

Cortical control of forelimb movement

Inauguraldissertation
zur
Erlangung der Würde eines Doktors der Philosophie
vorgelegt der
Philosophisch-Naturwissenschaftlichen Fakultät
der Universität Basel

von

Wuzhou Yang

2022

Originaldokument gespeichert auf dem Dokumentenserver der Universität Basel
edoc.unibas.ch

Genehmigt von der Philosophisch-Naturwissenschaftlichen Fakultät

auf Antrag von

Prof. Dr. Silvia Arber
Prof. Dr. Botond Roska
Prof. Dr. Carl Petersen

Basel, 20.09.2022

Prof. Dr. Marcel Mayor
Dekan der Philosophisch-
Naturwissenschaftlichen Fakultät

Table of Contents

1.	Summary.....	1
2.	Introduction.....	4
2.1.	Granular organization of cerebral cortex.....	5
2.2.	Diversity of cortical neurons	9
2.3.	Assembly of cortical circuits	12
2.3.1.	Excitatory circuits	12
2.3.2.	Inhibitory circuits	15
2.4.	Connecting cortical and subcortical structures	17
2.4.1.	Cortico-cortical networks.....	18
2.4.2.	Cortico-basal ganglia circuits.....	21
2.4.3.	Cortico-thalamo-cortical circuits.....	30
2.4.4.	Cortico-brainstem and cortico-spinal circuits	34
3.	Fine-grained structural and functional map for forelimb movement phases between cortex and medulla	40
3.1.	Abstract.....	41
3.2.	Introduction.....	42
3.3.	Results	47
3.3.1.	Medulla projection neurons reside preferentially in anterior cortex	47
3.3.2.	Cortex provides topographically organized synaptic input to latRM	52
3.3.3.	Cortical input to medulla is organized in 3D rostro-caudal columns	57
3.3.4.	Individual cortical neurons form collaterals along the rostro- caudal medulla	59
3.3.5.	Selective roles for MAC vs LAC in reaching vs handling.....	63
3.3.6.	Cortico-medullary synaptic organization extends into postsynaptic medulla.....	66
3.3.7.	Functional tuning of medulla neurons aligned with specific cortical input	68

3.3.8. Topography of cortico-medulla neurons extends to other subcortical structures	72
3.4. Discussion.....	77
3.4.1. Organization of cortical input to medulla and spinal cord for forelimb control	77
3.4.2. Organization of cortical input to medulla matches behavioral tuning of its neurons.....	79
3.4.3. Parallel cortical pathway logic generalizes to other motor centers	81
3.5. Methods.....	84
3.5.1. Key resources table	84
3.5.2. Resource availability	87
3.5.3. Animals	87
3.5.4. Method details	88
4. Conclusions and outlook	106
4.1. Hierarchical and interconnected motor pathways.....	106
4.2. Closed-loop organization for motor control	108
4.3. Open questions and challenges	109
5. Acknowledgments	111
6. References.....	112
7. Curriculum Vitae	133

Table of figures

Figure 2.1.1 Comparison of the brain of a mouse, a macaque monkey and a human, and the brain structures innervated by cortical projections in mice	5
Figure 2.1.2 Specificity of cortical regions.....	8
Figure 2.2.1 Different subtypes of cortical projection neurons	11
Figure 2.3.1 Architectures of cortical microcircuits	14
Figure 2.4.1 Cortico-cortical networks	19
Figure 2.4.2 Cortico-basal ganglia circuits	24
Figure 2.4.3 Cortico-thalamo-cortical circuits.....	31
Figure 2.4.4 Cortico-brainstem and cortico-spinal circuits	35
Figure 3.2.1 Scheme summarizing the cortical regions with different motor functions	43
Figure 3.3.1 Distribution of medullary and spinal projection neurons in the cortex ...	48
Figure 3.3.2 Medulla projection neurons reside preferentially in anterior cortex	49
Figure 3.3.3 Distribution of lumbar spinal projection neurons in the cortex	51
Figure 3.3.4 Cortex provides topographically organized synaptic input to latRM.....	53
Figure 3.3.5 Anterior cortex targets lateral rostral medulla.....	56
Figure 3.3.6 Cortical input to medulla is organized in 3D rostro-caudal columns.....	58
Figure 3.3.7 Individual cortical neurons form collaterals along the rostro-caudal medulla	61
Figure 3.3.8 Single MAC and LAC neurons from Mouselight database.....	62
Figure 3.3.9 Selective roles for MAC vs LAC in reaching vs handling	64
Figure 3.3.10 Cortico-medullary synaptic organization extends into postsynaptic medulla.....	67
Figure 3.3.11 Functional tuning of medulla neurons aligned with specific cortical input	70
Figure 3.3.12 Positively modulated latRM neurons in reaching and handling tasks ...	71

Figure 3.3.13 Topography of cortico-medulla neurons extends to other subcortical structures	75
Figure 3.3.14 Differences in synaptic targeting of cortico-medulla neurons extends to other subcortical structures	76
Figure 3.5.1 Analysis of electrophysiology data	99

Table of abbreviations

later rostral medulla	LatRM
striatum	Str
globus pallidus	GP
thalamus	Tha
zona incerta	ZI
subthalamic nucleus	STN
superior colliculus	SuC
red nucleus	RN
substantia nigra	SN
pontine nucleus	PN
pontine reticular nucleus	PRN
primary somatosensory cortex	S1
secondary somatosensory cortex	S2
primary motor cortex	M1
secondary motor cortex	M2
intratelencephalic neurons	IT neurons
extratelencephalic neurons	ET neurons
cortico-thalamic neurons	CT neurons
γ -aminobutyric acid	GABA
parvalbumin	PV
somatostatin	SST
vasoactive intestinal peptide	VIP
serotonin receptor 3A	5HT3aR
ventral tegmental area	VTA
5-hydroxytryptamine	5-HT
parafascicular thalamic nucleus	PF
ventromedial thalamic nuclei	VM
thalamic reticular nucleus	TRN
parasubthalamic nucleus	pSTN
striatal projection neuron	SPN
globus pallidus externus	GPe
globus pallidus internus	GPe
substantia nigra pars reticulata	SNr
substantia nigra pars compacta	SNc
anterolateral motor cortex	ALM
tongue/jaw motor cortex	tjM1
anterior cortex	AC
posterior cortex	PC
medial anterior cortex	MAC
lateral anterior cortex	LAC
adeno associated viruses	AAV
barrel cortex	BC
insular cortex	InsC
caudal forelimb area	CFA

cervical spinal cord	CSC
lumbar spinal cord	LSC
kernel density estimation	KDE
spinal trigeminal nucleus	Sp5
parvicellular reticular nucleus	PCRt
intermediate reticular nucleus	IRt
facial nucleus	7N
gigantocellular reticular nucleus	Gi
medial vestibular nucleus	MVe
ambiguus nucleus	Amb
solitary nucleus	Sol
lateral paragigantocellular reticular nucleus	LPGi
hypoglossal nucleus	12N
medullary reticular nucleus ventral part	MdV
medullary reticular nucleus, dorsal part	MdD
cuneate nucleus	Cu

1. Summary

Cortical control of movement is mediated by wide-spread projections impacting many nervous system regions in a top-down manner. Although much knowledge about cortical circuitry has been accumulated from local cortical microcircuits, cortico-cortical and cortico-subcortical networks, how cortex motor communicates to regions closer to motor execution, including the brainstem, is less well understood. In this dissertation, we investigate the organization of cortico-medulla projections and their roles in controlling forelimb movement. We focus on anatomical and functional relationships between cortex and lateral rostral medulla (LatRM), a region in caudal brainstem which is shown to be key in the control of forelimb movement.

We first uncover the organization of cortical neurons with connections to medulla. Using viral tracing approaches and reconstructions, we demonstrate that medulla-projecting cortical neurons reside preferentially in anterior cortical regions, in contrast to the well-studied cortico-spinal neurons, the majority of which is located in the relatively more caudal sensorimotor cortex. Within the anterior cortex, we define different domains with distinct projections to the medulla and spinal cord, including a lateral cortex region with exclusive access to medullary but not spinal circuits.

Secondly, our results reveal that medulla receives top-down cortical input in highly organized 3-dimensional rostro-caudal columns, targeted to and tiling forelimb regulatory regions in the medulla. We used high-resolution reconstructions of synaptic output patterns from many different identified cortical subregions. We find that the synaptic output from the anterior cortex to the medulla is organized into 3D columns extending throughout the length of the medulla, but in a pattern highly confined to lateral regions harboring skilled forelimb regulatory networks. Within this lateral

medullary space, neurons from different cortical locations generate synaptic output to distinct dorso-ventral positions, together tiling the entire space and giving rise to an exquisite 3D structural organization between cortex and medulla. This topographic and columnar organization is also followed at the level of individual cortical neurons that give rise to multiple terminal arborizations along the rostro-caudal axis of the medulla as revealed by analysis of single neuron tracing data. Additionally, the synaptic dorso-ventral topography is also reflected in the medullary neurons receiving input from the cortex that follow the same logic.

Thirdly, we find that medial- vs lateral anterior cortex regulate forelimb reaching and handling phases and are connected selectively to reaching- and handling tuned medulla neurons. Using loss-of-function experiments of selective cortical subregions, *in vivo* electrophysiological recordings in freely behaving mice and optogenetics, we probe cortical function as well as connectivity between cortex and behaviorally tuned neurons in the lateral medulla. Through these experiments, within the anterior cortex, we define a medial cortical region essential for forelimb reaching. Strikingly this region is preferentially connected to medulla neurons tuned to forelimb reaching. In contrast, we find a lateral cortical region to be essential for food handling and connected in a highly specific manner to medulla neurons tuned to food handling and manipulation but not reaching. Thus, within the small space of the lateral medulla, there is extraordinary matching between cortical function and behavioral tuning of connected neurons in the medulla, together central to the execution of distinct phases of behavior.

Lastly, the topography of cortico-medulla neurons we have discovered extends to other subcortical structures. Using a combination of retro- and anterograde viral tracing as well as high resolution imaging and reconstructions, we find that the logic of

anatomically segregated target innervation by medulla-projecting cortical neurons in different cortical regions extends to other subcortical motor structures. Specifically, medulla-projecting cortical neurons also, at the same time, exhibit highly selective collateralization patterns to other motor centers. These findings extend the concept of how collaterals interact with highly specific circuits within the hierarchy of the motor system. This extension of the topographic organization to other motor centers emphasizes the organization of parallel outputs from different cortical domains to major centers of motor control and argues for an anatomical/circuit structure basis at the core of functional segregation and output processing from within cortical domains.

Together, our findings reveal the precise anatomical and functional organization between different cortical regions and matched postsynaptic neurons in the caudal brainstem, tuned to different phases of one carefully orchestrated behavior, which advance the our knowledge on circuit mechanisms involved in the control of body movements, and unravel the logic of how the top-level control region in the mammalian nervous system – the cortex – intersects with a high degree of specificity with command centers in the brainstem and beyond.

2. Introduction

Movement is the most fundamental way for animals to interact with the environment. Animals can execute diverse forms of body movement in order to adapt to different circumstances. Some movement like locomotion requires many muscles in the whole body and those muscles contract with a regular rhythm to produce stereotypical movement. For some other movement implemented by individual limbs or fingers like food handling, precise muscle control needs to be generated and the movement can be various and flexible. To construct those diverse movements, a complex motor system with structures and neuronal circuits distributed throughout the entire nervous system is involved to signal and orchestrate behaviors, including the cortex, basal ganglia, thalamus, brainstem and spinal cord, where multiple levels of computation are implemented to allow animals to survive, adapt, and explore in the world (Heekeren et al., 2008; Lemon, 2008; Shepherd, 2013; Wang et al., 2017; Steinmetz et al., 2019; Pinto et al., 2019; Steinmetz et al., 2019; Roy et al., 2022; Arber and Costa, 2022).

What makes human beings special from other animals? Evolution has brought human beings the largest brain among extant primates, which is believed to empower human mental ability (Figure 2.1.1A) (Williams and Herrup, 1988). One of the most illustrious characteristics of the human brain is the expansion of the cerebral cortex with evolution, which is correlated with general intelligence and other indicators of cognitive capacities (Figure 2.1.1A) (Sousa et al., 2017). Motor function is an important ability that allows human beings to utilize and demonstrate their intelligence and cognition. Therefore, the cortical control of movement is a key attribution that distinguishes human beings from other species. The unique feature of the cerebral cortex with its access to almost all motor related structures of the brain places it as an ideal entry point

to unravel the organization of neuronal circuits for execution, choice, and coordination of movement (Figure 2.1.1B).

2.1. Granular organization of cerebral cortex

In the cerebral cortex of mice, around 80% of the cortical neurons are glutamatergic excitatory including cortical projection neurons, and the remaining approximately 20% of neurons are inhibitory which are mostly γ -aminobutyric acid (GABA)ergic interneurons providing local inhibition (Harris and Mrsic-Flogel, 2013). While inhibitory cortical neurons originate from the ganglionic eminences in the ventral pallium and then migrate tangentially to the dorsal telencephalon, excitatory cortical neurons are generated from radial glial cells in proliferative transient embryonic zones near the surface of the cerebral lateral ventricles (ventricular and subventricular zones) (Figure 2.1.2A) (Rakic, 2009). The postmitotic neurons derived from radial glial cells migrate radially along the radial glial fibers and each generation bypasses the previous one, a phenomenon known as the inside-out gradient of neurogenesis (Rakic, 2009).

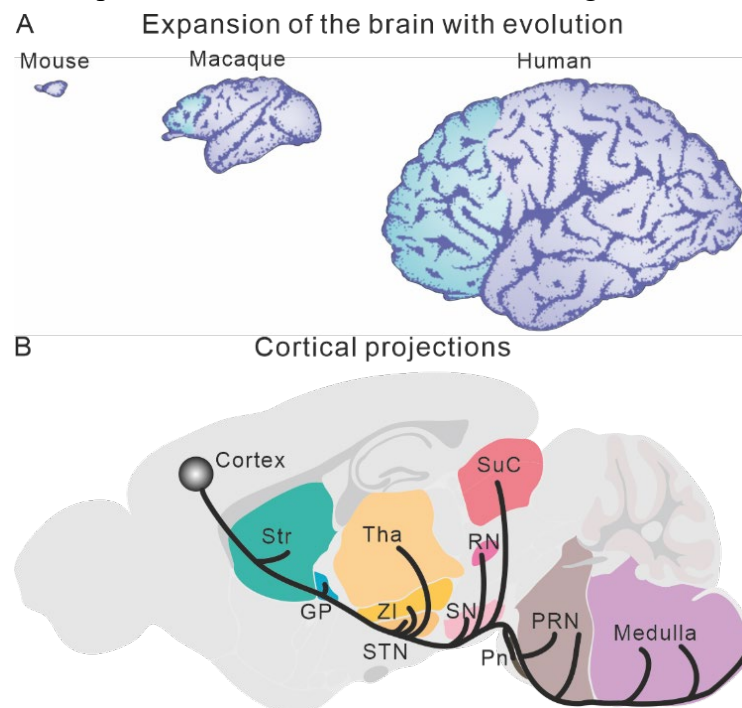


Figure 2.1.1 Comparison of the brain of a mouse, a macaque monkey and a human brain, and the brain structures innervated by cortical projections in mice

(A) The cerebral hemispheres of a mouse, a macaque monkey and a human brain, respectively, are drawn to approximately the same scale (adapted from (Rakic, 2009)).

(B) Cortical projections to subcortical brain regions which are related to motor functions. Abbreviations refer to *Table of abbreviations*.

Although the cerebral cortex appears to be a uniform, six-layer structure, it can be defined into specific subregions by different criteria. For example, the first observation of body movement induced by electric stimulation on cortical regions paved the way to uncover the motor function of cerebral cortex (Ferrier and Burdon-Sanderson, 1875; Fritsch and Hitzig, 2009). Further knowledge about the cerebral cortex comes from Ramón y Cajal who revealed the anatomy of different cell types (Cajal, 1899; Sotelo, 2003). Based on the cytoarchitectural organization, many cortical regions were delineated, such as Brodmann areas in human cortex (Figure 2.1.2B) (Brodmann, 1909). Henceforth, finer stimulation of the cortex mapped a more detailed organization of sensory and motor cortices, which are described as cortical homunculi (Figure 2.1.2C) (Penfield and Boldrey, 1937). Such functional mapping approaches, together with advances on anatomical tracing (Gerfen and Sawchenko, 1984; Lanciego and Wouterlood, 2020), lead to a classic view of a hierarchical organization of cortical regions, where the primary somatosensory cortex (S1) receiving sensory input, the primary motor cortex (M1) controlling specific body/limb movements, and the secondary motor cortex (M2, or premotor cortex), as a higher order region, indirectly modulating movements through intracortical connections with M1 (Figure 2.1.2D).

However, even though the cerebral cortex exhibits subregional specificity, the functions of different cortical regions are controversial. For example, different ways of stimulation of motor cortex in rodent, either electrically or optogenetically, produce different cortical maps corresponding to movements (Harrison et al., 2012; Miri et al., 2017; Tennant et al., 2011; Wang et al., 2017). In monkeys, prolonged stimulation of primary motor and premotor cortex evoke coordinated and complex forelimb movements, implying a converged repertoire with diverse motor programs in the cerebral cortex (Graziano et al., 2002). Moreover, different subregions in motor cortex

can be overlapping. For example, the secondary motor cortex in mouse is also viewed as primary whisker motor cortex (Mayrhofer et al., 2019). More surprisingly, whisker movement can be elicited by stimulation of whisker sensory cortex (Matyas et al., 2010). In forelimb movement, sensory cortex also show important roles in motor control (Conner et al., 2021; Mathis et al., 2017). These combined results suggest a more complicated organization of cerebral cortex than what might have been anticipated, likely arisen from the diversity of cortical neurons, which is only beginning to be elucidated in recent years.

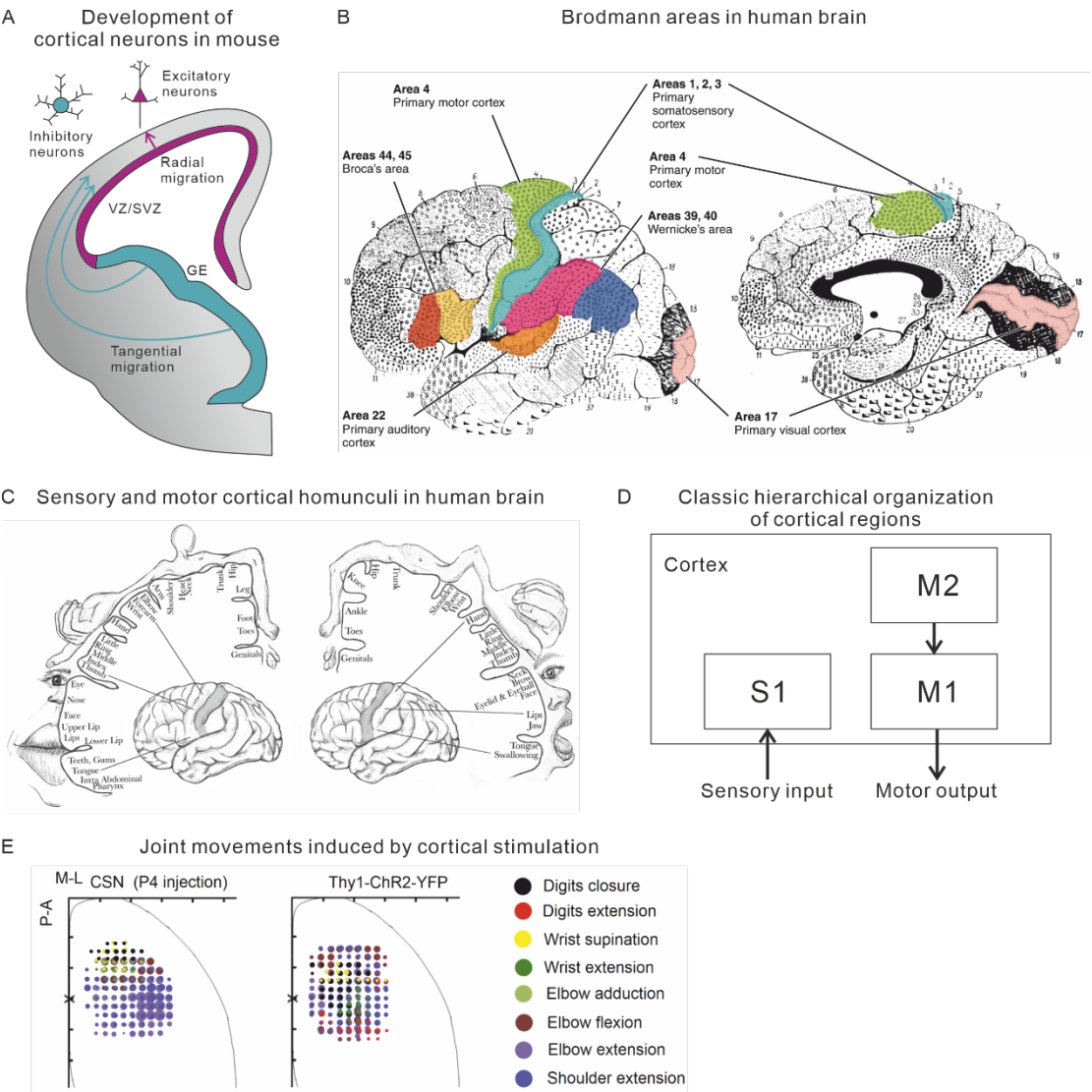


Figure 2.1.2 Specificity of cortical regions
 Legend on next page.

Therefore, further knowledge about the cerebral cortex calls for high level of granularity using multimodal approaches including anatomy, molecular and function to study the cerebral cortex on the basis of neuronal subtypes. Recent advances with deep single-cell RNA sequencing in visual and motor cortex reveal more than 100 neuronal subtypes (Tasic et al., 2018). Interestingly, while GABAergic neuronal subtypes are shared across cortical areas, most subtypes of glutamatergic neurons are exclusive to only one cortical region (Tasic et al., 2018). The regional specificity in glutamatergic but not GABAergic neurons might originate from respective developmental programs (Di Bella et al., 2021). Visual and motor cortices are functionally different and distantly placed, but it is still unknown if specificity exists in spatially closer cortical regions with similar functions. Other work takes advantage of retrograde viruses to label a specific population of cortical projection neurons, the cortico-spinal neurons, and demonstrates the differential use of motor cortex areas in behavioral phases of a forelimb-guided food pellet retrieval task (Wang et al., 2017). It is worth noting that, depending on the subtype of cortical neurons, optogenetic stimulation on the same cortical region elicits different patterns of movement (Figure 2.1.2E) (Wang et al., 2017), suggesting that the specificity of cortical regions is related to the granularity of the neuronal subtypes. Thus, it is of great interest and importance to put the puzzle pieces of the cerebral cortex together, especially from the perspective of the motor cortex, which provides a good

Figure 2.1.2 Specificity of cortical regions

- (A) Scheme shows a cross section of half of a mouse fetal forebrain. In rodents, ventricular and subventricular zones (VZ/SVZ) generate excitatory neurons while ganglionic eminences (GE) are the main source of inhibitory neurons.
- (B) Brodmann areas in human brain (adapted from (Brodmann, 1909)).
- (C) Sensory and motor homunculi in human cerebral cortex (adapted from <https://www.ebmconsult.com/articles/homunculus-sensory-motor-cortex>).
- (D) a classic view of a hierarchical organization of cortical regions for sensory and motor functions.
- (E) Motor maps of all joint movements elicited by opto-stimulation in mice with ChR2 expressed in cortico-spinal neurons and Thy1-ChR2 mice (adapted from (Wang et al., 2017)).

opportunity to align the properties of cerebral cortex from multiple dimensions such as molecular, anatomy and function to understand the logic of cortical organization.

2.2. Diversity of cortical neurons

Cortical projection neurons consist of three major excitatory subtypes: intratelencephalic (IT), extratelencephalic (ET, also referred to as pyramidal tract) and cortico-thalamic (CT) neurons (Figure 2.2.1A) (Shepherd, 2013; BRAIN Initiative Cell Census Network (BICCN), 2021; Muñoz-Castañeda et al., 2021). IT neurons in layer 2 to 6 project to the striatum and other cortices. ET neurons in lower layer 5 project to the striatum as well as targets outside the telencephalon such as thalamus, brainstem and spinal cord. CT neurons in layer 6 project almost exclusively to thalamus and weakly to striatum. IT and ET neurons can be further divided into subgroups based on their projection targets (Figure 2.2.1A). IT neurons in layers 2/3 and 6 have cortico-cortical projections, whereas those in upper layer 5 have not only cortico-cortical but also cortico-striatal projections (Shepherd, 2013; BRAIN Initiative Cell Census Network (BICCN), 2021; Muñoz-Castañeda et al., 2021). ET neurons, which send axon collaterals to many targets, can be separated into two non-overlapping populations: upper ET neurons project to thalamus while terminating rostral to medulla, and lower ET project to medulla but avoid the thalamus (Economo et al., 2018; BRAIN Initiative Cell Census Network (BICCN), 2021; Muñoz-Castañeda et al., 2021). Moreover, there are incredibly diverse subtypes of inhibitory interneurons, which can be organized into three large classes based on the expression of Parvalbumin (PV), Somatostatin (SST), and the serotonin receptor 3A (5HT3aR). The alignment among molecular, morphological and electrophysiological features of interneurons are extraordinarily complicated (Ascoli et al., 2008; Kepecs and Fishell, 2014; Lim et al., 2018; BRAIN Initiative Cell Census Network (BICCN), 2021).

As the motor cortex hosts many different types of neurons with projections to many subcortical structures, it is strategically suited as a hub for information integration and commands broadcasting. To achieve these functionalities, the motor cortex requires infrastructures to receive input information from multiple sources as the first step, secondly to deliver commands and/or modulation to motor execution centers and thirdly interface and/or compute between available information and final execution. To start with, cortical projection neurons need to receive prolific excitatory and inhibitory inputs from multiple cortical and subcortical cell classes. To this end, they utilize basal and apical dendrites, which allow dendritic computation through linear and/or nonlinear mechanisms (Figure 2.2.1B) (London and Häusser, 2005). For example, coincident inputs to different regions of the apical dendrite in layer 5 excitatory neuron evokes bursts of axonal action potentials that would not be expected from the linear summation of the individual inputs (Larkum et al., 1999; Williams and Stuart, 2002). Action potentials back-propagating to dendrites, which activate the dendritic spines coincidentally with presynaptic inputs in a certain time interval, have been shown to modulate the efficacy of synaptic connections (Markram et al., 1997). Interestingly, dendritic activity in visual cortical layer 2/3 neurons recorded by *in vivo* calcium imaging reveals that even in one dendritic branch, preferred orientations can be different, while the dendritic segments exhibiting the same orientation preference are widely distributed throughout the dendritic tree (Jia et al., 2010). Furthermore, a more detailed analysis of the dendritic activity in dendritic spines suggests that the spines that share the visual features with the soma are placed at the primary branches of the dendrite while those with different visual features are located at the high-order branches (Iacaruso et al., 2017). These results demonstrate that at the cellular level, a single cortical neuron synthesizes diverse information, and the functional output of the neuron

depends on dendritic computation. In motor cortex, dendritic signal processing is also important in motor control, which is shown by the reorganization of dendritic spines associated with the process of motor learning (Xu et al., 2009). However, the cellular mechanisms of how convergent presynaptic input in the motor cortex give rise to behavior output remain unclear. In addition, cortical neurons express different receptors rendering neuromodulation from multiple resources (Figure 2.2.1B), such as noradrenergic input from the locus coeruleus (Wang et al., 2007), dopaminergic input from the ventral tegmental area (VTA) (Gaspar et al., 1995; Seong and Carter, 2012), 5-hydroxytryptamine (5-HT; also known as serotonin) input from the dorsal raphe nucleus (Araneda and Andrade, 1991; Ju et al., 2020) and cholinergic input from the nucleus basalis (Dembrow et al., 2010; Poorthuis et al., 2013). The different forms of neuromodulations that cortical neurons receive no doubt contribute to the diversity of cortical neuron responses and influence information processing.

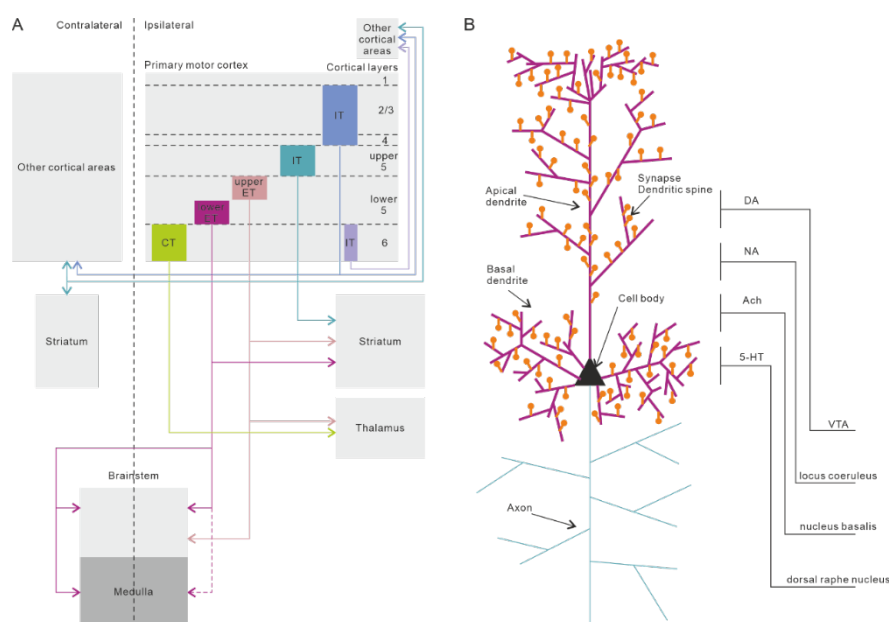


Figure 2.2.1 Different subtypes of cortical projection neurons

- (A) Summary scheme of cortical projection neurons in different cortical layers and their projection targets.
- (B) A representative cortical projection neuron with dendrites (magenta) and axons (cyan), as well as neuromodulatory inputs including dopamine (DA), noradrenaline (NA), acetylcholine (ACh) and 5-hydroxytryptamine (5-HT) signaling.

Thus, it is conceivable that cortical neurons, which exhibit incredible diversities in terms of genetic and epigenetic traits, developmental programs, neuronal morphology, electrophysiological properties and neuromodulation receptors, receive and process neuronal signals in multiple ways. It would be interesting to further study how the different types of the cortical neurons are built into circuits, which subcellular compartments are interconnected, and how information flow occurs. Moreover, it will be of great clinic value to study not only the physiological functions e.g. learning or decision making, but also malfunctional conditions e.g. Parkinson disease or schizophrenia.

2.3. Assembly of cortical circuits

To further process neuronal signals, individual excitatory and inhibitory cortical neurons are assembled into different forms of neuronal microcircuits with specific patterns of synaptic connectivity which are hardwired by developmental programs and can also be rewired dynamically by neuronal plasticity. The microcircuits serve as the building blocks to construct complicated neuronal networks for cortical computations to take place. Understanding the architectures of microcircuits helps to bridge the gap between individual neurons and the function of the brain.

2.3.1. Excitatory circuits

The canonical connectivity of the excitatory cortical neurons is well established (Harris and Mrsic-Flogel, 2013) as I will briefly summarize (Figure 2.3.1A). In this canonical circuit, Layer 4 neurons receive input from thalamus and project to all layers but most strongly layer 2/3 neurons, and subsequently layer 2/3 IT neurons project to layer 5. While the upper layer 5 IT neurons possess local connections to layer 2/3, the lower layer 5 ET neurons lack local output but send long range axons with collaterals

to striatum, thalamus and brainstem. ET neurons can be further split into thalamus projecting (upper ET) and medulla projecting (lower ET) neurons (Economo et al., 2018). ET neurons collect input within a cortical column with little local output within the column while send long-range projections outside telencephalon, which therefore serve as an output station which accumulates information from an entire cortical column, and broadcasts processed information to distant targets (Brown and Hestrin, 2009). Layer 6 are mostly cortico-thalamic neurons with local projections preferentially targeting layer 4 inhibitory neurons (Thomson, 2010) and provide long-range projections to the thalamus (Muñoz-Castañeda et al., 2021). It is worth noting that, while sensory cortices have layer 4, a specific recipient layer for thalamic input that carries peripheral sensory information, motor cortex only possess a very thin layer of layer 4 which has only been acknowledged recently (Yamawaki et al., 2014; BRAIN Initiative Cell Census Network (BICCN), 2021).

How are these different subtypes of neurons wired together forming stereotypical circuits? Interestingly, a single progenitor cell can give rise to preferentially connected excitatory neurons of multiple subtypes in different layers (Yu et al., 2009) mediated by transient electrical synapses (Yu et al., 2012). In visual cortex, neurons arising from the same progenitor are more likely to be synaptically connected and share orientation preference than unrelated ones (Figure 2.3.1B) (Li et al., 2012). These studies suggest that the hardwired columnar connectivity can be generated through early developmental processes. Moreover, cortical circuits can also be shaped by postnatal experience. The Hebbian plasticity, known as “fire together, wire together”, argues for the strengthening of interconnected neurons to be tuned to similar or commonly co-occurring features (Hebb, 2002). In line with this rule, in the visual cortex, excitatory neurons sharing similar visual features tend to be more interconnected than

those who are differently tuned (Ko et al., 2011). These data suggest the existence of multiple intermingled subnetworks of highly interconnected cortical neurons in cortical areas (Figure 2.3.1C).

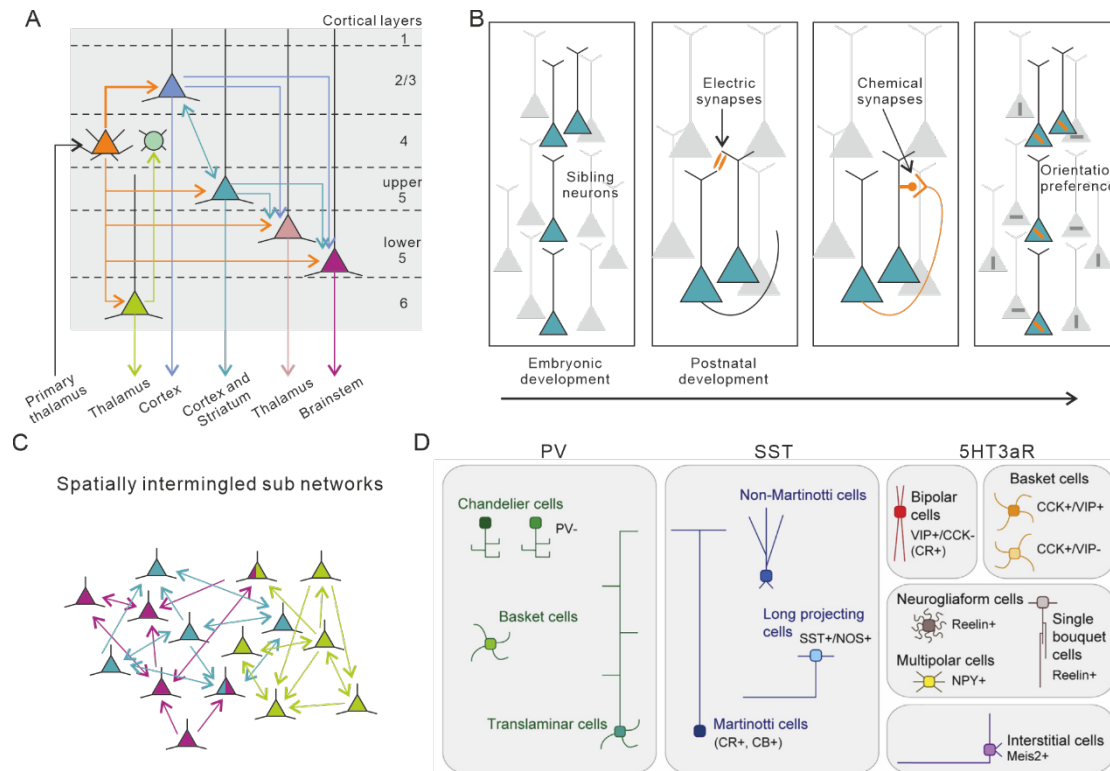


Figure 2.3.1 Architectures of cortical microcircuits

- (A) Scheme illustrating the canonical connectivity of cortical excitatory neurons.
- (B) Neurons developed from the same progenitor cell migrate towards the brain surface to form lineages of sibling neurons across the cortical layers. At early stage, sibling neurons are preferentially connected by electric synapses which disappear as development proceeds and chemical synapses are preferentially established between sibling neurons thereafter. In a later developmental phase, sibling neurons respond to similar sensory features, such as the orientation of visual stimuli (adapted from (Mrsic-Flogel and Bonhoeffer, 2012)).
- (C) Proposed fine structure of cortical circuits with multiple intermingled subnetworks of highly interconnected excitatory neurons. Colored triangles represent neurons in the same subnetwork. Striped triangles show neurons belonging to different subnetworks. Arrows indicate synaptic connections (adapted from (Harris and Mrsic-Flogel, 2013)).
- (D) Scheme depicting the main classes of cortical interneuron in the mouse cerebral cortex based on the expression of PV, SST, and 5HT3aR (adapted from (Lim et al., 2018)).

The principles of cortical circuit establishment in sensory cortices, with a combination of molecular cues and activity-dependent synaptic plasticity, shed light on understanding the assembly of the motor cortical circuits, such that multiple and dynamic motor subcircuits for different motor programs might co-exist in motor cortical areas forming spatially intermingled while separately interconnected ensembles. Notably, a significant difference between sensory and motor function is that sensory information needs to be relatively faithfully obtained from the external environment while motor behaviors can be remarkably flexible. Relatedly, sensory cortices show reduced plasticity after critical period (Erzurumlu and Gaspar, 2012; Hensch, 2005), while motor cortex seems to keep a certain level of plasticity throughout adulthood (Sanes and Donoghue, 2000). Indeed, layer 2/3 IT neurons in motor cortex show dynamics of movement-related activities and emerge into a smaller population exhibiting reproducible spatiotemporal sequences of activity with learning (Peters et al., 2014), while during the learning course, cortical neurons are disengaged from movement control at later stage when the animals become expert (Hwang et al., 2019). Layer 5 cortico-spinal neurons, however, show heterogeneous and dynamic patterns of activity throughout learning, suggesting the formation and reorganization of several subnetworks encoding different parameters of movement (Peters et al., 2017). Further studies to uncover the development and dynamics of neuronal microcircuits in the motor cortex which contribute to diverse forms of motor behaviors will be particularly interesting (Figure 2.3.1C).

2.3.2. Inhibitory circuits

Proper functionality of critical neuronal circuits also requires the participation of inhibitory interneurons. Three major classes of interneurons (PV+, SST+ and 5HT3aR+), each of which can be further divided into subgroups, form diverse motifs

of circuits together with excitatory neurons to enrich the cortical circuits (Figure 2.3.1D) (Jiang et al., 2015; Lim et al., 2018; Luo, 2021).

PV⁺ neurons, distinguished as fast spiking neurons, consist of three main subgroups. The major subtype is the basket cells whose axons form synapses on the soma and proximal dendrites of pyramidal cells and other interneurons (Hu et al., 2014). Chandelier cells, with the characteristic morphology of their elaborated axonal arbor that resembles a chandelier light fixture, target the axon initial segment (Taniguchi et al., 2013). And a minor subset of PV⁺ neurons, called translaminar interneurons, targets excitatory neurons across several layers (Bortone et al., 2014).

SST⁺ neurons contain Martinotti and non-Martinotti cells as the major types. Martinotti cells are characterized by an ascending axon that arborizes profusely in layer 1. They preferentially target the tuft dendrites of excitatory cells and mediate disynaptic inhibition (Hilscher et al., 2017; Silberberg and Markram, 2007). Non-Martinotti cells innervate PV⁺ basket cells primarily and lack axons in layer 1 (Pfeffer et al., 2013; Xu et al., 2013). SST⁺ inhibitory neurons also encompass a minor group of long-range GABAergic projection neurons involved in sleep regulation which innervate other cortical areas (Dittrich et al., 2012).

5HT_{3A}R⁺ neurons are more heterogeneous. The major class is bipolar cells expressing vasoactive intestinal peptide (VIP) which are mainly disinhibitory for their preferential inhibition on SST⁺ and PV⁺ interneurons (Pi et al., 2013; Jiang et al., 2015). Multipolar VIP⁺ cells are different from bipolar interneurons which co-express the neuropeptide cholecystokinin and make synapses on the soma of excitatory neurons and other interneurons (Kawaguchi and Kubota, 1998; Tasic et al., 2018). There are also some VIP⁺ interneurons abundant in layer 1 including neurogliaform cells and

single bouquet cells. Neurogliaform cells possess dense and characteristic axonal arbor with expression of reelin and neuropeptide Y mediating volumetric GABA transmission (Lee et al., 2010; Oláh et al., 2007), while single bouquet cells have axonal ramifications that extend to deep layers of the cortex (Jiang et al., 2015; Tasic et al., 2018).

Together, diverse inhibitory neurons, along with different excitatory neurons, establish synapses on distinct subcellular compartments of their targets to build neuronal microcircuits for information processing. It will be remarkably interesting to reveal the detailed microcircuit organization of defined neuronal populations and their functions in different context. The assembly of cortical neurons forms various circuit motifs and architectures such as feedforward excitation, feedforward and feedback inhibition, lateral inhibition and mutual inhibition (Jiang et al., 2015; Luo, 2021), which are embedded in bigger circuits across multiple brain regions to enable neural computations and functions. Interestingly, compared with mouse cortex, human cortex shows significantly increased proportion of non-neuronal cells, suggesting that the non-neuronal cells might play an important role in modulating cortical neuronal circuits especially in the human cortex (Fang et al., 2022). Moreover, the higher percentage of inhibitory neurons and IT neurons implies that these neuronal types might be important in building more complicated cortical neuronal circuits in human cortex (Fang et al., 2022).

2.4. Connecting cortical and subcortical structures

The microcircuits in individual cortical regions alone are not sufficient to carry out complicated functions. Nearly all brain functions, including sensory, motor and cognitive functions, rely on a distributed network of regions, which requires not only

the generation of relevant patterns of activity within each region, but also the appropriate communication of activity among different cortical regions as well as subcortical structures including basal ganglia, thalamus, brainstem and spinal cord (Heekeren et al., 2008; Lemon, 2008; Shepherd, 2013; Wang et al., 2017; Steinmetz et al., 2019; Pinto et al., 2019; Steinmetz et al., 2019; Roy et al., 2022; Arber and Costa, 2022).

2.4.1. Cortico-cortical networks

It is well known that different cortical regions are highly interconnected. Cortical regions form segregated subnetworks which show elevated interconnection within and are linked together by some hub regions (Figure 2.4.1A) (Oh et al., 2014; Zingg et al., 2014). The intratelencephalic (IT) neurons across layer 2 to 6 output to distant cortical regions, and therefore serve as the neuronal population mediating cortico-cortical communications. Recent studies reveal a diverse range of IT neuron subtypes with various forms of cortico-cortical projections. For example, in motor cortex, molecularly distinct IT neurons in different cortical layers show different patterns of projection to other cortical areas (Muñoz-Castañeda et al., 2021). At single-neuron level, the combination of output targets from one single neuron can be diverse, suggesting the existence of widely interconnected while highly selective subnetworks in cerebral cortex (Han et al., 2018; Winnubst et al., 2019; Muñoz-Castañeda et al., 2021). IT neurons target other cortical areas in a laminar specific manner as observed in both non-human primate (Rockland and Pandya, 1979) and rodent (Harris et al., 2019), which conform to the canonical cortical microcircuit in many ways (Figure 2.4.1B). For example, IT neurons in the barrel cortex (the primary sensory cortex [S1] for whisker perception) with distinct electrophysiological properties provide respective projections to secondary sensory cortex (S2) and primary motor cortex (M1) and

innervate different layers of the targeted cortical areas (Figure 2.4.1B) (Yamashita et al., 2013). The highly selective pathways diverge information from S1 to M1 and S2 separately which underlie computing different sensory properties (Chen et al., 2013). Moreover, whisker motor cortex targets the apical dendrite of layer 5 neurons in barrel cortex, which potentiates the activity of layer 5 neurons coding whisker sensory signal (Xu et al., 2012).

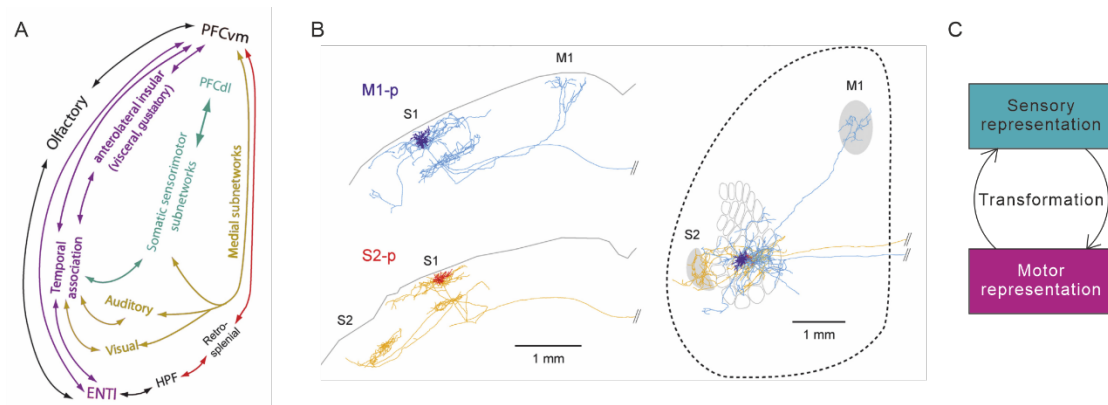


Figure 2.4.1 Cortico-cortical networks

- (A) Scheme showing cortico-cortical network information flow in a top-down view of the cortex. Colored pathways are corresponding subnetworks. Note prefrontal cortex as the hub of multiple subnetworks (adapted from (Zingg et al., 2014)).
- (B) In mouse S1, two distinct subclasses of layer 2/3 neurons project to M1 and S2, innervating different layers of targeted cortical regions (adapted from (Yamashita et al., 2013)).
- (C) Scheme showing the transformation of neuronal representations between sensory and motor cortices.

The networks with interconnected cortical areas allow for complex information processing. A simple motif that the excitatory cortical neurons can form is excitatory recurrent circuitry which enables reinforcement of the sensory signaling and amplification of the sparse input from multiple sources (Douglas et al., 1995). With the interconnected cortical neurons, the neuronal activity is processed in distributed cortical networks which increase the fault tolerance of the neuronal coding to be more to be resistant to errors and recover the required information when perturbed (Inagaki et al., 2019). Moreover, cortical areas forming multi-level neuronal networks allow more

complex computation for the extraction of different features from sensory modalities. For example, visual perception can be distributed in primary and high order visual cortical areas tuned to basic (e.g., the orientation) and more complex visual features (e.g., the pattern motion and the curvature of an object), respectively, and these cortical areas are interconnected to enable specialized information streams across multiple areas (Born and Bradley, 2005; Niell and Scanziani, 2021), showing the existence of the functional subnetworks to process visual information. Other sensory modalities like auditory (Kaas and Hackett, 2000) and vibrissal (Petersen, 2019) perception also require multiple levels of processing to extract information in different dimensions. Although cortical long-range inter-areal connections are mediated by excitatory neurons, it could also result in inhibition of targeted cortical regions depending on the postsynaptic neuronal population. For example, secondary motor cortex specifically targets PV⁺ interneurons in auditory cortex and leads to suppression of excitatory neurons in auditory cortex during movement, which might play a role in facilitating hearing and auditory-guided behaviors (Schneider et al., 2014).

Conceptually, movement and perception are always linked together (Figure 2.4.1C). For example, mice actively touch an object with their whisker to establish a neuronal representation of it (Petersen, 2019). Moreover, vision can only be achieved by continued eye movement and fixation of gaze in some animal species (Martinez-Conde et al., 2004). Therefore, approaching the external world and building a perception require the transformation of neuronal representations between sensory and motor cortical areas (Figure 2.4.1C) (Keller and Mrsic-Flogel, 2018). Similarly, interdisciplinary collaboration of sensory and motor systems is important for precise forelimb behaviors, where visual, tactile and proprioceptive sensitivity as well as complicated hand musculature including approximal and distal forelimb muscles are all

involved to allow dexterous interactions with objects by hands (Sobinov and Bensmaia, 2021). In non-human primate, it is believed that visually-guided forelimb movements are carried out by the interaction between the motor cortex and the posterior parietal cortex (Sobinov and Bensmaia, 2021). However, further knowledge about the cellular mechanisms of visuo-motor transformations are difficult to be obtained from monkey studies. In rodent, although visually-guided forelimb movements are not observed, other sensory modalities are involved in goal-oriented forelimb behaviors. For example, it has been shown that mice use olfaction to locate the water droplets and perform a forelimb reaching movement to get such droplets through this mechanism (Galiñanes et al., 2018). It will be particularly interesting to know how the olfactory-motor interaction contributes to determine the parameters in forelimb reaching task such as directionality.

Together, the organization of cortico-cortical projections allows inter-areal communication between functionally distinct cortical domains and diversifies cortical computations to fit with different behavioral scenarios. Uncovering the information flow among cortical domains will be instrumental to understand the logic of cortical computation (Markov et al., 2013; Keller and Mrsic-Flogel, 2018; Kohn et al., 2020).

2.4.2. Cortico-basal ganglia circuits

IT neurons in the cerebral cortex mediate not only cortico-cortical interaction but also cortico-subcortical communication. Layer 5 IT neurons are different from other IT neuronal populations with their intensive connections to striatum (Shepherd, 2013; Muñoz-Castañeda et al., 2021). In addition, ET neurons in layer 5 also send axonal collaterals to the striatum. Of note, studies with anatomical mapping and electrophysiological recording show that cortico-striatal projection follows a precise topographical organization (Hintiryan et al., 2016; Peters et al., 2021) (Figure 2.4.2A).

Highly organized circuits are preserved throughout basal ganglia circuits. Substantia nigra pars reticulata (SNr) neurons in different locations receive inputs from different subdomains of striatum which are involved in diverse functions (Lee et al., 2020; Foster et al., 2021) (Figure 2.4.2B). Distinct neuronal populations in SNr send output with multiple channels to different brainstem regions (McElvain et al., 2021) and thalamus including parafascicular (PF) and ventromedial (VM) thalamic nuclei (Foster et al., 2021) (Figure 2.4.2C). Finally, PF and VM thalamic nuclei provide topographical projections back to the cortex (Foster et al., 2021; Wang et al., 2021) and separate PF populations project to basal ganglia domains such as striatum, subthalamic nucleus (STN) and nucleus accumbens respectively with distinct functions (Mandelbaum et al., 2019; Watson et al., 2021; Zhang et al., 2022) (Figure 2.4.2D). These results reveal the existence of multiple distinct cortico-basal ganglia loops. Furthermore, PF receives direct cortical input (Mandelbaum et al., 2019), marking thalamus as an intersection among cortico-basal ganglia and cortico-thalamo-cortical circuits (Figure 2.4.2D). The cortico-thalamo-cortical circuits are discussed in the next section.

The striatum consists of at least two major types of neurons, the GABAergic striatal projection neurons (SPNs) as the most abundant type and a small population of interneurons which are GABAergic and cholinergic, while completely lacking excitatory glutamatergic neurons (Kreitzer and Malenka, 2008). The SPNs were historically called medium spiny neurons, due to their high spine density, negative resting potential, and low firing rates *in vivo* (Kreitzer and Malenka, 2008). SPNs can be further classified into two populations based on their gene expressions and axonal projections: neurons expressing D1-type dopamine receptors project to SNr with minor collaterals to the globus pallidus externus (GPe), and neurons with D2-type dopamine receptors send axons terminating in GPe (Arber and Costa, 2022) (Figure 2.4.2E). Both

SNr and GPe are comprised of GABAergic inhibitory neurons. SNr, together with globus pallidus internus (GPi), is considered as the output of basal ganglia circuits for its projection to brainstem nuclei, whereas GPe encompass projections to SNr as well as striatum, STN, thalamus and cortex. Therefore the circuits from D1 neurons to SNr are termed as the “direct pathway”, while the D2 neurons projecting to GPe are part of the “indirect pathway” (Arber and Costa, 2022) (Figure 2.4.2E).

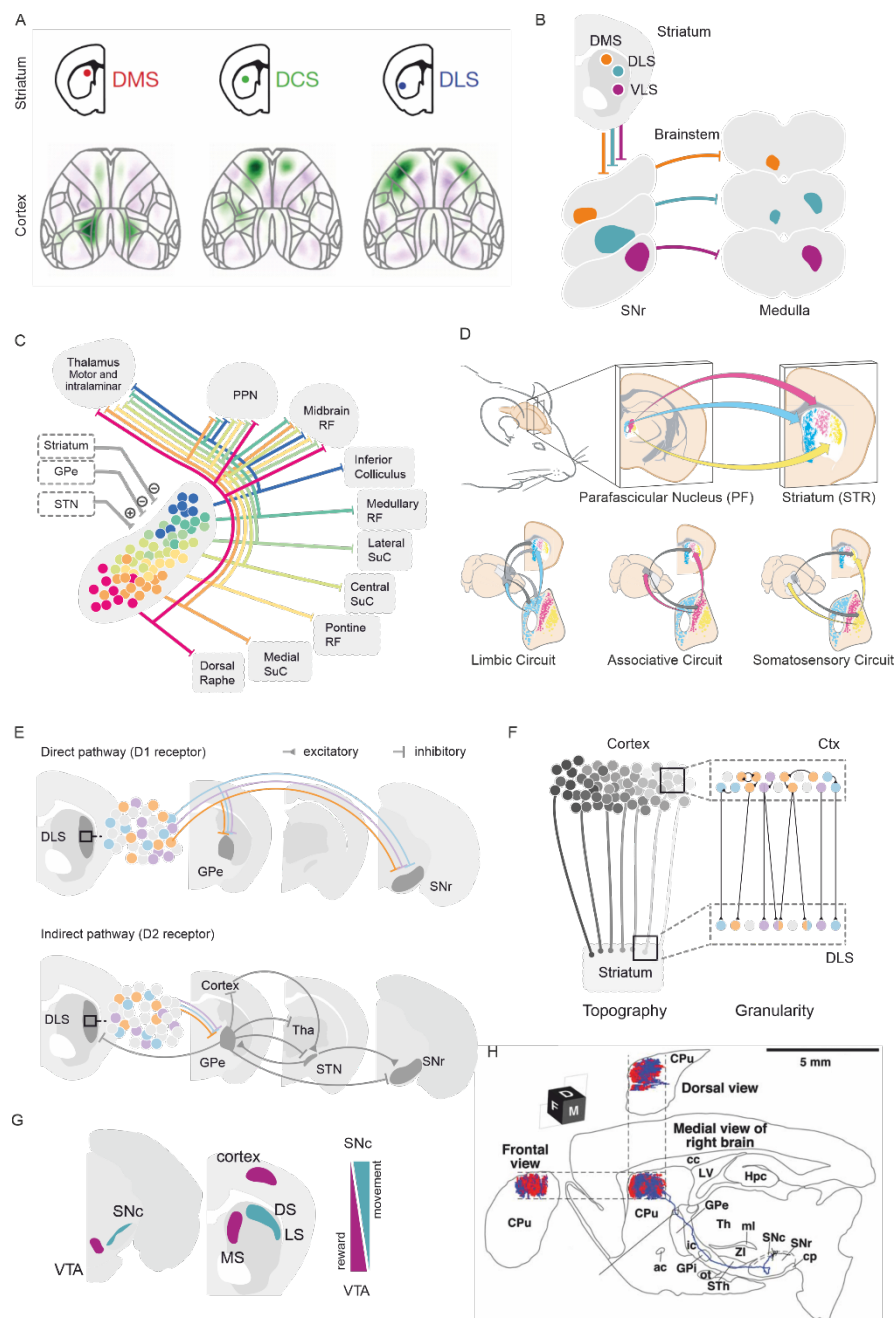


Figure 2.4.2 Cortico-basal ganglia circuits
Legend on next page.

The organization of direct and indirect basal ganglia pathways leads to the question of how they influence movement. At resting state, both GPi and SNr actively send inhibitory signals to their postsynaptic neuronal circuits, which inhibit the downstream brainstem structures tonically. When excitatory inputs from different cortices and related thalamic areas reach the striatum, the activation of D1 neurons could facilitate movement via the direct pathway by inhibiting SNr neurons and disinhibiting brainstem domains, while the activation of D2 neurons would suppress

Figure 2.4.2 Cortico-basal ganglia circuits

- (A) The activity in each striatal domain (dorsomedial striatum (DMS), red; dorsocentral striatum (DCS), green; dorsolateral striatum (DLS), blue) is correlated with the activity of the cortical region below, showing topographical connectivity between striatum and cortex (adapted from (Peters et al., 2021)).
- (B) Topographical projection from different striatal regions (dorsomedial striatum (DMS), orange; dorsolateral striatum (DLS), cyan; ventrolateral striatum (VLS), magenta) into different regions of the SNr. These distinct SNr subregions also target different downstream targets in the medulla (adapted from (Lee et al., 2020)).
- (C) Different SNr neuron populations project to specific brainstem targets (illustrated by different colors). All of these neurons also generate axonal collaterals to the pedunculopontine nucleus (PPN), midbrain reticular formation (RF) and the motor and intralaminar thalamus. Excitatory inputs are shown by triangular terminals (STN), and inhibitory inputs are shown by blunt arrows (striatum and GPe). (adapted from (McElvain et al., 2021)).
- (D) Three PF subpopulations revealed by projections to different striatal regions. These three PF subpopulations have different input–output connectivity patterns with the cortex and the striatum, suggestive of distinct functional roles. (adapted from (Mandelbaum et al., 2019)).
- (E) The direct (expressing D1 receptor, upper panel) and indirect (expressing D2 receptor, lower panel) pathways of basal ganglia circuits. D1 SPNs project directly to the SNr, with minor collaterals to the GPe, whereas D2 SPNs terminate in the GPe. GPe neurons project to the striatum, the STN, the SNr, the cortex and the thalamus. The STN, which is also part of the indirect pathway, targets the GPe and SNr. It receives cortical input directly which is the hyperdirect pathway. (adapted from (Arber and Costa, 2022)).
- (F) Cortical neurons target distinct regions in the striatum topographically (left). A fine level of functional granularity exist in cortical neurons and recipient neurons in the striatum (right, where different colors indicate functional granularity), suggesting that cortical input is a major driver input to the building of striatal ensemble activity (adapted from (Arber and Costa, 2022)).
- (G) Dopaminergic neurons in the SNc and VTA exhibit divergent axonal projections and divergent functional properties (left). SNc neurons project mostly to the dorsal striatum (DS), whereas VTA neurons preferentially target the medial and ventral striatum (MS) as well as the cortex (middle). The gradient depicting the relative proportion of dopaminergic neurons in the VTA or SNc being recruited during reward or movement (right) (adapted from (Arber and Costa, 2022)).
- (H) Reconstruction of the axons of a single dopaminergic neuron in SNc shown in the medial, dorsal and frontal views inside the striatum. Red and blue lines in the striatum indicate the axon fibers located in different compartments of the striatum (adapted from (Matsuda et al., 2009)).

movement via the indirect pathway by inhibiting GPe, releasing STN to activate, exciting SNr and inhibiting brainstem domains (Hikosaka et al., 2000; Nambu, 2008) (Figure 2.4.2E). Interestingly, direct and indirect pathways arising from a common striatal source converge in SNr, suggesting that SNr synthesizes and relay separately processed information from the direct and indirect pathways to brainstem motor centers (Foster et al., 2021), but the signals from each pathway may not arrive at the same time due to multiple synaptic connections in the indirect pathway which allows the integration of additional information, and different electrophysiological properties between D1 and D2 neurons resulting in disparities in the timing of depolarization (Sippy et al., 2015). Moreover, both direct and indirect pathways in the striatum are active during movement (Cui et al., 2013), and even at single-neuron level, activities of D1 and D2 neurons show similar movement specificity (Klaus et al., 2017), suggesting the simultaneous involvement of direct and indirect pathways in motor control. Perturbing neuronal activities of either D1 or D2 neurons at different phases alters movements in distinct ways (Tecuapetla et al., 2016), supporting the necessity of the coordinated activity of direct and indirect pathways to regulate movement (Figure 2.4.2E). Hence, based on the pro- and antikinetic natures of direct and indirect pathways respectively, the basal ganglia circuits might work as a “gas and brake” system to steer an action to be performed precisely. This yin-and-yang system posits that it could either program motor behaviors in a dual-tread manner by promoting the desired movements while suppressing the unwanted ones, or differentially control distinct groups of muscles in the same movement, as any movement requires a sequence of simultaneous contraction and relaxation of different muscles. However, SPNs are often quiescent owing to their intrinsic membrane properties (Kreitzer and Malenka, 2008), so to drive basal ganglia circuits, striatum requires excitatory inputs, most of which arise from the

cortex (Huerta-Ocampo et al., 2014). Therefore, parallel cortico-striatal projections from motor, sensory and frontal cortices activate different domains of striatum to allow the execution of desired movements, and furthermore, to ensure the proper performance of the movements, direct and indirect pathways are recruited in parcellated basal ganglia circuits to coordinate downstream motor programs carefully and precisely (Figure 2.4.2E) (Foster et al., 2021; Klaus et al., 2019). Interestingly, insular cortex, ventral striatum, central amygdala and the paraventricular nucleus (pSTN) are assembled into a hierarchical system similar to cortico-basal ganglia organization, which controls the termination of feeding behavior according to the internal states of the animal, expanding the principles of circuits assembly from motion to emotion (Barbier et al., 2020).

How do cortico-striatal circuits program diverse behaviors? Although it has been a long-term argument whether nature or nurture determines brain functions, well-coordinated movements need to be developed postnatally to adapt to different environments and scenarios (Dominici et al., 2011), in agreement with the view that the neuronal circuits, as a *tabula rasa* or a blank slate, are shaped by learning (Markram et al., 2011). Cortico-striatal circuits provide an example to demonstrate such experience-dependent reorganization for learning new behaviors (Costa et al., 2004; Di Filippo et al., 2009; Koralek et al., 2012; Znamenskiy and Zador, 2013). Given that striatal neurons require substantial glutamatergic inputs to be activated (Kreitzer and Malenka, 2008) and simultaneous recordings from the cortex and striatum show that striatum faithfully inherits cortical activity (Peters et al., 2021), a postulation arises that cortical neurons encode a movement and transmit the pattern of activity to a group of striatal neurons, forming a movement-related ensemble (Figure 2.4.2F). Plasticity at cortico-striatal synapses observed both *in vitro* (Fino et al., 2005) and *in vivo* (Xiong et al.,

2015; Fisher et al., 2017) provide a possible mechanism for cortex to influence and consolidate a subset of striatal neurons. In addition to SPNs which are involved in the formation of movement-related ensemble (Klaus et al., 2017), GABAergic and cholinergic interneurons in striatum also receive direct cortical input and participate in cortico-striatal circuits to modify the activity of SPNs (Kreitzer and Malenka, 2008; English et al., 2012). Moreover, manipulating activities of cortico-striatal neurons biases the behavior choice (Znamenskiy and Zador, 2013), showing the necessity of cortico-striatal communications in performing the desired movement. Strikingly, cortico-striatal plasticity also contributes to abstract skill learning, where mice control the activity of motor cortex without physical movement to reach a goal in a neuroprosthetic task (Koralek et al., 2012). During the course of learning, specific patterns of activity in striatal neurons emerges which undergo dynamic reorganization at different phases of learning (Yin et al., 2009) as well as in the processes of learning new task (Barnes et al., 2005). Cortical and striatal circuits might contribute to different learning processes or phases thereof, as learning of gross limb movements is rapid which can be impaired by either cortical or striatal inactivation, whereas refinement for fine motor skills takes longer and is heavily relied on motor cortex (Lemke et al., 2019). These results suggest that the striatal ensembles encode correlated behaviors by incorporating information from cortex (Figure 2.4.2F). However, a recent study also demonstrates that the striatal neurons are able to code and to control learned skilled movements without the involvement of the cortex (Dhawale et al., 2021). It is likely that, once the motor program is encoded in striatal circuits, excitatory input, such as thalamus, and/or with the synergy of dopaminergic input, is capable of driving the striatal ensembles to allow the execution of a behavior. Together, these studies provide

a picture of cortical neurons driving the activity of striatal neurons to form behavior-related neuronal ensembles to control diverse movements (Figure 2.4.2F).

What is the pushing force for action execution? Animals, including humans, act on the basis of the immediate result and/or the accumulated experience, either to increase the probability of an outcome or to reduce it (Seymour et al., 2007). The establishment of the relationships between actions and rewards requires the modulation of neuronal activity and the long-lasting modifications of the efficacy of synaptic transmission. Cortico-striatal circuits are thought to be the center of reward-related learning which could lead to positive reinforcement and habituation in physiological conditions (Yin and Knowlton, 2006), or obsessive-compulsive disorder and addiction in pathological situations (Kreitzer and Malenka, 2008; Bobadilla et al., 2017). The striatum can be assigned to two systems on the basis of connectivity and functionality (Figure 2.4.2G). The dorsal and lateral striatum are preferentially innervated by associative and sensorimotor areas of the cortex and mainly participates to movement generation and learning (Di Filippo et al., 2009). They receive inputs from dopaminergic neurons in the substantia nigra pars compacta (SNc) which exhibit transient activity during movement initiation and modulate the vigor of upcoming movements (Figure 2.4.2G) (Panigrahi et al., 2015; Howe and Dombeck, 2016; Silva et al., 2018). On the other hand, the ventral striatum is primarily innervated by limbic cortical areas and plays a crucial role during reward (Di Filippo et al., 2009). It receives dopaminergic afferents from the ventral tegmental area (VTA) which encode mainly reward-prediction error (Figure 2.4.2G) (Panigrahi et al., 2015; Howe and Dombeck, 2016; Silva et al., 2018). Midbrain dopaminergic neurons contribute to the motor control and reward-related learning by modulating the excitability of SPNs and the plasticity of their cortical inputs (Reynolds and Wickens, 2002; Shen et al., 2008).

Unlike cortico-striatal projections with specific topographical organization, axons from single dopaminergic neuron broadly invade a large region of the striatum (Matsuda et al., 2009) (Figure 2.4.2H). In line with the anatomical feature, dopaminergic neurons convey generic information of whether and how a behavior should be performed, and coincident specific cortical projections select the appropriate ensembles of SPNs to allow the performance of the movements (Silva et al., 2018). Dopamine signals can also be modulated by cholinergic interneurons in striatum, showing the interaction of multiple neuromodulators in the control of movement and learning (Cragg, 2006; Maurice et al., 2015). Cholinergic interneurons target the distal dopamine axons to induce action potential firing and dopamine release in striatum, which might gate or enhance the dopamine signals (Liu et al., 2022). In the situation when dopaminergic neurons are impaired such as Parkinson disease, the balance between D1 and D2 neurons is altered and the movement-related striatal ensembles are changed which lead to motor deficit, suggesting the essential role of dopamine in modulating the cortico-striatal activity as well as the communication of striatum to downstream targets (Parker et al., 2018; Maltese et al., 2021). Moreover, patients with Parkinson disease not only exhibit motor malfunctions such as bradykinesia, rigidity and rest tremor, but are also associated with many non-motor symptoms, e.g. disorders of sleep–wake cycle regulation, cognitive impairment (including frontal executive dysfunction, memory retrieval deficits, dementia and hallucinosis), disorders of mood and emotion, autonomic dysfunction (mainly orthostatic hypotension, urogenital dysfunction, constipation and hyperhidrosis), and sensory symptoms (hyposmia and pain) (Poewe et al., 2017), implying the diverse functions of dopamine system beyond motor control.

2.4.3. Cortico-thalamo-cortical circuits

Cerebral cortex receives extensive inputs from numerous thalamic nuclei (Hunnicutt et al., 2014; Harris et al., 2019). Traditionally, thalamus is regarded as a relay station for receiving afferent input from sensory pathways and transmitting this information to cerebral cortex (Figure 2.4.3A). Thalamic nuclei receiving direct ascending input from sensory nuclei are defined as the first order thalamic relays which subsequently project to cortical regions innervating layer 4 neurons to establish a topographic representation of the external sensory world in primary sensory cortices (Figure 2.4.3A) (Sherman and Guillery, 2005). Although individual thalamo-cortical connections are relatively weak and unable to drive cortical activity alone, synchronous pattern of activity drives layer 4 neurons to fire reliably (Bruno and Sakmann, 2006; Wang et al., 2010). It is also reported that deep layer neurons in barrel cortex, can be driven directly by thalamic stimulation (Constantinople and Bruno, 2013). Other thalamic nuclei which do not receive sensory afferent input are regarded as high order thalamic relays with projections to sensory, motor and associate cortices (Figure 2.4.3B) (Hunnicutt et al., 2014). Unlike the stereotypical sensory thalamo-cortical projection to primary sensory cortices which mainly target layer 4, the other cortices display a diverse layer-preferential innervation from thalamus. For example, in primary whisker motor cortex, sensory related thalamic nuclei are more likely to project to layers 2/3 and upper layer 5, whereas the motor related thalamic nuclei project to lower layer 5 (Hunnicutt et al., 2014). Moreover, ventral medial (VM) thalamus provides biased projections to layer 1 in anterolateral motor cortex (ALM) and connects with apical tuft dendrites of layer 5 ET neurons which project back to VM (Guo et al., 2018). These observations suggest a diverse and complex nature of thalamo-cortical projections,

expanding the traditional view that thalamus as a simple relay station transmits sensory information from peripherals to the cerebral cortex.

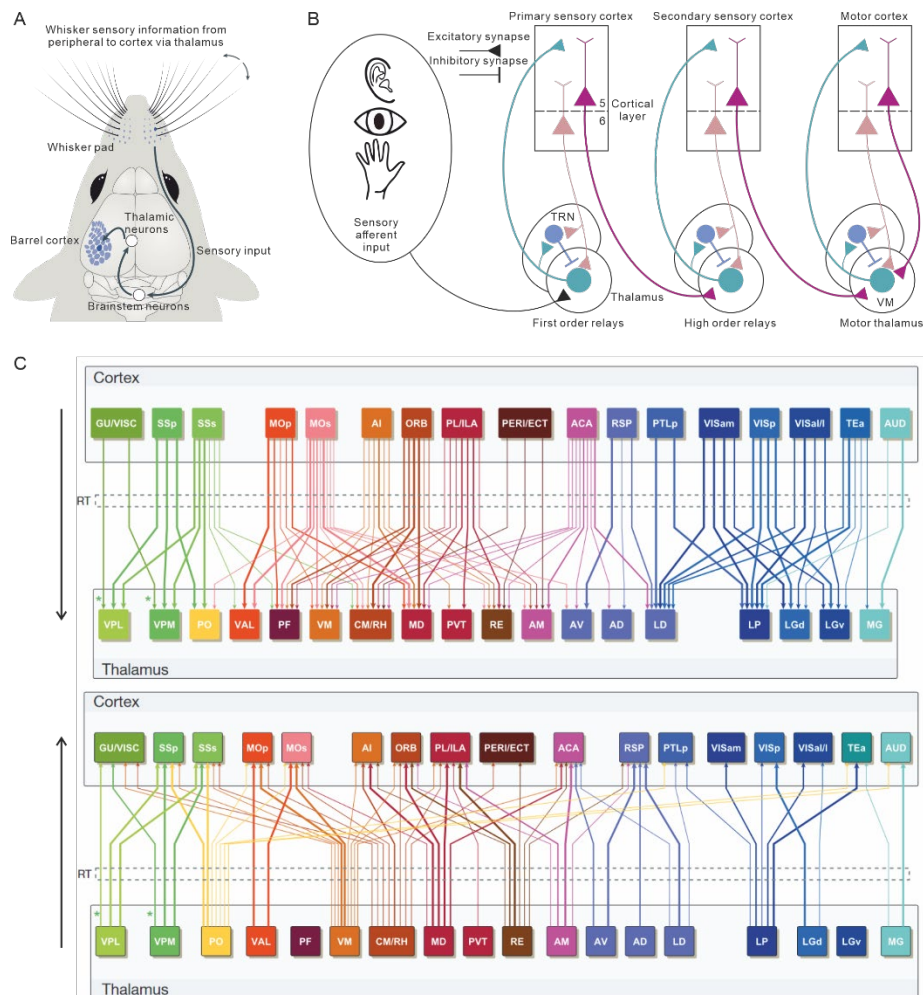


Figure 2.4.3 Cortico-thalamo-cortical circuits

- (A) Sensory input derived from whisking reaches brainstem neurons and thalamus which relays the neuronal signals to the barrel cortex (primary somatosensory cortex for whiskers). The barrel cortex is topographically organized into units corresponding to individual whiskers (adapted from (Petersen, 2019)).
- (B) Classic view of cortico-thalamic circuits. Sensory information from the periphery is relayed via first order thalamic nuclei to primary sensory cortex. Layer 6 CT cells provide feedback “modulator” input to sensory thalamus while also targeting TRN. Layer 5 ET neurons bypass TRN and provide strong “driver” input to higher order thalamus, which relays the signal to higher order cortex. The TRN provide inhibitory input to the thalamus. In motor-related thalamus, VM receives input from both layer 5 ET and layer 6 CT neurons, forming reciprocal loops involving between motor cortex and VM (adapted from (Collins and Anastasiades, 2019)).
- (C) Scheme showing connections between major cortical regions and thalamic nuclei (upper, cortex to thalamus; lower, thalamus to cortex). Colors indicating different cortical regions and their corresponding thalamic nuclei. See https://static-content.springer.com/esm/art%3A10.1038%2Fnature13186/MediaObjects/41586_2014_BFnature13186_MOESM69_ESM.xlsx for the full name of each region (adapted from (Oh et al., 2014)).

Thalamic nuclei not only project to cerebral cortex but also receive separate cortical inputs from different cortical regions through cortico-thalamic projections (Oh et al., 2014; Harris et al., 2019; Huo et al., 2020). For example, PF is not only embedded in cortico-basal ganglia circuits with input from SNr and output to cortex (Foster et al., 2021; Wang et al., 2021), but also innervated by topographical cortical inputs, such as the medial PF preferentially targeted by prefrontal cortex, the central PF innervated by motor cortex and the lateral PF receiving somatosensory cortex axons (Mandelbaum et al., 2019). Cortico-thalamic projection is mediated by a subset of layer 5 ET neurons as well as layer 6 CT neurons (Sherman and Guillery, 2005; BRAIN Initiative Cell Census Network (BICCN), 2021). A classic view suggests that layer 5 ET neurons provide “driver” (thick axon with large synaptic boutons) input to higher order thalamic nuclei, so as to relay information from first order to high order thalamic nuclei, while layer 6 CT neurons provide “modulator” (thin axons and small synapses) input to the same thalamic nucleus where the thalamo-cortical projections come from as well as the thalamic reticular nucleus (TRN, the main inhibitory resource in thalamus), which therefore provide feedback projections to the thalamus (Figure 2.4.3B) (Guillery and Sherman, 2002; Collins and Anastasiades, 2019). Accordingly, it posits that the innervation patterns of cortical layer 5 and 6 neurons are different. However, recent advances with transgenic mice and viral tracing approaches to systematically investigate the cortical and thalamic connectivity show similar cortico-thalamic projection patterns from layer 5 and layer 6 neurons to thalamic nuclei (Harris et al., 2019). As both cortico-thalamic and thalamo-cortical neurons are excitatory, the cortico-thalamo-cortical circuits are considered as a recurrent excitatory system (Figure 2.4.3B). Indeed, *in vivo* electrophysiological recordings and optogenetic perturbation on both cortex and thalamus show that the maintenance of persistent activity in those

two structures require bidirectional connectivity between cortex and thalamus, which is important for the preparation of voluntary movement (Guo et al., 2017). In the cortico-thalamo-cortical circuits, thalamo-cortical projections might play a more important role, because inhibition of cortex only reduce the activity of thalamus but does not affect the thalamic response to signal (Inagaki et al., 2022), while proper cortical activity relies on thalamic input as inactivating the thalamus perturbs cortical activity and disrupts forelimb movements (Sauerbrei et al., 2020). Clinically, patients with persistent vegetative state are linked to thalamic abnormality (Adams et al., 2000) and the restoration of thalamo-cortical connectivity is related to the recovery from persistent vegetative state (Laureys et al., 2000), suggesting a pivotal role of the thalamo-cortical system to keep the proper excitability of the brain.

However, simple reciprocal cortico-thalamo-cortical loops would lead to uncontrolled oscillations in the cortex and thalamus. Recent studies with systematic anatomical tracing show that the cortico-thalamo-cortical circuits are not organized in a point-to-point fashion forming simple loops; rather, different cortical regions and multiple thalamic nuclei are interconnected, revealing a complicated network of cortico-thalamo-cortical circuits with a hierarchical organization (Figure 2.4.3C) (Oh et al., 2014; Harris et al., 2019). This observation fits with the “no-strong-loops” hypothesis proposed to explain the proper function of the cortico-thalamo-cortical circuits while avoiding over-excitation (Crick and Koch, 1998), which suggests nontrivial ways for information processing between cortex and thalamus. Moreover, layer 6 CT neurons send collaterals to the TRN (Figure 2.4.3B), the main inhibitory domain in thalamus, which play a dual role in inhibiting and facilitating the cortico-thalamo-cortical circuits (Crandall et al., 2015; Takata, 2020) and are suggested to be involved in gain control (Olsen et al., 2012). Interestingly, molecular and

electrophysiological distinct populations of inhibitory neurons, sitting at different subdomains of TRN, participate into separated thalamic subnetworks (Lam and Sherman, 2015; Li et al., 2020; Martinez-Garcia et al., 2020). Together, these data reveal the existence of a complex interaction between cortex and thalamus. Future works deciphering the cortico-thalamo-cortical circuits to understand the computational mechanisms require detailed specificity of thalamic neurons spanning molecular identities, anatomical features and functional properties.

2.4.4. Cortico-brainstem and cortico-spinal circuits

In the end, to perform a behavior, all movement-related information needs to be transmitted to regions for motor execution, including the brainstem and spinal cord. Although spinal cord is not able to initiate movements alone, as complete spinal cord injury leads to inability to move muscles controlled by spinal segments below the lesion, despite the presence of the functional circuits in the spinal cord, neuronal circuits in brainstem provide basic input to drive spinal cord to work. A striking example comes from a loss of function experiment in decerebrate rats which were subjected to the removal of the whole brain structures except medulla, and those rats were still able to produce irregular and fragmented movements (Berridge, 1989). Indeed, some neuronal circuits in brainstem and spinal cord, known as central pattern generators, are the corner stones to construct stereotypical patterns of movement including locomotion, respiration and orofacial movement (Figure 2.4.4A) (Goulding, 2009; Smith et al., 2013; Moore et al., 2014; Ruder and Arber, 2019). However, an well-coordinated behavior requires a sequence of orchestrated muscle activities with real-time sensory update for timely adjustment of movement, which cannot be achieved by brainstem and spinal cord individually; rather, it requires multiple descending pathways to command different parameters of the action (Figure 2.4.4A) (Lemon, 2008).

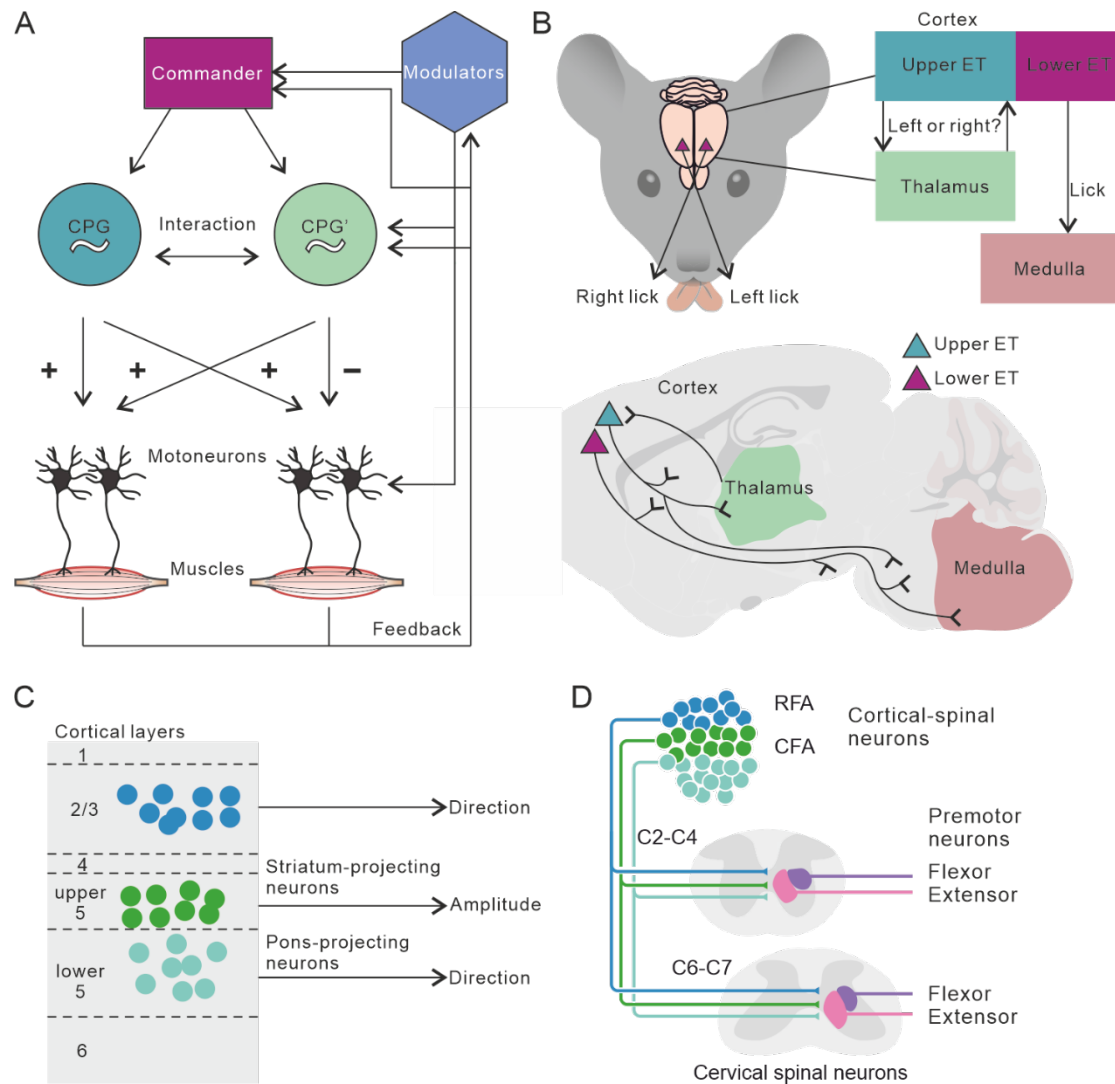


Figure 2.4.4 Cortico-brainstem and cortico-spinal circuits

- (A) Scheme of a proposed model for execution of different movements. CPGs bear stereotypical motor programs with direct or indirect innervation with motor neurons to coordinate muscle activity. CPGs interact and coordinate with each other. Command and modulation systems arbitrate the execution and parameters of different movements by gating or selecting separate CPGs. Peripheral feedback ensures the appropriate performance and provide motor error signals to improve the motor programs (modified based on (Moore et al., 2014)).
- (B) Cortical neurons influence the directional bias of licking in a delayed discrimination task. Upper ET neurons and thalamic neurons form reciprocal connections during delay period, while activity of lower ET neurons signal contralateral licking. Lower ET neurons send axons to medulla but avoid thalamus, whereas Upper ET neurons terminate axonal projections rostral to medulla (Li et al., 2015; Inagaki et al., 2022).
- (C) Layer 2/3 and pons-projecting cortical neurons are tuned to direction of forelimb movement while striatum-projecting cortical neurons represent amplitude (Galiñanes et al., 2018; Park et al., 2022).
- (D) Cortico-spinal neurons located in different cortical regions (rostral forelimb area (RFA), caudal forelimb area (CFA)) terminate in different dorso-ventral domains of the cervical spinal cord and exhibit different recruitment profiles during skilled forelimb behaviors. Axon terminals of different cortical neurons are matched with a positional matrix of premotor neurons in the spinal cord, where extensor premotor neurons are located more medially and flexor premotor neurons are located more laterally (Wang et al., 2017).

In spite of the essential roles of many brain regions in motor control, the necessity of motor cortex is controversial, as chronic lesions on cortex in rodents do not show obvious movement deficit but only impair motor learning (Kawai et al., 2015). However, even though in rodents the motor cortex appears to be dispensable for the performance of movement, it is crucial in primate. Motor cortex or cortical tract lesions on non-human primates (Friel et al., 2007; Lemon et al., 2012; Murata et al., 2008; Zaaime et al., 2012) and humans such as stroke patients (Lang and Schieber, 2004; Brown, 2006; Jones and Adkins, 2015) lead to movement impairment. The critical contribution of cerebral cortex on motor control in non-human primates and humans, might be owing to the monosynaptic projections in primates from motor cortex to motor neurons controlling distal limb muscles, which seems to have evolved for dexterous and fractionated digit movements (Heffner and Masterton, 1975; Kuypers, 1982; Nakajima et al., 2000; Rathelot and Strick, 2006, 2009). In mice, cortical connections to motor neurons are established at early postnatal stage, which are subsequently eliminated during later developmental stages, and strikingly, mice that maintain the monosynaptic connections from cortex to motor neurons in adulthood have been suggested to exhibit superior manual dexterity than normal mice (Gu et al., 2017). Moreover, acute inactivation of motor cortex in rodents disrupts forelimb behavior execution (Otchy et al., 2015). These results argue for the crucial role of motor cortex in motor control even for rodents.

Many studies have emerged to illustrate the properties of cortical populations on the basis of their projections targets. Orofacial movements have attracted much attention to reveal the functions of cortical subtypes. Cortical areas controlling orofacial movement communicate with brainstem premotor neurons via distinct pathways to regulate motor neurons involved in different aspects of orofacial behavior (Mercer

Lindsay et al., 2019). In areas controlling the tongue movement, including anterior lateral motor cortex (ALM) and tongue/jaw motor cortex (tjM1), the neuronal activity ramps up before the onset of tongue movement and is necessary for contralateral licking (Figure 2.4.4B) (Li et al., 2015; Mayrhofer et al., 2019). More specifically, medulla projecting neurons in ALM are necessary to initiate movements as silencing this population is enough to occlude licking, whereas cortico-thalamic projections convey neuronal activity at preparatory stage before movement onset (Figure 2.4.4B) (Inagaki et al., 2022). Together, these studies on orofacial movements put forward a model in which the medulla projecting cortical neurons accumulate information from the cortical region and broadcast the signal to brainstem [which can also be regarded as the “spinal cord” for orofacial movement owing to the presence of both premotor and motor neurons controlling orofacial muscles (Takato et al., 2021)] for motor execution (Figure 2.4.4B). This postulation fits with the morphological properties of layer 5 ET neurons and the canonical organization of cortical microcircuit discussed above (Figure 2.3.1A).

However, studies on cortical connections to brainstem regions involved in the regulation of forelimb movements are limited, despite the important role of the medulla in the control of different aspects of skilled forelimb movement including reaching and handling (Esposito et al., 2014; Ruder et al., 2021). While cortical silencing interrupts forelimb movements, it is not clear if the contribution comes from cortico-brainstem neurons (Guo et al., 2015). Some efforts have been taken to record the neuronal activity of cortico-brainstem neurons to elucidate the functional tuning properties in forelimb movement. For example, comparing the activity of striatum-projecting and pons-projecting neurons reveals functional tuning to different parameters of forelimb movement, where striatum-projecting neurons preferentially represent amplitude while

pons-projecting neurons are biased to direction (Figure 2.4.4C) (Park et al., 2022). It is also reported that layer 2/3 neurons display activity tuned to directional selectivity during forelimb reaching (Figure 2.4.4C) (Galiñanes et al., 2018). Further studies with higher granularity might reveal more detailed tuning features of cortical projection neurons as striatum-projection neurons contains both IT and ET neurons, pons-projecting neurons can be further divided into thalamus-projecting ET neurons and medulla-projecting ET neurons, and even more subtypes exist in all of those populations (Economo et al., 2018; BRAIN Initiative Cell Census Network (BICCN), 2021).

Compared to cortico-brainstem projections, cortico-spinal projections have been intensively studied in the context of forelimb movement control. In a study screening molecular defined spinal interneuron subtypes with transgenic mice to determine the preference of cortical input, some of the subtypes receive inputs from both motor and sensory cortices while some receive biased input from one cortical area (Ueno et al., 2018). Specifically silencing the motor recipient subpopulation in spinal cord leads to deficits in skilled reaching while inhibition of the sensory recipient subpopulation causes deficits in food pellet release (Ueno et al., 2018). Moreover, cortical neurons in different regions contact different spinal segments and laminae, such that the axons from caudal cortex terminate at rostral cervical segments and at the dorsal lamina which host extensor interneurons, while those from rostral cortex innervate throughout the rostral to caudal cervical segments and shift ventrally targeting flexor interneurons (Figure 2.4.4D) (Wang et al., 2017). In line with the axonal segregation, ablation of rostral and caudal cortico-spinal neurons cause impairment of food pallet reaching and retrieval, respectively (Figure 2.4.4D) (Wang et al., 2017). The specificity of cortico-spinal innervation might come from differential developmental programs

which undergo axonal retraction after birth (Sahni et al., 2021a, 2021b). In addition to spinal cord, the cortico-spinal neurons also send collaterals to other brain regions. A recent study shows that synaptic connections from cortico-spinal neurons to the striatum are stronger on D1 neurons than that on D2 neurons (Nelson et al., 2021), suggesting that the cortico-spinal neurons recruit direct and indirect pathways of basal ganglia circuits differently.

In sum, although evidence is accumulated on cortico-brainstem and cortico-spinal neurons, knowledge about how the cortex influences the brainstem neuronal circuits is still limited, partially due to the technical difficulties to access the circuits. It will be particularly informative to locate the specific cortico-brainstem pathways for forelimb movement and to reveal the contribution of cortical inputs to the downstream circuits in the construction of movements. Further work will reveal how cortical inputs modulate the movements in a real-time manner and how they shape and reorganize the neuronal circuits in learning of new movements or recovering from injury and stroke. With the intention to approach these questions, the central aim of this dissertation is to elucidate the organization and function of cortical control on brainstem circuits for forelimb movement.

3. Fine-grained structural and functional map for forelimb movement phases between cortex and medulla

Wuzhou Yang^{1,2}, Harsh Kanodia^{1,2} and Silvia Arber^{1,2,3}

¹ Biozentrum, Department of Cell Biology, University of Basel,
4056 Basel, Switzerland

² Friedrich Miescher Institute for Biomedical Research
4058 Basel, Switzerland

³ lead contact

Correspondence to S.A.
silvia.arber@unibas.ch

3.1. Abstract

The cortex influences movement by its widespread projections to many nervous system regions using top-down control. Skilled forelimb movements require brainstem circuitry in the medulla, yet how cortex communicates with these modules remains unexplored. Here we reveal a fine-grained anatomical and functional map between anterior cortex (AC) and medulla in mice. Distinct cortical regions generate three-dimensional synaptic columns tiling the lateral medulla, topographically matching the dorso-ventral positions of postsynaptic neurons tuned to distinct forelimb action phases. While medial AC (MAC) terminates ventrally, connects to forelimb-reaching tuned neurons and its silencing impairs reaching, lateral AC (LAC) influences dorsally positioned neurons tuned to food handling, and its silencing impairs handling. Cortico-medullary neurons also extend collaterals to other subcortical structures through a segregated channel interaction logic. Our findings reveal precise alignment between cortical location, its function, and specific forelimb-action tuned medulla neurons, thereby clarifying interaction principles between these two key structures and beyond.

3.2. Introduction

Motor cortex is the evolutionarily most recent addition to the motor system and influences many regions of the central nervous system (Lemon, 2008). It projects to diverse regions of the motor system processing information relevant to execution and learning of movements. These include well studied forebrain regions, most notably basal ganglia and thalamus, and structures much closer to motor output, in particular the spinal cord and the brainstem. Uncovering organizational principles of how the motor cortex interacts with different processing stations in the hierarchy of the motor system is of key importance to understand its function.

Although motor cortex is often referred to as a coherent unit, multiple dimensions of anatomical and functional diversity exist. As recent work in the motor cortex revealed, cortical cellular diversity is defined by many parameters including neuronal morphology, molecular, genetic and epigenetic traits, developmental programs as well as electrophysiological properties (BRAIN Initiative Cell Census Network (BICCN), 2021; Di Bella et al., 2021; Winnubst et al., 2019). Ultimately, communication and function of cortical neurons is defined by their integration into circuits with specific synaptic input and output patterns. A classical way to probe cortical output potential has been to monitor behavioral patterns elicited by microstimulation of cortical regions. With specificity according to targeted cortical regions, these experiments revealed the generation of movement of different body parts, or of goal-directed movements upon longer stimulation trains (Ferezou et al., 2007; Graziano et al., 2002; Tennant et al., 2011; Wang et al., 2017). In line with these data and based on recording and perturbation experiments, a cortical map with assignment of functions is beginning to emerge in mice (Figure 3.2.1), including control of forelimbs (Economo et al., 2018; Guo et al., 2015; Mathis et al., 2017; Morandell and

Huber, 2017; Peters et al., 2017; Tennant et al., 2011), whiskers (Matyas et al., 2010; Sreenivasan et al., 2015) and tongue-jaw (Li et al., 2015; Mayrhofer et al., 2019; Mercer Lindsay et al., 2019). Described roles include learning (Kawai et al., 2015; Peters et al., 2014, 2017; Wang et al., 2017), decision making and movement preparation (Li et al., 2015) as well as precision and adjustments of flexible movements (Bollu et al., 2021; Heindorf et al., 2018; Lemke et al., 2019). Strikingly, striatal neurons inherit information from the cortex in precise topography, as shown by both anatomical mapping (Alexander et al., 1986; Hintiryan et al., 2016) and electrophysiological recordings in behaving mice, with parallel encoding of rich behavioral parameters by cortical and striatal neurons (Peters et al., 2021). Together, these findings suggest a modular cortical organization with communication specificity to subcortical structures. Therefore, unraveling the principles guiding the organization and function of cortical channels to subcortical neurons central to the orchestration of movement is essential to understand how cortical cell types influence execution and learning of movements. Answering these questions will be particularly informative close to the execution of motor programs, most notably the brainstem and the spinal cord, where movement-relevant information is translated into action.

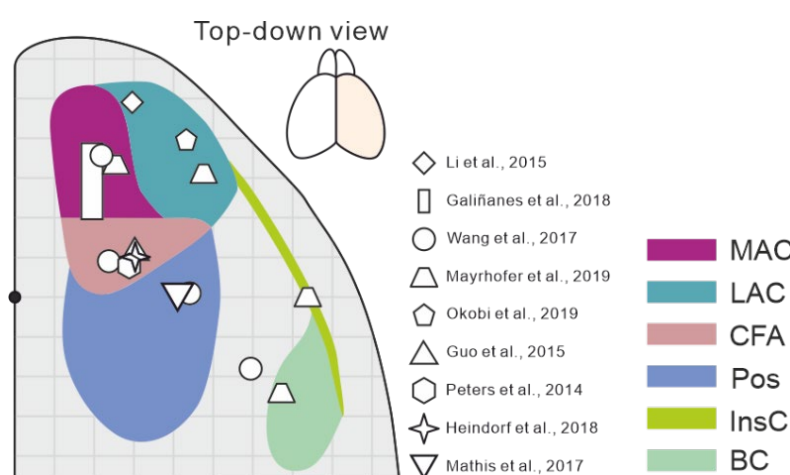


Figure 3.2.1 Scheme summarizing the cortical regions with different motor functions

Scheme summarizing the cortical regions related to forelimb, whisker and orofacial movement from different previous studies. Respective references can be found in the reference list

Skilled forelimb movement is well-suited to address these questions since it requires voluntary control mechanisms to generate precisely timed sequences of muscle activations with different phases, is evolutionarily conserved, and involves cooperation across many nervous system regions including the cortex (Hyland and Jordan, 1997; Iwaniuk and Whishaw, 2000; Yakovenko et al., 2011). A forelimb behavior evolutionarily conserved across species is reaching for and handling food (Iwaniuk and Whishaw, 2000). This behavior consists of timely transport of the hand to the food location through forelimb reaching, food grasping, the retraction of the hand to bring the food close to the mouth, and food manipulation before and during consumption. Recent work in mice provides evidence that neuronal circuits in the most caudal part of the brainstem i.e. the medulla play an important role in the control of different aspects of skilled forelimb movement including reaching and handling (Esposito et al., 2014; Ruder et al., 2021). Experiments in macaque monkeys in which descending cortical axons were cut at mid-brainstem levels, leaving parts of the medulla and all of the spinal cord devoid of cortical input, resulted in profound defects in forelimb movements without affecting posture, locomotion and other forms of body movement (Lemon et al., 2012). Similar defects were also observed upon lateral but not medial descending brainstem pathway lesions (Lemon et al., 2012). The combined findings of these lesion experiments and the identification of medullary circuits involved in skilled forelimb movement in mice (Esposito et al., 2014; Ruder et al., 2021) raise the possibility that cortical input to the lateral medulla might contribute to the control of forelimb movement. Thus, pairing the use of forelimb-based food retrieval as motor behavioral model system on the one hand, with probing circuit interactions between cortex and forelimb-regulating medullary circuits on the other hand, represents a perfect opportunity to elucidate principles of functional organization involving cortex.

The cortex communicates with subcortical structures through two classes of projection neurons. While intratelencephalic (IT) neurons do not extend axons beyond the telencephalon, extratelencephalic (ET) neurons also establish projections to targets outside the telencephalon (BRAIN Initiative Cell Census Network (BICCN), 2021; Shepherd, 2013), and are thus relevant for the here-addressed question. In addition, recent work revealed the division of ET neurons into two populations (BRAIN Initiative Cell Census Network (BICCN), 2021; Economo et al., 2018): A medulla-projecting population, which is active during late phases of movement preparation aligned with movement initiation, execution and termination; and a thalamus-projecting population, which is active mostly during early preparatory time windows (Economo et al., 2018; Inagaki et al., 2022). Whether and how the medulla projecting population interacts with functionally distinct subpopulations in the medulla involved in forelimb movements, possibly breaking down the cortico-medullary functional interaction code, is currently unknown.

Focusing on neuronal substrates and interaction principles required to construct skilled forelimb movements in mice, here we systematically mapped communication topography between cortex and medulla. We found that anterior cortical input is the most prominent source and organized specifically into three-dimensional dorso-ventral synaptic columns within the lateral medulla. We define a medial cortical region essential for forelimb reaching and preferentially connected to reaching-tuned medulla neurons, as well as a lateral cortical region essential for food handling and connected to handling-tuned medulla neurons. We also find that the logic of anatomically segregated target innervation by different medulla-projecting cortical neurons extends to other subcortical motor structures by collateralization. Together, these findings reveal the precise anatomical and functional organization between different cortical

regions and matched postsynaptic neurons in the caudal brainstem, tuned to different phases of one carefully orchestrated behavior.

3.3. Results

3.3.1. Medulla projection neurons reside preferentially in anterior cortex

To determine the location of cortical neurons with projections to the medulla of adult mice, we used adeno-associated viruses (AAVs) with retrograde targeting potential (Tervo et al., 2016) expressing a nuclear tag marker protein (rAAV-nTag) (Figure 3.3.2A). We targeted the lateral rostral medulla (latRM), a region with established roles in the control of forelimb movement (Ruder et al., 2021). We compared the distribution of latRM cortical projection neurons to that of cortical neurons with projections to the cervical spinal cord, visualized by retrograde AAV injections at cervical levels C5-C7 (Figure 3.3.1, Figure 3.3.2A). As expected, cortical neurons retrogradely marked from the latRM or cervical spinal cord were confined to locations with strong bias contralateral to injection sites in cortical areas mostly implicated in sensory-motor functions (Figure 3.3.1, Figure 3.2.1, data not shown). Notably however, we observed organizational differences between the two types of projection neurons along both rostro-caudal and medio-lateral cortical axes (Figure 3.3.1).

We reconstructed the position of retrogradely-labeled contralateral cortical neuronal cell bodies, following a widely-used brain atlas with a numerical coordinate frame as reference (Paxinos and Franklin, 2007). These reconstructions revealed different cortical territories with respect to occupancy by latRM and cervical spinal cord projection neurons (Figure 3.3.2B). First, a caudal cortical domain was occupied predominantly by cervical projection neurons with only few latRM projection neurons. Second, both types of neurons were found in a rostral antero-medial region and a very lateral caudal domain (barrel cortex, BC). Third, a cortical region bridging the two intermingled territories, with most neurons laterally adjacent to the anterior-medial

cortical domain and extending into the insular cortex (InsC) was almost exclusively occupied by latRM- but not cervical spinal cord projection neurons. These data suggest that most cortical neurons with access to latRM reside in the anterior cortex. In addition, a segregation into a medial and lateral region occurs within the anterior cortex: medial anterior cortex (MAC) harbors neurons with projections to medulla and spinal cord while lateral anterior cortex (LAC) has privileged access to the medulla but not cervical spinal cord. Both of these domains are rostral to the classically defined caudal forelimb area (CFA) (Guo et al., 2015; Tennant et al., 2011).

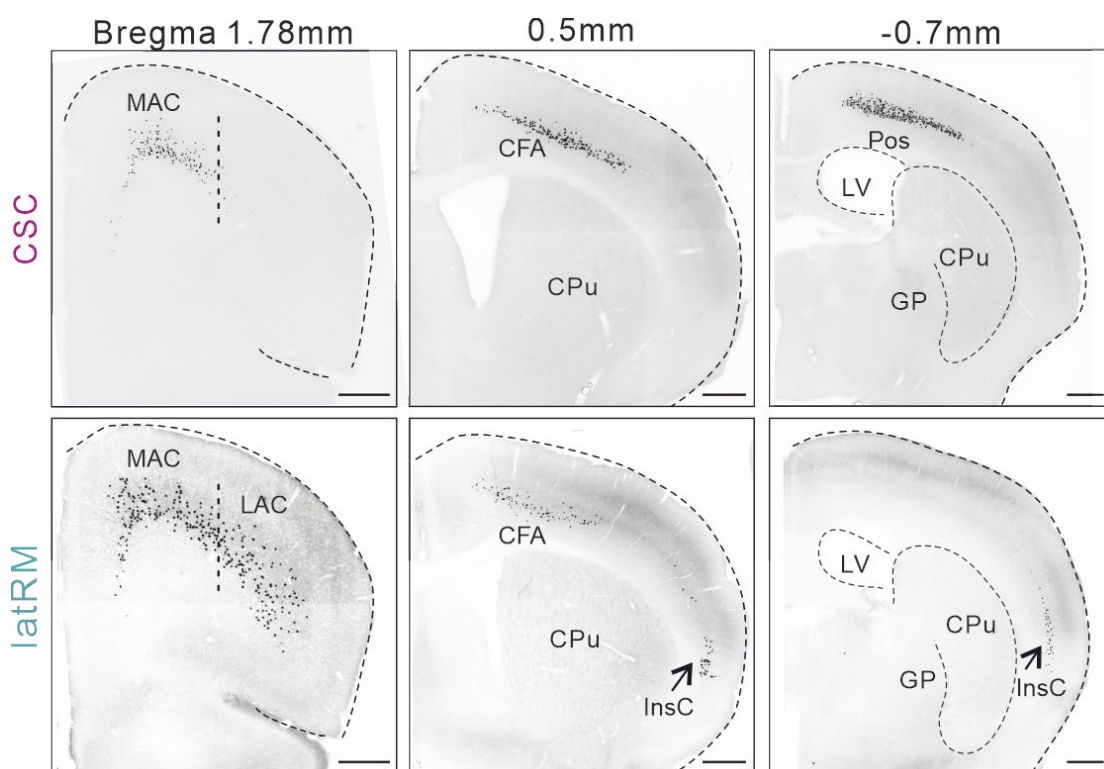


Figure 3.3.1 Distribution of medullary and spinal projection neurons in the cortex

Representative coronal sections at different rostro-caudal levels showing distribution of cortico-spinal and cortico-medullary neurons labeled by injection strategy shown in Figure 3.3.2A. Scale bar, 0.5mm.

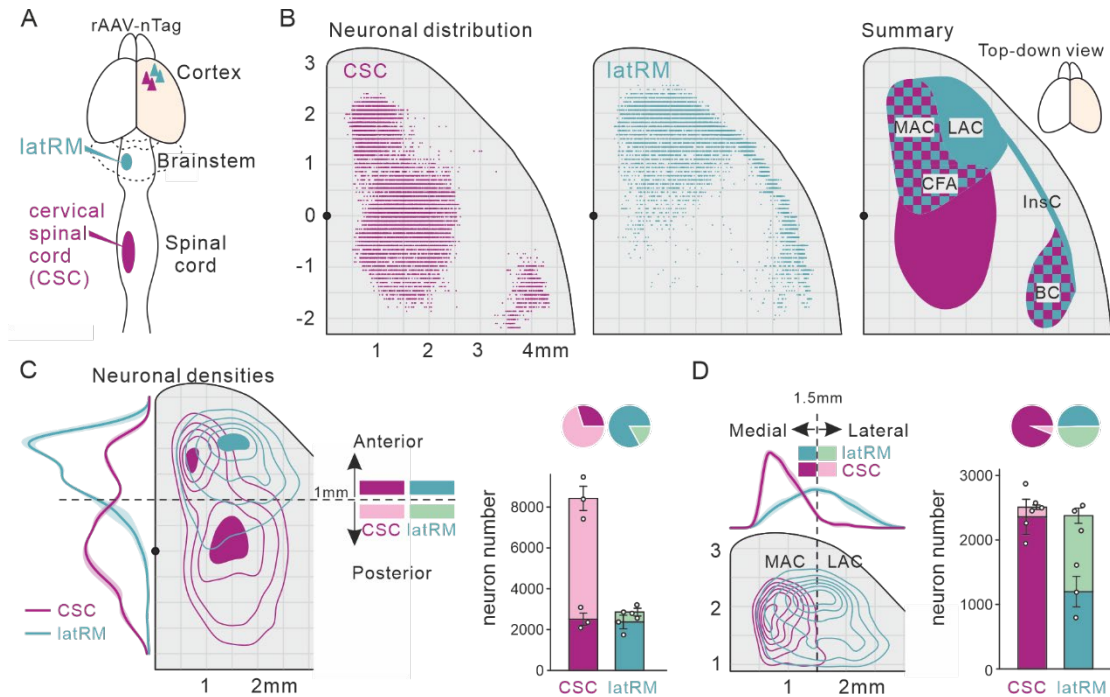


Figure 3.3.2 Medulla projection neurons reside preferentially in anterior cortex

- (A) Strategy for retrograde labeling of cortical neurons from lateral rostral medulla (latRM) and cervical spinal cord (CSC).
- (B) Neuronal distribution of cortico-CSC and cortico-latRM neurons (one example mouse each) from top-down view of cortex. The black marker on the midline indicates bregma. Right panel illustrates the exclusive or overlapping regions of the two neuronal populations shown in magenta (CSC) and cyan (latRM) respectively. MAC, medial anterior cortex; LAC, lateral anterior cortex; CFA, caudal forelimb area; InsC, insular cortex; BC, barrel cortex.
- (C) Density curves (left, mean \pm SEM) show averaged cell density of cortico-CSC and cortico-latRM neurons along the antero-posterior axis. The contour plots (middle) show the 2-dimensional (antero-posterior and medio-lateral) distribution of the respective projection neurons within sensory-motor cortical regions. The dashed line at 1mm anterior to bregma indicates the boundary of anterior (AC) and posterior (PC) cortex. Quantification of respective cell proportions and number (mean \pm SEM) in AC and PC for each cortical population (right; $n=3$ for each population).
- (D) Left panel: Averaged cell density of cortico-CSC and cortico-latRM neurons along the medio-lateral axis in AC is shown with density curves (top, mean \pm SEM). The 2-dimensional distribution of the averaged cell density of cortico-CSC and cortico-latRM neurons in AC is shown with a contour plot (bottom). The dashed line is 1.5mm lateral to the middle line which indicates the boundary of medial anterior (MAC) and lateral anterior (LAC) cortex in our study (see text for details). Right panel: Quantification of labeled cell proportions and numbers (mean \pm SEM) in MAC and LAC for each population ($n=3$ for each population).

To quantify these differences and more clearly delineate the observed domains, we plotted the density of neurons labelled using kernel density estimation (KDE), focusing on sensory-motor cortical regions (Figure 3.3.2C). This revealed an anterior and a posterior distribution center for cervical projection neurons (Figure 3.3.2C; relative to bregma; Anterior center: AP+1.8mm and ML+0.7mm; Posterior center: AP+0.3mm and ML+1.5mm), with the caudal center close to the previously described CFA (relative to bregma; AP+0.5mm and ML+1.5mm; Figure 3.2.1) (Guo et al., 2015; Tennant et al., 2011). In contrast, the peak of the distribution for latRM projection neurons was located laterally within the anterior cortex (Figure 3.3.2C; relative to bregma; AP+2mm and ML+1.5mm), due to the extension of these neurons into the lateral cortex. Most of the latRM projecting neurons ($84.3 \pm 3.7\%$; $n=3$; Figure 3.3.2E) were located rostral to +1mm from bregma, the reported anterior edge of CFA (Tennant et al., 2011). Henceforth, we refer to the domain anterior to this boundary as the anterior cortex (AC), while the cortical domain posterior to it is referred to as the posterior cortex (PC).

Within AC, the vast majority of cervical spinal projection neurons were located medial to +1.5mm relative to Bregma ($94.1 \pm 1.0\%$; $n=3$), whereas latRM projection neurons were distributed about equally medially and laterally to this boundary (medial: $49.7 \pm 3.3\%$ of AC latRM projecting neurons; Figure 3.3.2D). These results allow for the delineation of a medial anterior cortex (MAC) domain, in which neurons reside projecting to cervical spinal cord and/or latRM, and an adjacent lateral anterior cortex (LAC) domain, in which almost exclusively latRM projection neurons but very sparse spinal cord projection neurons reside (Figure 3.3.2D).

To contrast these AC domains communicating with subcortical regions implicated in the control of forelimb movements, we also determined the location of

cortical neurons with projections to the lumbar spinal cord, involved in the regulation of hindlimb movement. In agreement with previous work (Kamiyama et al., 2015), we found that these neurons were located very caudally within motor cortical territory (Figure 3.3.3; center relative to bregma at AP -1mm and ML+1.2mm), demonstrating a lack of overlap in cortical location between latRM and lumbar spinal cord projection neurons.

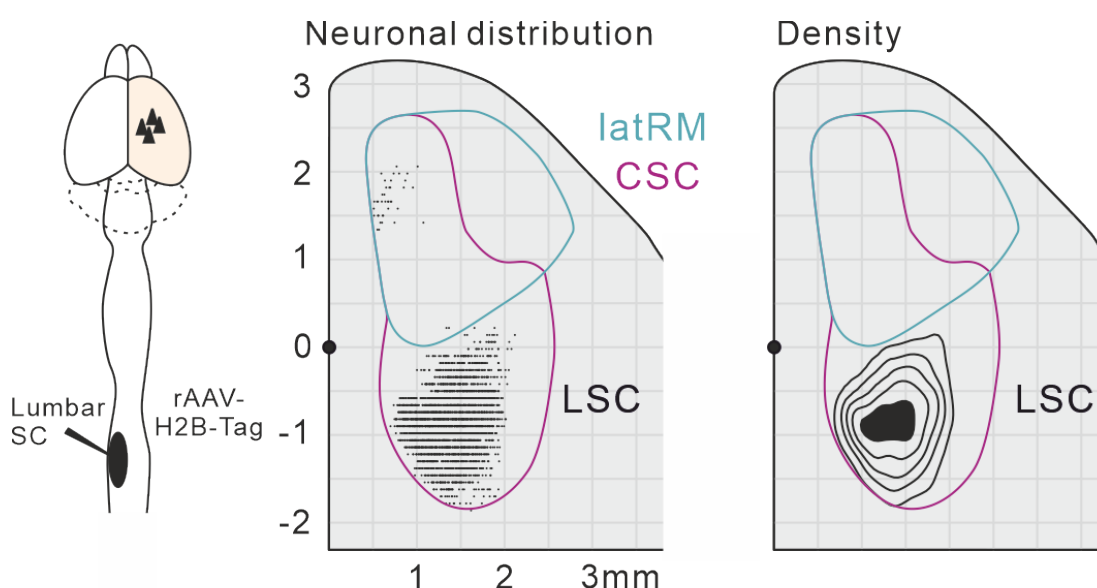


Figure 3.3.3 Distribution of lumbar spinal projection neurons in the cortex

Left panel: Strategy for retrograde labeling of lumbar spinal cord projecting cortical neurons. Middle panel: Representative example showing the neuronal distribution of cortico-lumbar neurons. Contour traces denote boundaries for cervical spinal cord (CSC) and latRM projecting neurons respectively. Right panel: 2D reconstruction of averaged neuronal density distribution of cortico-lumbar neurons ($n = 3$).

Together, our results demonstrate that cortical regions have differential access to latRM and the spinal cord. Cortical access to the latRM occurs preferentially from AC. Within this domain, cortical neurons with selective access to latRM but not to the spinal cord define the LAC, while MAC harbors both populations of cortical neurons (Figure 3.3.1, Figure 3.3.2D). These lateral anatomical characteristics extend into the InsC, which also does not contain spinal projection neurons. The delineation of these

cortical domains based on retrograde tracing raises the question of whether a more fine-grained spatial organization might exist for the communication between cortex and the medulla.

3.3.2. Cortex provides topographically organized synaptic input to latRM

We therefore next carried out systematic injections of AAVs into the cortex of adult wild-type mice (n=30), using our retrograde map as a guide to define cortical areas of interest. We injected a cocktail of Cre-conditional AAVs to express different marker proteins targeted to the cytosol (CytTag), the synapse (SynTag), and the nucleus (nTag) of infected neurons together with an AAV-Cre to induce their expression (Figure 3.3.4A). This approach visualized axonal projections, synaptic terminals, and cell bodies of infected neurons located in sensory-motor cortex and InsC covering the domains of interest defined by retrograde injections. Through visualizing the cytosolic tag (CytTag) in the medulla, we found that, as expected, descending cortical axons extended ipsilateral to injection, and most axon collaterals emerging in the medulla crossed the midline to shoot towards the contralateral side (data not shown). We restricted further analysis to the medulla contralateral to cortical injection.

We first determined the distribution of synaptic input to the medulla from the different cortical injection sites, detecting synaptic puncta based on SynTag immunofluorescence (Figure 3.3.5A). Focusing first on the facial motor nucleus (7N) level (bregma -6mm; Figure 3.3.5B), we compared synapse numbers across all cortical injection sites (Figure 3.3.4B, Figure 3.3.5C). We found that AC including MAC and LAC contributed the highest number of synaptic puncta (Figure 3.3.4B). Lower numbers were contributed by CFA and InsC, with the sparsest synaptic contribution from domains posterior to CFA (here referred to as Pos) (Figure 3.3.4B).

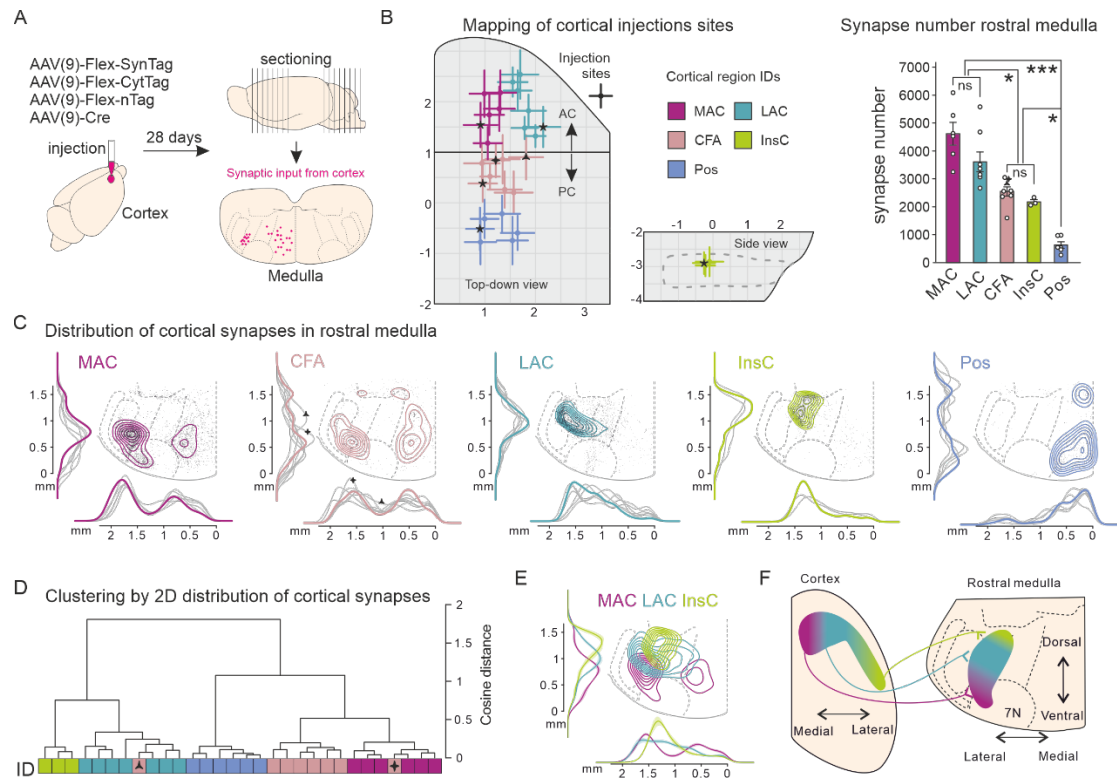


Figure 3.3.4 Cortex provides topographically organized synaptic input to latRM

- (A) Strategy for cortical injections to map cortico-medullary projections.
- (B) Left panel: Injection sites color-coded by cortical regions. Stars indicate the injection sites of examples shown in C. Right panel: Bar plot (mean \pm SEM) displaying number of synapses in rostral medulla from different cortical injection sites grouped as shown in the left panel. Triangle and diamond shapes indicate injection sites marked in C and D. MAC, $n = 6$; LAC, $n = 7$; CFA, $n = 8$; InsC, $n = 3$; Pos, $n = 6$. $*p < 0.05$; $***p < 0.001$; ns, not significant.
- (C) Distribution of cortical synaptic puncta and density in rostral medulla including dorso-ventral and medio-lateral densities from representative injections in different cortical regions. Colored curves show one example density distribution from each cortical region (injection sites indicated in B with stars), while the grey curves are dorso-ventral and medio-lateral densities from all other injection sites in the corresponding cortical regions. Triangle and diamond shapes in CFA plot indicate injection sites marked in B.
- (D) Clustering of the injection sites based on the spatial distribution patterns of cortical synapses in rostral medulla from all individual injection sites shown in B. Triangle and diamond shapes denote the injection site in B residing at the border between AC and PC.
- (E) Averaged synaptic densities of 2D distribution including dorso-ventral and medio-lateral densities (mean \pm SEM) from MAC, LAC and InsC in rostral medulla overlaid (MAC, $n = 6$; LAC, $n = 7$; InsC, $n = 3$).
- (F) Scheme summarizing the fine-grained map in latRM receiving synaptic input from cortex revealed by our work.

These cortical synaptic abundance differences were observed also at two more caudal medullary levels up to the hypoglossal motor nucleus (12N) level (Figure 3.3.5B-D). Together, these findings demonstrate that AC regions produce anatomically more pronounced synaptic input to the medulla than PC regions.

To determine which regions of the medulla are the main targets for synaptic input from the cortex, we analyzed data from all cortical injection sites for their synaptic distribution at the 7N level. We pooled injection sites according to the regions defined by retrograde infection (MAC, LAC, CFA, InsC and Pos) and mapped the 2D synaptic densities along medio-lateral and dorso-ventral axis (Figure 3.3.4C). We found that synaptic distributions from MAC and CFA exhibited a bimodal distribution along the medio-lateral axis, although MAC showed more pronounced synaptic terminations in the latRM. In contrast, synaptic output from LAC and InsC injections were biased laterally. Synaptic output from Pos injection sites, while generally sparse as described above, avoided latRM territory and instead was directed to the medially located gigantocellular nucleus region (Gi; Figure 3.3.4C). We confirmed these findings by calculating a laterality index to estimate the lateral bias of the synaptic distribution, demonstrating that indeed the four cortical regions with the most abundant synaptic contribution to the 7N level (MAC, LAC, CFA and InsC) also exhibited higher values in the laterality index (Figure 3.3.5E).

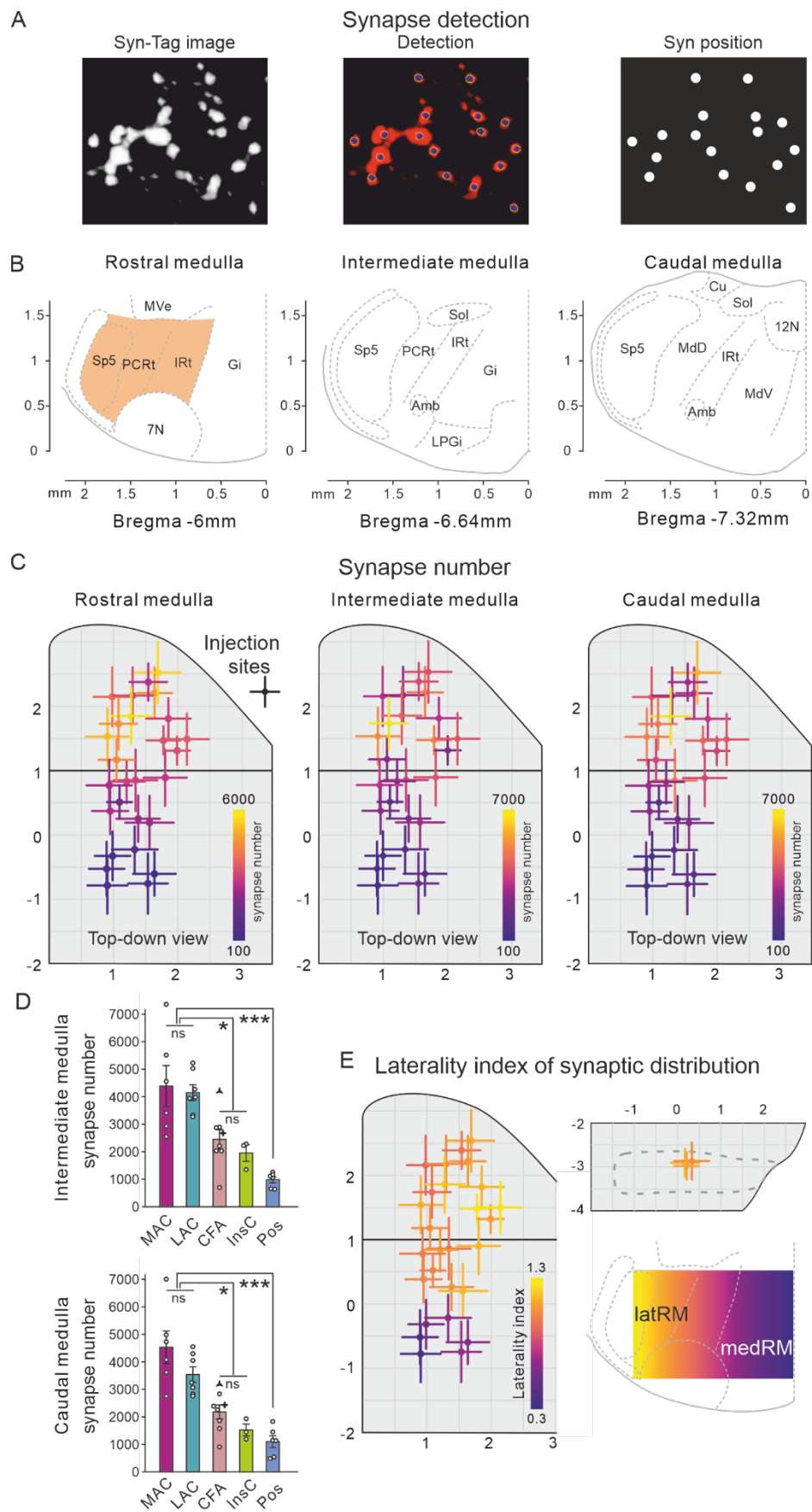


Figure 3.3.5 Anterior cortex targets lateral rostral medulla
Legend on next page.

In addition to the medio-lateral organization, we also observed a topographic organization of synaptic input along the dorso-ventral axis according to the source of its cortical origin (Figure 3.3.4C). MAC and CFA-derived synaptic input was directed to the most ventral region of the latRM, followed by a region with highest input from LAC and abutted by input from InsC most dorsally along the latRM axis (Figure 3.3.4C, E). These data demonstrate that the latRM is the main cortical synaptic target at the 7N level. Moreover, cortical input to the latRM is topographically arranged, with synaptic input from InsC, LAC and MAC tiling the latRM along its dorso-ventral axis (Figure 3.3.4C).

The synaptic distribution patterns for the injections within each cortical domain (MAC, LAC, CFA, InsC, and Pos) were markedly more correlated and similar to the other injections within the group as demonstrated by a hierarchical clustering dendrogram (Figure 3.3.4D). Strikingly, we found that different cortical injection sites from within the here defined anatomical boundaries clustered together, indicating that they share similar synaptic distribution patterns and confirmed the demarcation of these

Figure 3.3.5 Anterior cortex targets lateral rostral medulla

- (A) Representative example of synaptic terminal analysis with high-resolution imaging and Imaris spot detection.
- (B) Schematic showing the three medullary levels analyzed in this study as rostral, intermediate and caudal medulla, respectively according to (Franklin and Paxinos, 2007). Color-coded region is the area here referred to as lateral rostral medulla (latRM). Sp5, spinal trigeminal nucleus; PCRt, parvicellular reticular nucleus; IRt, intermediate reticular nucleus; 7N, facial nucleus; Gi, gigantocellular reticular nucleus; MVe, medial vestibular nucleus; Amb, ambiguus nucleus; Sol, solitary nucleus; LPGi, lateral paragigantocellular reticular nucleus; 12N, hypoglossal nucleus; MdV, medullary reticular nucleus, ventral part; MdD, medullary reticular nucleus, dorsal part; Cu, cuneate nucleus.
- (C) Synapse numbers in rostral, intermediate and caudal medulla from cortical injection sites shown in Figure 3.3.4B.
- (D) Number of synapses at corresponding medullary levels from cortical sites grouped as shown in Figure 3.3.4B (mean \pm SEM). Triangle and diamond shapes indicate injection sites marked in Figure 3.3.4B. MAC, $n = 6$; LAC, $n = 7$; CFA, $n = 8$; InsC, $n = 3$; Pos, $n = 6$. $*p < 0.05$; $***p < 0.001$; ns, not significant.
- (E) Laterality indices of the synaptic distributions from individual injection sites in the cortex and summary scheme (bottom right) depicting the high density of cortical synapses in the lateral (latRM)- as opposed to the medial (medRM) rostral medulla.

boundaries. There were two injection sites that did not obey the clustering hierarchy, which were however along the rostral edge of the CFA boundary invading MAC or LAC territory respectively, explaining the seeming discrepancy (Figure 3.3.4B, D). Together, these findings demonstrate that the majority of 7N medullary level cortical synapses are directed towards the lateral medulla and derived from AC including MAC, LAC and InsC. These synapses tile the lateral medulla along the dorso-ventral axis in a fine-grained map (Figure 3.3.4F).

3.3.3. Cortical input to medulla is organized in 3D rostro-caudal columns

To determine whether and how this revealed spatial organization so far detected at one rostro-caudal medulla level might generalize to the three-dimensional extent of the medulla, we next applied the same analysis to intermediate and caudal medulla levels (Figure 3.3.6A; Figure 3.3.5B). We chose the hypoglossal (12N) level as caudal medulla (bregma -7.32mm), and a level midway between these two positions as intermediate medulla (bregma -6.64mm) (Paxinos and Franklin, 2007) (Figure 3.3.5B). We found that the highest density of synaptic terminals derived from MAC was confined to ventral territory at both intermediate and caudal medulla levels (Figure 3.3.6A, B). In contrast, analysis of synaptic output from LAC revealed a termination zone dorsally adjacent to terminals from MAC, and analogous analysis of InsC synaptic output resulted in the most dorsal termination zone in sequence (Figure 3.3.6A, B). These findings were confirmed by analyzing the peak of highest synaptic density along the dorso-ventral axis across the three rostro-caudal levels, with each of the cortical groups peaking at a similar dorso-ventral level along the rostro-caudal medulla axis (Figure 3.3.6C).

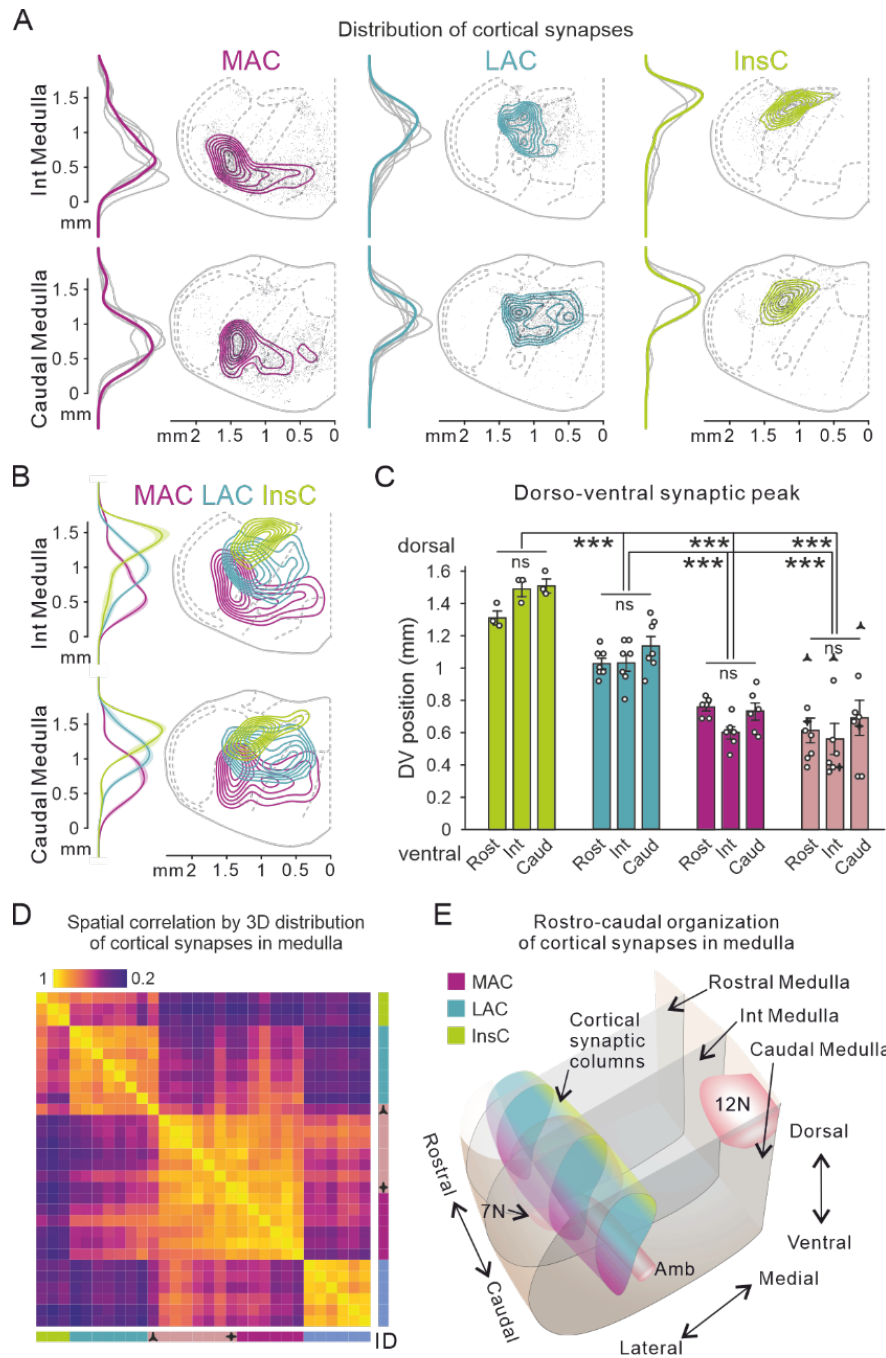


Figure 3.3.6 Cortical input to medulla is organized in 3D rostro-caudal columns

- (A) Distribution of cortical synaptic puncta and density at intermediate and caudal medulla levels from representative injections in MAC, LAC and InsC indicated in Figure 2B with stars, including density of neurons in the dorso-ventral axis. Grey curves are the respective density traces from other injection sites in the corresponding cortical regions.
- (B) Overlaid 2D distribution of averaged synaptic densities and average density along the dorso-ventral axis (mean \pm SEM) from MAC, LAC and InsC (MAC, $n = 6$; LAC, $n = 7$; InsC, $n = 3$).
- (C) Dorso-ventral position of peak of the distribution of synapses from MAC, LAC, InsC and CFA injections at the three analyzed medullary levels (mean \pm SEM). ** $p < 0.01$; *** $p < 0.001$; ns, not significant.
- (D) Spatial correlation analysis of the synaptic distribution patterns using the three analyzed medullary levels.
- (E) 3D scheme of cortical input to the rostro-caudal axis of the medulla.

We constructed a spatial similarity matrix of the different injection sites in the cortex combining information on the synaptic organization from all three medullary levels to obtain a 3D distribution of the synapses (Figure 3.3.6D). Indeed, this analysis showed that all injection sites fall into the groups assigned by retrograde tracing displaying higher correlation of synaptic distribution patterns within the group than across groups. Moreover, LAC and InsC as well as MAC and CFA are more correlated to each other, while Pos was the least correlated with all other groups (Figure 3.3.6D). We conclude that the synaptic output of MAC, LAC and InsC is directed to rostro-caudally arranged columns along the medullary dorso-ventral axis (Figure 3.3.6E), thus extending the logic of cortical synaptic organization within the medulla to a 3D configuration.

3.3.4. Individual cortical neurons form collaterals along the rostro-caudal medulla

We next asked whether these three-dimensional medullary cortical axon terminal columns are the product of individual cortical neurons each giving rise to several collateral branches and associated synapses along the rostro-caudal axis, or alternatively whether they represent a composite of arborizations each exhibiting only one restricted termination zone along the rostro-caudal axis. To address this question, we turned to the MouseLight project from the Janelia Research Campus (Winnubst et al., 2019). In this database, the axonal arborization of individual mouse brain neurons was reconstructed, including cortical neurons. We searched the available library for cortical neurons within the here-analyzed cortical territory with axons ramifications in the medulla and found both MAC (n=7) and LAC (n=6) neurons (Figure 3.3.7A, B; Figure 3.3.8). In agreement with our own overall tracing experiments (Figure 3.3.6E), we observed a differential dorso-ventral synaptic distribution of axon terminals within

the lateral medulla when separately grouping MAC and LAC neurons together (Figure 3.3.7C).

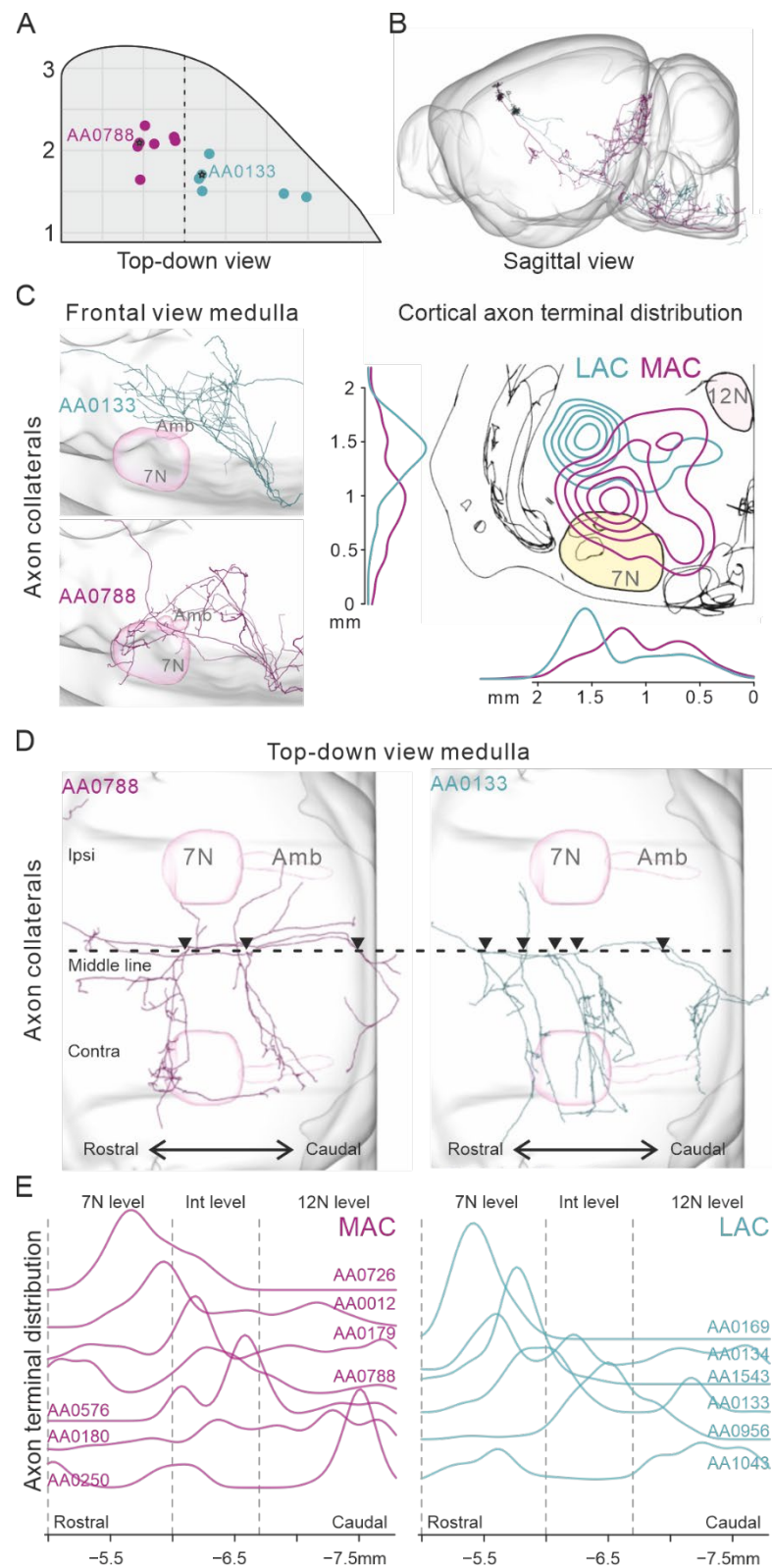


Figure 3.3.7 Individual cortical neurons form collaterals along the rostro-caudal medulla
Legend on next page.

Analysis along the rostro-caudal dimension showed that within the medulla, the main axon projected in the pyramidal tract ipsilateral to cortical cell body location, in agreement with our overall population analysis. We observed quite some variability at the level of individual neurons with respect to the extent of axonal arborization and presumptive associated synaptic boutons generated (Figure 3.3.8). However, collaterals from the parent axon generally branched off at multiple rostro-caudal levels, exhibiting proliferative axonal growth within the lateral medulla, with a preference for the side contralateral to cortical cell body location (Figure 3.3.7D, E; Figure 3.3.8). We visualized and quantified the distribution of axon terminals of all available neurons, plotted their density along the rostro-caudal axis in the medulla and observed that neurons generally had axon terminals distributed at multiple levels in the antero-posterior dimension (Figure 3.3.7E). This analysis demonstrates that while the sum of reconstructed axon terminals of individual cortical neurons never filled the entire rostro-caudal extent, individual MAC and LAC neurons generally synaptically contact the lateral medulla at multiple locations within the overall rostro-caudal medullary column. Together, our analysis demonstrates that cortical input to the medulla even at the single neuron level does not represent a simple point-to-point communication but rather follows a signaling mode with interactions in a three-dimensional volume at multiple locations of the medulla in a top-down manner.

Figure 3.3.7 Individual cortical neurons form collaterals along the rostro-caudal medulla

- (A) Schematic showing the soma location of neurons in the Mouselight database identified in the MAC and LAC (MAC: $n = 7$; LAC: $n = 6$). Neuronal morphology was mirrored when needed, so the somas are all displayed in the right hemisphere. Stars denote the two representative neurons shown in B, C and D.
- (B) Neuronal processes of one MAC and one LAC neuron marked with stars in A overlaid and shown in the sagittal view in 3D model.
- (C) Left: Frontal view of axons in the medulla from the two example neurons. Right: 2D, dorso-ventral and medio-lateral axon terminal distribution in the medulla shown in coronal view from all neurons in A.
- (D) Top-down view of axons in the medulla from the two examples neurons (triangles: axonal collaterals exiting from parent main axon at multiple rostro-caudal levels).
- (E) Rostro-caudal axonal terminal distribution of single cortical neurons in medulla.

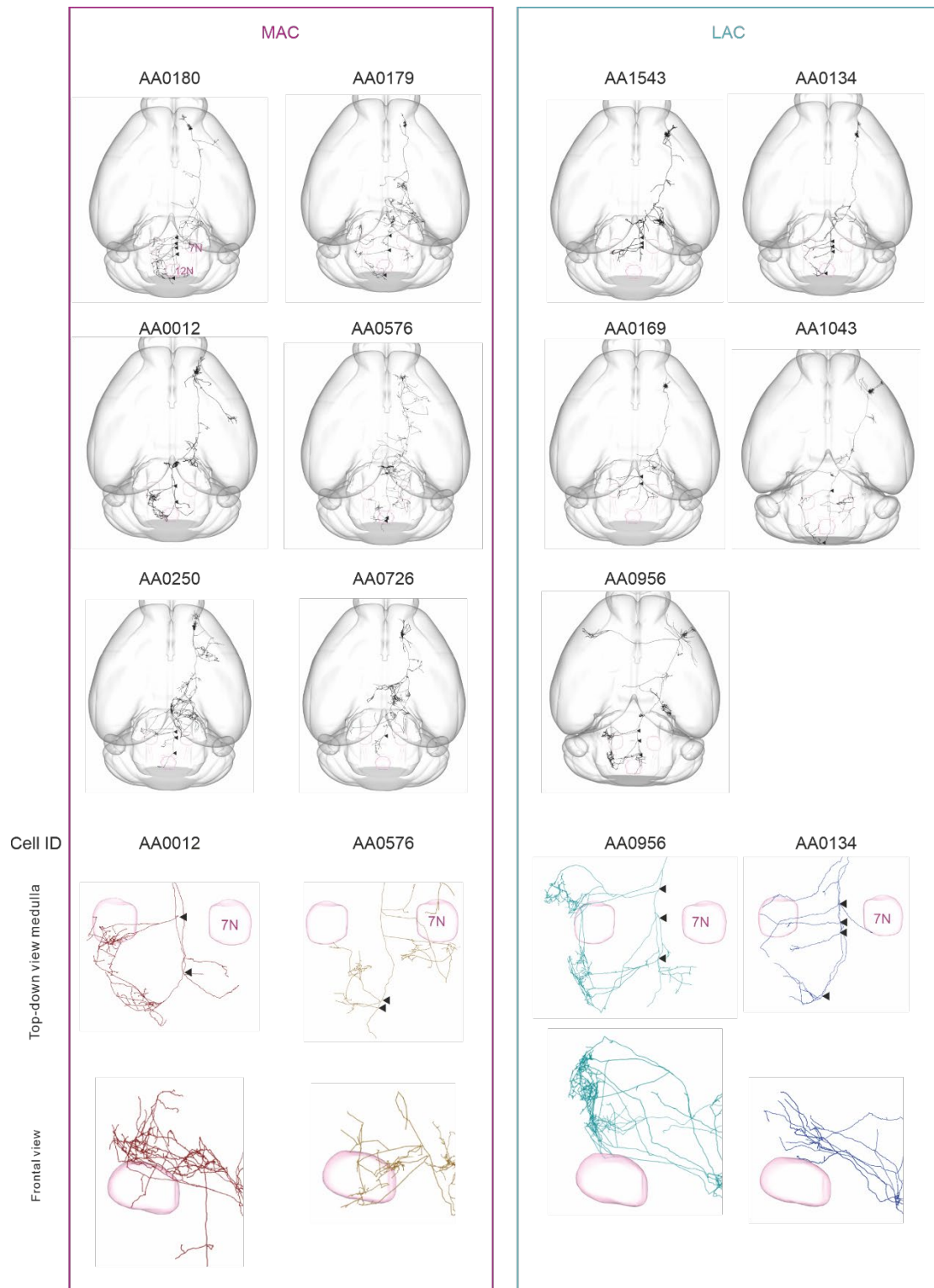


Figure 3.3.8 Single MAC and LAC neurons from Mouselight database

Upper panel: Top-down view of overall axonal processes from single MAC (magenta) and LAC (cyan) neurons.

Lower panel: Top-down (upper) and frontal view (lower) zoom-in views of axonal processes in the medulla from single cortical neurons at higher magnification.

3.3.5. Selective roles for MAC vs LAC in reaching vs handling

Given the striking difference in anatomical input organization from MAC and LAC to forelimb-regulating regions in the medulla respectively, we next set out to probe the function of these two cortical domains in forelimb control. We trained mice to perform a pellet reaching and food manipulation task, which we had previously shown to recruit specific latRM neurons in a task- and behavioral phase dependent manner (Ruder et al., 2021). We analyzed its two main phases, i.e. the food retrieval phase comprised of a directed forelimb reaching and retrieval action, as well as the consummatory phase during which mice handle the food pellet while eating.

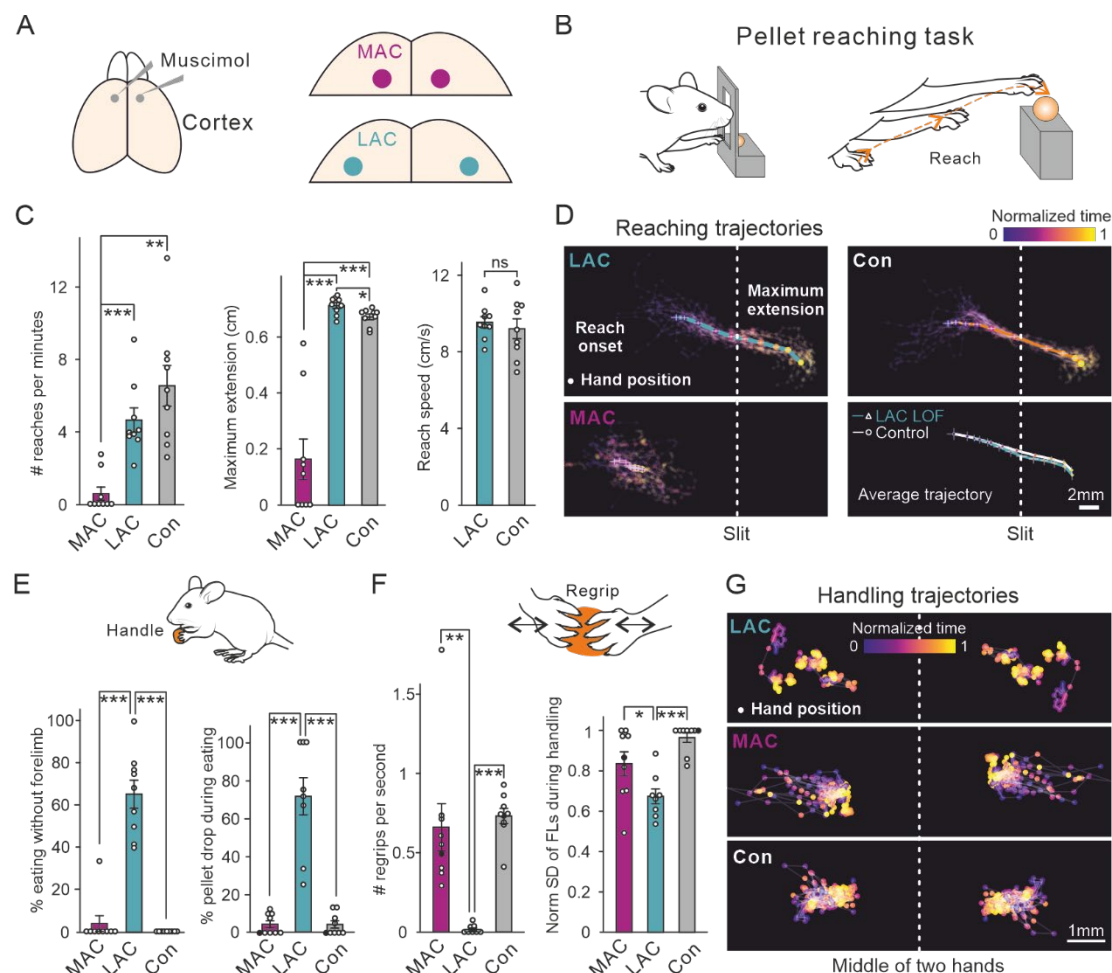


Figure 3.3.9 Selective roles for MAC vs LAC in reaching vs handling
Legend on next page.

We tested the effect of acute silencing by cortical muscimol injections into either MAC or LAC on behavioral performance (Figure 3.3.9A). After 7 days, mice were well-trained to retrieve a food pellet presented to them outside a slit of a plastic box by reaching (Figure 3.3.9B). During this first behavioral phase of the assay, silencing of MAC, but not LAC had a dramatic effect on reaching (Figure 3.3.9C, D), essentially leading to the complete inability to extend the forelimb through the slit towards the presented food pellet (Video S1). Quantitative analysis of behavior from high speed videos by tracking reaching trajectories using DeepLabCut (DLC) (Mathis et al., 2018) demonstrated a highly significant decrease in the number of executed reaches per minute and the maximum extension of the forelimb towards the pellet in

Figure 3.3.9 Selective roles for MAC vs LAC in reaching vs handling

- (A) Strategy for silencing of identified cortical domains using bilateral muscimol injections into MAC or LAC.
 - (B) Pellet reaching task illustrating the elaboration of the reaching trajectory.
 - (C) Quantification of the number of reaches per minute (left), maximum extension of the forelimb from the slit (middle) and speed of reaching (right) with silencing of MAC and LAC as compared to control (mean \pm SEM, $n = 9$ mice).
 - (D) Trajectories of reaching with silencing of MAC or LAC as compared to control condition. Trajectories shown in the top and lower left panels are trajectories from one example mouse. The colored curves are averaged trajectories from all grey curves in each silencing condition (LAC, 30 trials; MAC, 22 trials; Con, 31 trials). Lower right panel: Average trajectories comparison for LAC silencing and control conditions ($n = 9$ mice). Dots colored by normalized time denote the paw position at corresponding normalized timepoints during reaching. Averaged paw positions are shown as mean \pm SEM.
 - (E) LAC silencing impairs food handling. Upper panel: Scheme of a mouse handling a food pellet. Lower panel: Bar plots showing the percentage of food handling bouts without the use of forelimbs (left, mean \pm SEM, $n = 9$ mice) and percentage of handling bouts terminating with the dropping of the food pellet (right, mean \pm SEM, $n = 8$ mice). One mouse (black dots in MAC and Con) used exclusively the mouth (and not hands) to consume food in LAC silencing condition.
 - (F) Quantification of number of regrips per second during the handling bout (left) and normalized standard deviation of the limb mid-point centered trajectories (right) across experimental conditions ($n = 8$ mice). Black dots in MAC and Con denote the one mouse which used exclusively the mouth to consume food in LAC silencing condition. Inserted scheme on top: Indication of the quantified regrip movements characteristic of forelimb food handling.
 - (G) Limb mid-point centered trajectories of the forelimbs during food handling from one example mouse compared across the different experimental conditions during 7 handling bouts of an example mouse. Dots colored by normalized time denote the paw position at corresponding normalized timepoints during handling.
- * $p < 0.05$; ** $p < 0.01$; *** $p < 0.001$; ns, not significant.

MAC silenced mice compared to either LAC silenced or control mice (Figure 3.3.9C, D). Moreover, while reaching speed could not be quantified from MAC silenced mice owing to their inability to reach, LAC- silenced mice were not different from control mice in this parameter (Figure 3.3.9C).

A strikingly different result was obtained when we analyzed the second behavioral phase of the assay, which consisted of handling/manipulating food and consuming it (Figure 3.3.9E; Video S2). LAC silencing led to deficits in food manipulation, due to which the mice consumed food directly from the ground for long periods of time, without engaging their forelimbs to manipulate it, while MAC-silenced or control mice used almost exclusively their forelimbs to eat (Figure 3.3.9E). Moreover, in the phases when LAC-silenced mice used the forelimbs to hold food, we observed they frequently dropped the food pellet, a property neither observed in MAC-silenced nor control mice (Figure 3.3.9E). To determine why LAC-silenced mice resorted to eat without forelimb food manipulation as is the stereotypical behavior for mice, we carefully analyzed the episodes during which they hold food pellets in their hands and compared them to corresponding episodes in MAC-silenced or control mice (Figure 3.3.9F, G; Video S2). We found that during food pellet manipulation, mice exhibit stereotyped regrip movements (regrips) with their distal forelimbs and digits. These regrips were observed at comparable frequency in MAC-silenced and control mice, but were essentially absent in LAC-silenced mice (Figure 3.3.9F). The loss of regrips in LAC-silenced mice was also evident from the decrease in the movement of the distal forelimbs during handling, which we quantified based on DLC tracking as the standard deviation of the forelimb hand positions during a handling bout (Figure 3.3.9F).

Together, these results demonstrate that MAC and LAC are essential for mice to proficiently perform the food pellet reaching and handling task, but strikingly, they

are needed for distinct behavioral phases. While MAC is required for the reaching phase of the task, in agreement with previous optogenetic silencing experiments (Galiñanes et al., 2018), LAC is essential for handling and manipulation phases of the task recruiting distal forelimb muscles, but completely dispensable for the reaching phase.

3.3.6. Cortico-medullary synaptic organization extends into postsynaptic medulla

The strikingly different roles of MAC and LAC in controlling reaching and handling raised the question of which neurons in the latRM are the targets for these different cortical inputs. With the goal to record from medullary neurons to assess the identity of cortical input in relation to their behavioral tuning, we first determined the location of latRM neurons postsynaptic to different cortical regions. To achieve this goal, we took advantage of an AAV serotype exhibiting anterograde transfer potential for recombinase expressing cargos (Zingg et al., 2017, 2020). We injected a cocktail of AAVs expressing different recombinases (AAV(1)-Cre and AAV(1)-FLP) into two different cortical regions (MAC and LAC, or LAC and InsC respectively) together with a cocktail of corresponding reporter constructs (AAV(9)-flex-CytTag1 and AAV(9)-ftr-CytTag2) into latRM contralateral to cortical injections (Figure 3.3.10A, B). Since the reporter viruses for the two recombinases were co-injected in latRM, this strategy allowed to probe whether latRM neurons postsynaptic to one or the other cortical input region are spatially organized. Combinatorial postsynaptic mapping of latRM neurons from MAC and LAC revealed an overall more ventral position for MAC-recipient medulla neurons, while analogous experiments from LAC and InsC resulted in InsC-recipient neurons in a more dorsal position than LAC counterparts (Figure 3.3.10C). Quantification of marked medulla neurons over all injections allowed to determine the distribution of these neurons in the latRM (Figure 3.3.10D; Video S3). We found that

MAC-input neurons were located most ventrally, followed by LAC- and InsC- input neurons with highest densities in progressively more dorsal positions (Figure 3.3.10D; Video S3). Strikingly, the overall neuronal distribution patterns in latRM were reminiscent of the synaptic input patterns from the corresponding cortical regions (Figure 3.3.4C). Together, these findings demonstrate that the communication from different cortical regions to the medulla is highly organized and that postsynaptic recipient neurons in the latRM faithfully follow the distribution of cortical synaptic input.

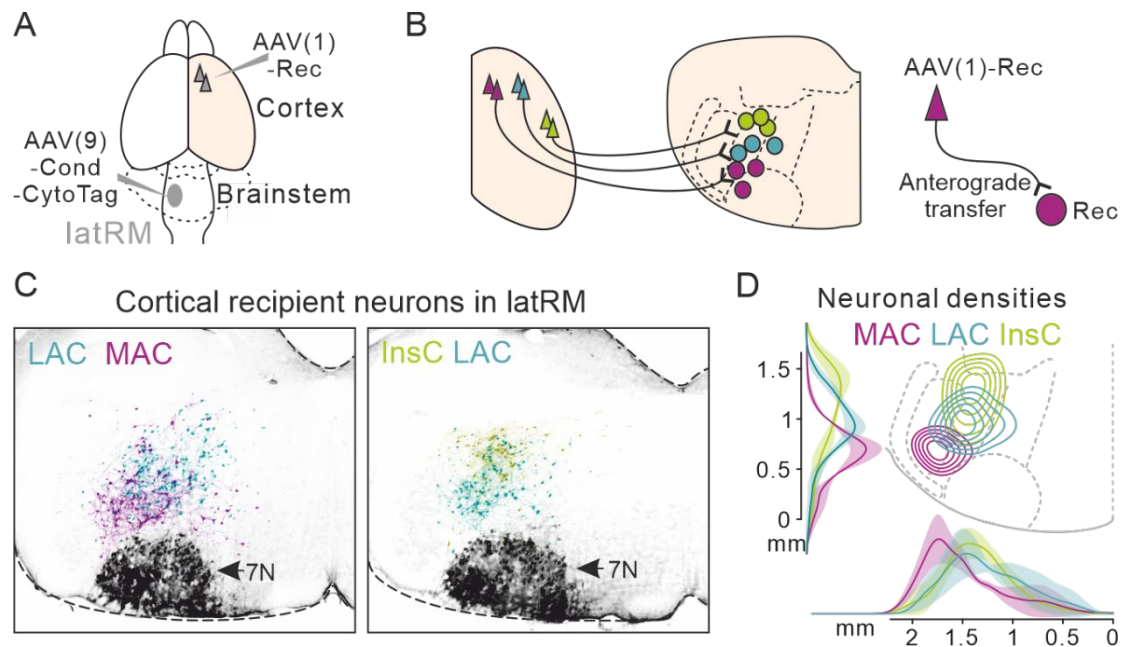


Figure 3.3.10 Cortico-medullary synaptic organization extends into postsynaptic medulla
 (A) Strategy for labeling medulla neurons with cortical input from different cortical regions.
 (B) Scheme showing the strategy of using AAV(1) virus to label postsynaptic neurons through anterograde transfer of Recombinase (Rec) expressing virus.
 (C) Representative coronal rostral medulla sections from two mice showing the infected postsynaptic neurons receiving input from MAC, LAC and InsC.
 (D) Averaged 2D, dorso-ventral and medio-lateral density distribution of postsynaptic neurons in the rostral medulla receiving input from MAC (n=3), LAC (n=4) and InsC (n=3).

3.3.7. Functional tuning of medulla neurons aligned with specific cortical input

To determine whether individual latRM neurons receive preferential functional cortical input from MAC or LAC and how this relates to their behavioral tuning during skilled forelimb movement, we next used *in vivo* electrophysiological recordings in latRM combined with cortical stimulation by optogenetics (Figure 3.3.11A). We delivered short pulses (50ms) of light to either stimulate MAC or LAC neurons while recording activity from single units in latRM. Through this approach, we identified 21 MAC- and 15 LAC-modulated latRM neurons, defined by an increase in firing rate at short latencies in response to cortical stimulation (putative monosynaptic AC>latRM connections; significant increase in firing rate at latencies <20ms; Figure 3.5.1).

We next determined the tuning properties of these cortically tagged latRM neurons to the different behavioral phases of the pellet reaching and handling task (Figure 3.3.11B). We recorded from a total of 726 neurons in latRM. Consistent with previous study (Ruder et al., 2021), neurons in latRM (54.1%; 393/726) were positively modulated during different phases of the forelimb tasks (Figure 3.3.12). Focusing specifically on the MAC and LAC cortically tagged populations, we found that latRM neurons optogenetically tagged from MAC exhibited strikingly different behavioral tuning properties to the ones tagged from LAC (Figure 3.3.11C-E). Averaged population activity of all MAC- or LAC-tagged neurons showed that the MAC-tagged population exhibited an increase in firing rate preceding the onset of forelimb reaching, while the LAC-tagged population sharply increased firing rate only thereafter (Figure 3.3.11D, left). In contrast, the LAC-tagged population exhibited increasing firing preceding food handling onset, while the MAC-tagged population sharply downregulated its activity around this behavioral transition with the onset of handling

(Figure 3.3.11D, right). This was also reflected in the activity of the single latRM neurons giving rise to the population activity. While LAC-tagged latRM neurons almost exclusively showed increases in activity corresponding to the onset of handling and manipulation of the food pellet, individual MAC-tagged neurons showed transient increase in activity that over all analyzed neurons tiled the behavior space of the reaching task preceding the handling of the food pellet (Figure 3.3.11D, E).

Together, these experiments provide striking functional evidence for highly selective interactions between cortex and latRM neurons with respect to different behavioral phases of forelimb movement. While LAC input is directed almost

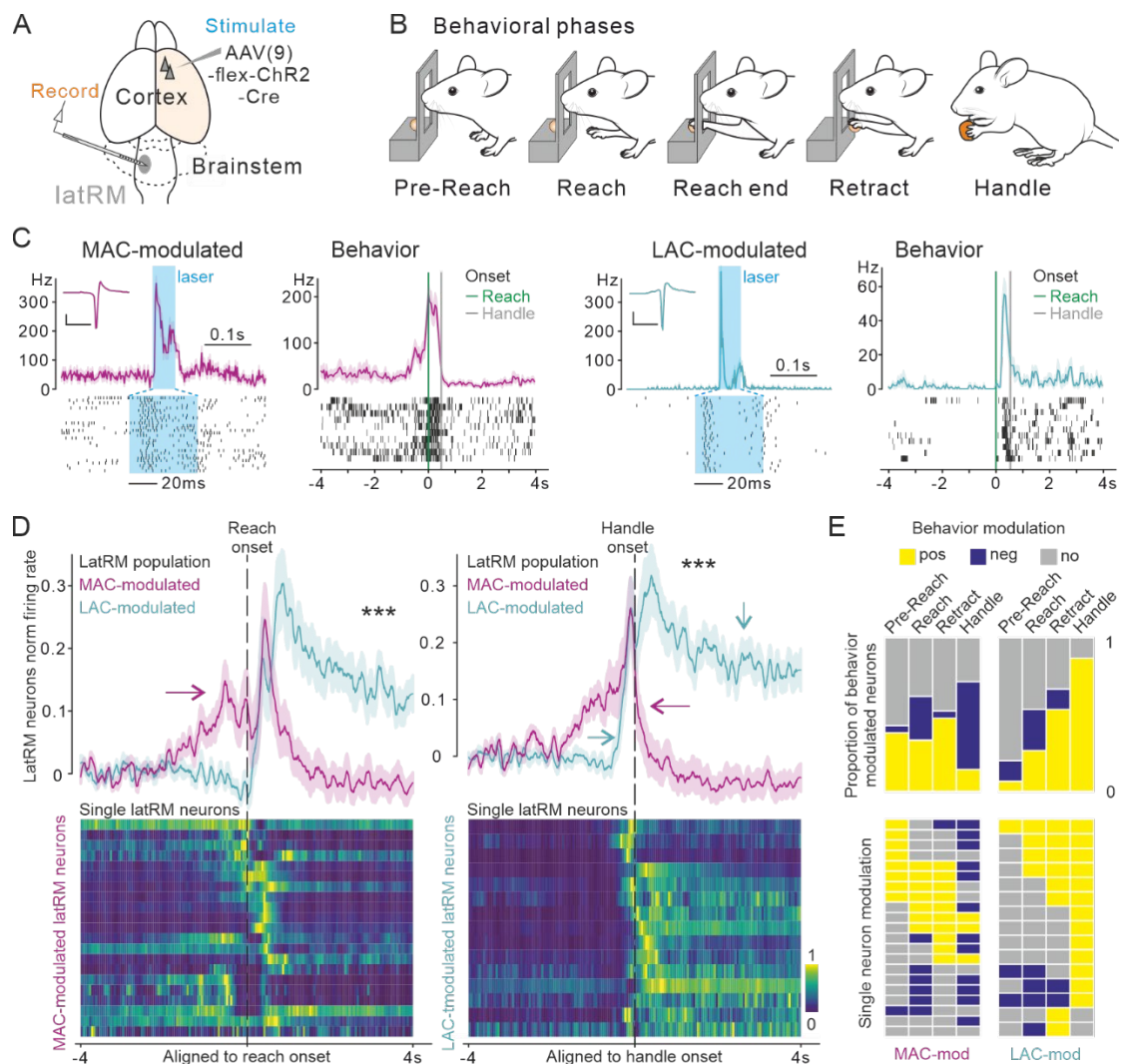


Figure 3.3.11 Functional tuning of medulla neurons aligned with specific cortical input
Legend on next page.

exclusively to latRM neurons tuned to handling, MAC input is preferentially directed to latRM neurons active during phases preceding food manipulation (pre-reaching, reaching, retraction).

Figure 3.3.11 Functional tuning of medulla neurons aligned with specific cortical input

- (A) Strategy to identify the effect of cortical input to latRM neurons upon stimulation of ChR2 expressing cortical neurons while performing extracellular silicon probe recordings in the latRM in freely moving mice during reaching and handling task.
- (B) Schematic representation of different phases of the reaching and handling task which we annotated in the behavioral videos to quantify modulation of neuronal activity during different action phases encompassing the task.
- (C) Example units showing the effect of cortical stimulation and activity of the same unit during the task. The left 2 panels (magenta) show the average firing rate (top) and raster plot (bottom) of an example unit that responded to the stimulation of the MAC with low latency (left-most) and that during the reaching task shows a striking increase in firing during pre-reach and reach phase of the behavior. The right 2 panels (cyan) are the average firing rate (top) and raster plot (bottom) of an example unit that responds to the stimulation of the LAC and during behavior shows a strong increase in activity during the retraction and handling phases of the task (right-most). Insets: Average waveforms from the two displayed neurons. Scale bar, 100 μ V (vertical) and 1ms (horizontal).
- (D) Upper panels: Population level activity of MAC-tagged (magenta) and LAC- tagged (cyan) latRM neurons using the average normalized firing rate of the respective populations aligned to reaching onset (left) or handling onset (right). Lower panels: Baseline subtracted and normalized firing of single neurons for the MAC-tagged (left, aligned to reach onset) and LAC-tagged (right, aligned to handle onset) populations. *** $p < 0.001$; MAC-tagged neurons, $n = 21$ from 5 mice; LAC- tagged neurons, $n = 15$ from 8 mice.
- (E) Upper panel: Proportion of MAC- or LAC- tagged neurons modulated during the different behaviors compared between the two neuronal populations. Lower panel: Modulation of each corresponding neuron shown in panel D (yellow: positive modulation, blue: negative modulation; grey: no modulation).

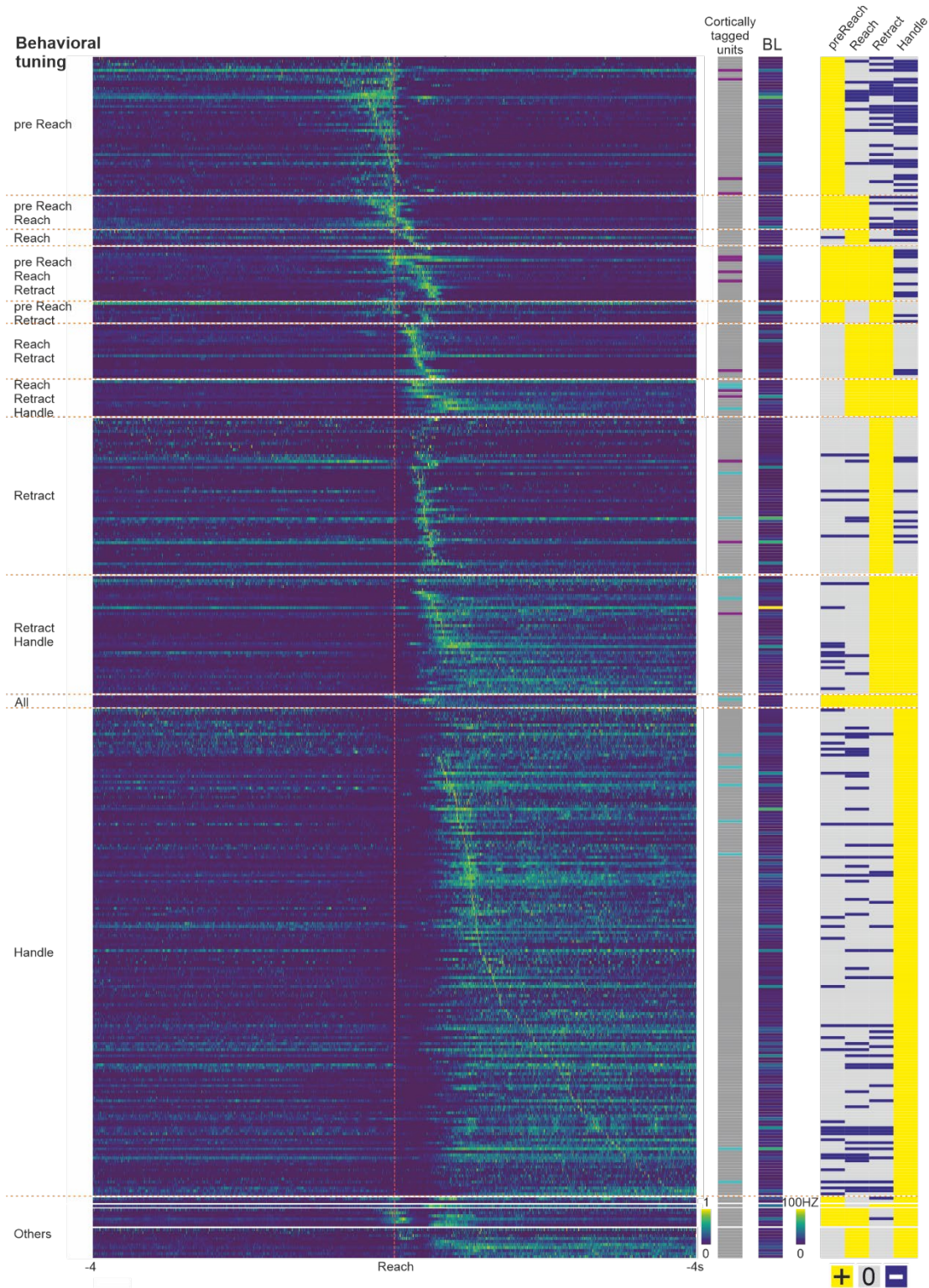


Figure 3.3.12 Positively modulated latRM neurons in reaching and handling tasks

Heatmap showing the normalized firing rate of all single neurons in latRM positively modulated in reaching and handling (n=393). On the right, neuron identity is indicated in magenta (MAC tagged), cyan (LAC tagged) or grey (not tagged) depending on tagging properties, next to its baseline firing rate (BL) and the modulation in different behavioral phases (yellow: positive modulation; blue: negative modulation; grey: no modulation).

3.3.8. Topography of cortico-medulla neurons extends to other subcortical structures

The striking anatomical and functional output organization of medulla-projecting cortical neurons raises the question of whether and how these populations collateralize to subcortical motor system targets other than the medulla, and whether segregation of cortical channels is also observed. This is interesting in light of recent observations that cortical output neurons stratify into two populations based on whether or not they innervate thalamic targets (Economo et al., 2018), and that cortical neurons with projections to the cervical spinal cord preferentially target striatal D1-receptor expressing neurons (Nelson et al., 2021). We therefore analyzed the collateralization patterns of latRM-projecting MAC, LAC and InsC neurons to several subcortical regions. As subcortical structures within the general motor cortical output pathway with known overall cortical input we selected (1) the superior colliculus, an important multi-sensory integration center in the midbrain, (2) the striatum, the input layer to basal ganglia circuitry, (3) the subthalamic nucleus (STN), the excitatory intermediate target within the indirect basal ganglia pathway and target for the hyperdirect pathway from the cortex, and (4) substantia nigra (SN), the biggest basal ganglia output nucleus in rodents.

We injected retrograde AAV expressing Cre recombinase into latRM to selectively induce CytTag and SynTag expression specifically in medulla projecting cortical populations in different cortical regions (MAC, LAC and InsC) (Figure 3.3.13A). Consistent with single neuronal tracing data (Figure 3.3.7), axon collaterals from marked cortico-medulla neurons targeted exclusively territory ipsilateral to cortical injection subcortically rostral to the medulla, but exhibited a biased targeting of axons to regions contralateral to injection within the medulla (Figure 3.3.13A, data

not shown). Therefore, we analyzed the synaptic output patterns of MAC-, LAC- or InsC-latRM projection neurons to the ipsilateral striatum, STN, SN and superior colliculus (Figure 3.3.13A). The quantification of synaptic distribution allowed us to score the similarity of synaptic patterns in target structures either considering all of these subcortical target structures (Figure 3.3.13B), or by individual target structures (Figure 3.3.13C-F). We found that latRM projection neurons located in MAC also establish collaterals and synaptic input to a restricted domain of the motor layers of the superior colliculus sparing its most lateral corner of innervation, an intermediate part of the lateral striatum, the ventral domain of the STN, as well as to a ventral intermediate region of the SN pars reticulata (SNr; Figure 3.3.13C-F; Figure 3.3.14). In contrast, LAC neurons with axons to the medulla also terminated in the lateral most corner of the superior colliculus, a ventral part of the lateral striatum, the dorsal domain of the STN, and in a lateral dorsal domain of the SNr (Figure 3.3.13C-F; Figure 3.3.14). Lastly, we analyzed InsC neurons with collaterals to the medulla and found these to be distinct in the elaboration of collaterals to other subcortical structures from MAC and LAC. Specifically, while there was some overlap between LAC and InsC output in the superior colliculus, these were still distinct enough to segregate the cortical domains in the computational similarity analysis. Moreover, LAC and InsC output was strikingly segregated within the STN region, where InsC input targeted the adjacent para-STN region rather than the STN proper, and no significant input was observed for InsC to the SNr (Figure 3.3.13C-F; Figure 3.3.14). We also evaluated axonal terminations of cortico-medullary projection neurons in the thalamus, which in agreement with previous work (Economo et al., 2018) did not represent a major target structure for either of these three populations (data not shown).

Together, these findings demonstrate that the here characterized different populations of cortico-medulla projection neurons not only follow a highly granular logic for how their synaptic input targets medullary neurons. Strikingly, at the same time, these neurons establish collaterals to several other subcortical regions with patterns of high spatial organization and distinction, thereby generalizing the logic of how these neurons interact within the motor system.

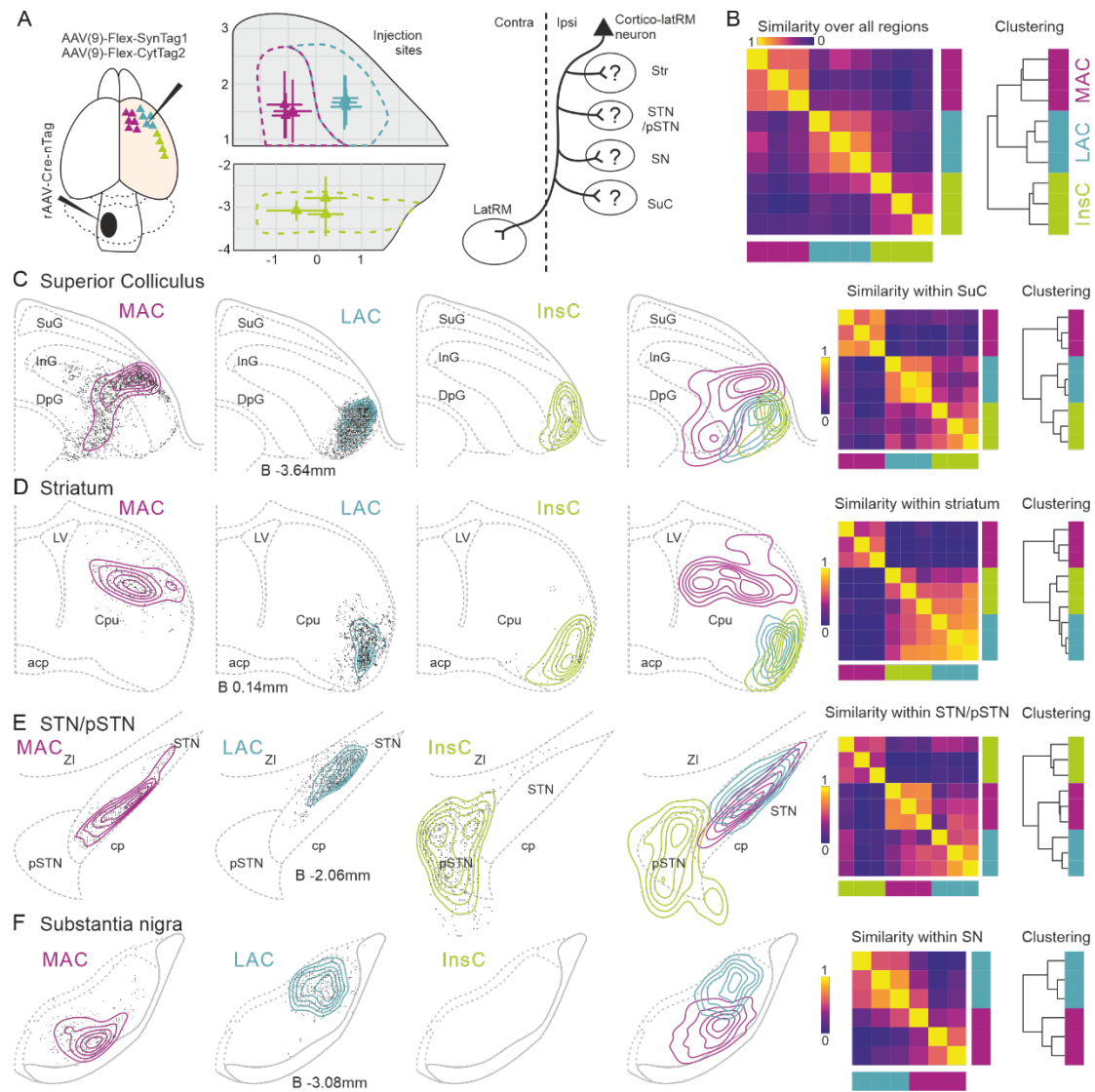


Figure 3.3.13 Topography of cortico-medulla neurons extends to other subcortical structures

- (A) Strategy for anterograde tracing cortico-medullary neurons in different cortical regions (left), cortical injection sites (middle), and scheme for regions of analysis for collateral arborization patterns of cortico-medulla neurons subtypes (right) (MAC, $n = 3$; LAC, $n = 3$; InsC, $n = 3$). Abbreviations: Str, striatum; STN/pSTN, subthalamic nucleus/parathalamic nucleus; SN, substantia nigra; SuC, superior colliculus; Ipsi, ipsilateral side; Contra, contralateral side.
- (B) Spatial correlation analysis (left) and clustering (right) of the synaptic distribution patterns in different subcortical regions across all levels shown in C-F and Figure S8 from individual injections.
- (C-F) Example representative 2D reconstruction of synaptic puncta and density distributions in superior colliculus (C), striatum (D), STN/pSTN (E) and substantia nigra (F) from 3 mice with labeled cortico-medullary neurons in MAC, LAC and InsC, respectively. Middle panel: 2D reconstruction of averaged synaptic density distribution from different cortical regions overlaid. Right panel: Spatial correlation analysis and clustering of the synaptic distribution patterns from individual injections at the subcortical regions from all levels analyzed in Figure 3.3.13 and Figure 3.3.14.

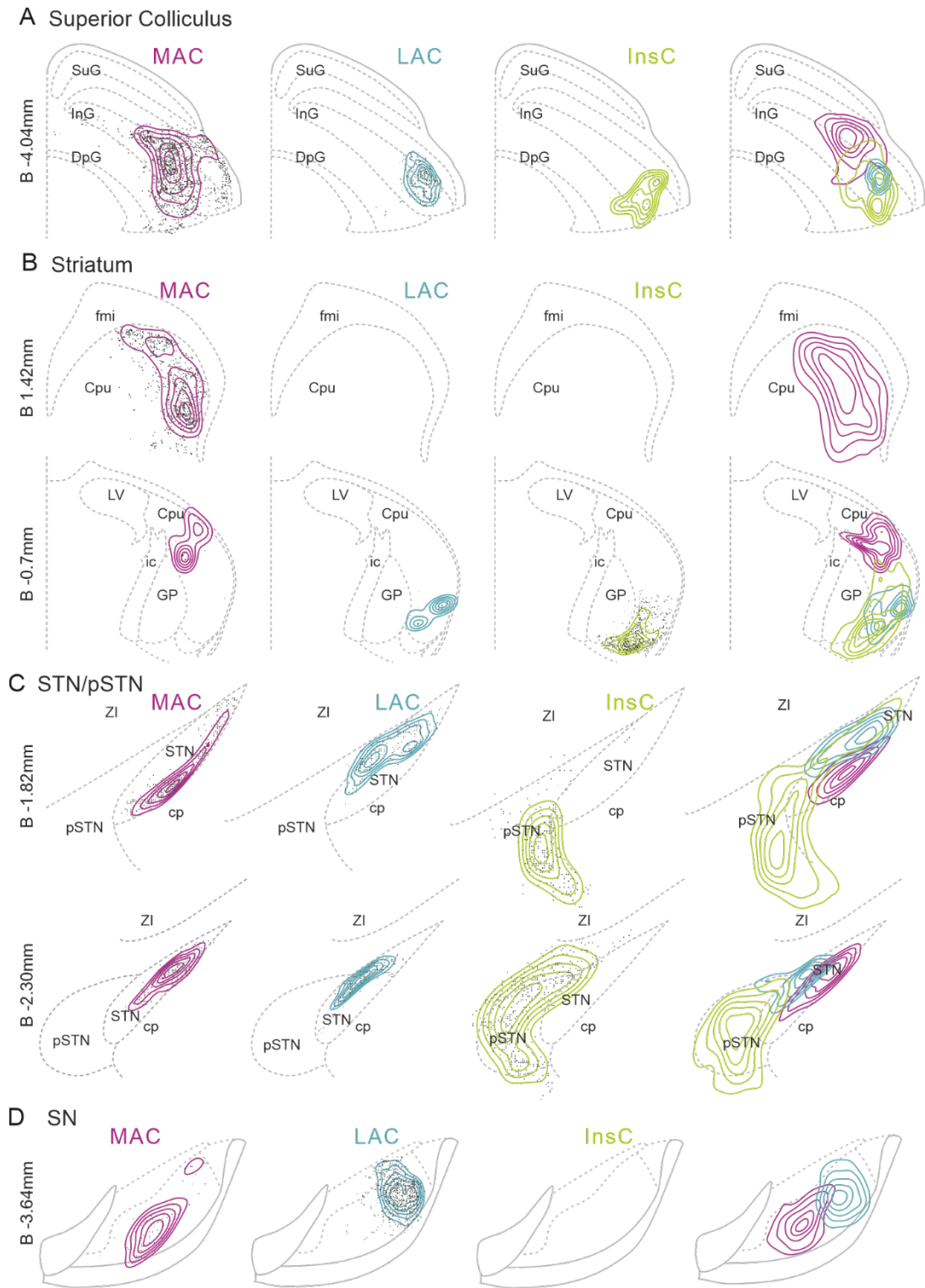


Figure 3.3.14 Differences in synaptic targeting of cortico-medulla neurons extends to other subcortical structures

(A-D) Example 2D reconstruction of synaptic puncta and density distributions in superior colliculus (A), striatum (B), STN/pSTN (C) and substantia nigra (D) at denoted levels from 3 mice with labeled cortico-medullary neurons in MAC, LAC and InsC. Right panel, 2D reconstruction of averaged synaptic density distribution from MAC, LAC and InsC overlaid.

3.4. Discussion

Understanding how the cortex influences subcortical movement centers requires to elucidate the principles of how cortex and subcortical structures interact. The medulla is a major cortical target in the motor output system (Economo et al., 2018) involved in key aspects of forelimb movement control (Esposito et al., 2014; Ruder et al., 2021), defining the focus of this study. Here we demonstrate that the cortex elaborates highly specific channels targeting precisely arranged 3D columns in forelimb- movement controlling regions in the medulla, preferentially interacting with neurons tuned to specific forelimb action phases. We demonstrate that these channels are aligned with the functional requirement of respective cortical regions in reaching and handling phases of forelimb movement. Our findings shed light on how large cortical territory topographically influences behaviorally-tuned circuits in the medulla in a top- down manner with channels of high functional precision. We discuss the organizational logic of these signaling strategies, the implications of our findings for understanding motor system function and how these findings generalize to other motor centers.

3.4.1. Organization of cortical input to medulla and spinal cord for forelimb control

Cortico-spinal neurons have been a main focus of studies on neuronal control of forelimb movement, demonstrating differential access to spinal segments, axonal termination zones or connectivity to spinal neurons for different cortical populations (Lemon, 2008; Morecraft et al., 2013; Nelson et al., 2021; Sahni et al., 2021b; Ueno et al., 2018; Wang et al., 2017). Our work uncovers a striking organization for synaptic interactions between cortex and medulla, and identifies LAC as a cortical domain without access to the spinal cord but strong interactions with the medulla. Interestingly,

high-density synaptic input to the medulla is preferentially derived from anterior cortical territory and targets regions of the medulla implicated in forelimb control (Esposito et al., 2014; Ruder et al., 2021), while sparing subregions implicated in full-body behaviors including the magnocellular and gigantocellular nucleus (Capelli et al., 2017; Cregg et al., 2020; Usseglio et al., 2020). In contrast, the majority of cortico-spinal neurons resides more caudally and establishes much sparser medullary collaterals. Focusing on anterior cortical territory, neurons with no spinal projections need to mandatorily signal through medullary circuits, as an intermediate signaling center to influence forelimb movement, without direct access to spinal circuits.

Our findings demonstrate that in mice, at a first level of organization, AC preferentially innervates forelimb related medulla regions, and is further subdivided according to its overall interaction hierarchies with medulla and/or spinal cord. A second level of organization relates to how synaptic input from different cortical domains terminates within the medulla. In the rostral medulla, cortical synaptic terminals tile the lateral domain from ventral to dorsal, with MAC elaborating its synaptic input most ventrally, neighbored by LAC input more dorsally, and InsC input most dorsally along this axis. Strikingly, these dorso-ventrally arranged synaptic sites of highest density extend along the length of the medulla, thereby generating 3D synaptic columns of shared cortical origin. These cortex-derived synaptic columns are not only discernable by overall synapse analysis, but also at the level of single neuron reconstructions with multiple termination zones along the rostro-caudal axis. Through this signaling strategy, single cortical neurons can contact neurons in the medulla across distinct neuroanatomical domains of its rostro-caudal axis, thereby providing precisely organized parallel top-down synaptic input to these neurons.

3.4.2. Organization of cortical input to medulla matches behavioral tuning of its neurons

A key question is whether and how the striking anatomical organization observed between cortex and medulla underlies functional organization. We found that optogenetic stimulation of MAC elicits putative monosynaptic excitatory responses preferentially in latRM neurons tuned to forelimb reaching but not handling phases of the pellet task. We also found that acute MAC silencing selectively disrupts reaching associated phases of the behavior but not handling, compatible with previous work in which optogenetic inactivation of specific cortical sites within MAC but not of neighboring regions efficiently blocks reaching initiation and diverts ongoing reaching trajectories (Galiñanes et al., 2018). Noteworthy also in this context, layer 2/3 neurons in this part of the cortex are tuned to directionality of forelimb reaches (Galiñanes et al., 2018), a property also exhibited by some latRM neurons (Ruder et al., 2021). In contrast, we found that LAC silencing disrupts food handling but not reaching behavior, and that LAC neurons connect preferentially to handling but not reaching tuned latRM neurons. Interestingly, different regions within LAC, notably its most anterior (referred to as anterior lateral motor cortex; ALM) and lateral domain (referred to as tongue/jaw motor cortex; tjM1) were previously studied in the context of orofacial behaviors including licking (Bollu et al., 2021; Li et al., 2015; Mayrhofer et al., 2019) or singing (Okobi et al., 2019) (Figure 3.2.1). Thus, further topography may exist within LAC to coordinate orofacial movements and handling-related forelimb movements, behaviors frequently occurring in parallel when mice consume food, through activity within LAC subregions and downstream connected circuits. This hypothesis is in agreement with work mapping the functional impact of cortical stimulation sites in head-fixed mice through optogenetics, eliciting a variety of muscle contraction patterns involving both orofacial and forelimb muscles, as well as forelimb movements towards the mouth similar to the

ones occurring during food handling (Mercer Lindsay et al., 2019). Moreover, neurons presynaptic to motor neurons innervating orofacial muscles also reside in the medulla (Mercer Lindsay et al., 2019), making it plausible that LAC cortico-medullary neurons have access to these pathways as well, and that different subregions of LAC might have functionally distinct targets within latRM. Together, these combined studies lend support to a model in which the influence of MAC is primarily on preparation and execution of forelimb reaching and trajectory elaboration, while LAC produces top-down modulation to coordinate forelimb handling and orofacial behaviors.

Our findings resonate with recent work on the organization of communication pathways within the medulla and to the spinal cord. Of note, excitatory neurons in the latRM stratify into at least four anatomically distinct subpopulations based on their axonal projections and these populations can serve as an entry point to elicit distinct forelimb behaviors by optogenetic stimulation (Ruder et al., 2021). Excitatory latRM neurons projecting to the spinal cord are anatomically distinct from two groups of latRM neurons terminating in the caudal medulla. While spinally-projecting latRM neurons elicit forelimb reaching behavior, more complex and digit-involving forelimb movements including hand-to-mouth or grooming are elicited by stimulation of the latter populations (Ruder et al., 2021). Moreover, excitatory neurons in the MdV located in the caudal medulla are required for the grasping but not reaching phase of the pellet task (Esposito et al., 2014). Thus, intra-medulla information processing appears to generate forelimb movements more complex than reaching, and therefore top-down impact of LAC exclusively to this region rather than in addition directly to the spinal cord might serve the purpose of diversifying complex forelimb behaviors and perhaps also allowing for more behavioral flexibility and adjustments; not least because coordination of forelimb and orofacial movement from within this caudal brainstem

structure is strategically best placed. In contrast, forelimb reaching behavior has also behavioral manifestations independent of feeding, including the need for direct sensory feedback at the level of the spinal cord itself. Processing circuits for action control would therefore be most conveniently placed directly in the spinal cord, where also somatosensory feedback from limbs can further impact reaching trajectories. In summary, the striking anatomical and functional pairing of cortico-medulla projection neurons residing in distinct cortical regions with behavioral-phase tuned neurons in the medulla provides insight into the principles of how the cortex communicates differentially through fine-grained functionally distinct channels with medullary and spinal circuits very close to the generation of movement.

This logic of organization might not only be suitable to influence execution of behavioral phases but also has the potential to be involved in learning new movements involving forelimbs where instructions for learned content might be transferred to subcortical populations by modifying connectivity patterns through plasticity, similar to modifications occurring in the striatum (Lemke et al., 2019). Inspection of synaptic arborization patterns of single reconstructed cortical neurons in the medulla shows tremendous differences ranging from very few synaptic boutons to large arbors with many sites. Analysis of these patterns across learning and functional recovery after injury or stroke has the potential to reveal whether and how these processes might modify connectivity at the intersection between cortex and medulla.

3.4.3. Parallel cortical pathway logic generalizes to other motor centers

Because of the widespread axonal arborization of cortical output neurons and the diversity of cortical neurons, it is crucial to elucidate principles of synaptic interaction between cortex and subcortical structures at the level of defined populations. Indeed, analysis of visual cortex single neuron long-range projections has revealed that

most neurons innervate multiple targets but that there is an emerging logic with respect to target identity rather than a selection of random targets (Han et al., 2018).

Our analysis of synaptic output patterns specifically from cortical neurons projecting to the medulla allowed us to determine whether cortical populations establishing distinct channels to medullary subregions also do so at the same time to other levels in the motor system hierarchy. Indeed, we found that medulla-projecting MAC, LAC and InsC neurons also arborize differentially in the superior colliculus, striatum, subthalamic region and substantia nigra, generating non-overlapping output channels. The data demonstrate that medulla projecting cortical neurons from different cortical domains elaborate very specific output channels also with regards to their projections to other subcortical regions. How the different collateral pathways established along the motor system by one population of cortico-medullary neurons collaborate in the production and learning of movement will be an interesting avenue to pursue in the future.

The logic of organization might be similar to one revealed recently within basal ganglia circuits, where striatal projection neurons of the direct pathway use parallel communication channels for axon collaterals to the intermediate processing station globus pallidus externa (GPe), but exhibit a more convergent mode of communication to its output layer in the substantia nigra pars reticulata (SNr) (Foster et al., 2021). Moreover, even within similar overall arborization to a region, specific neuronal subtypes can establish preferential synaptic contacts with subsets of neurons in the target region, as was recently shown to occur for connectivity of cortico-spinal neurons to striatal neurons (Nelson et al., 2021). Future work will reveal how strategies of convergent and divergent signaling modes contribute to computations in the motor system across its hierarchy. Our work advances this understanding in demonstrating the

precisely matched functional organization between different cortical regions and brainstem centers involved in the regulation of skilled forelimb movements.

3.5. Methods

3.5.1. Key resources table

REAGENT or RESOURCE	SOURCE	IDENTIFIER
Antibodies		
chicken anti-GFP	Invitrogen	Cat# A10262; RRID: AB_2534023
chicken anti-Myc	Invitrogen	Cat# A21281; RRID: AB_2535826
Rabbit anti-GFAP	Millipore	Cat# AB5804; RRID: AB_2109645
goat anti-ChAT	Millipore	Cat# AB144P; RRID: AB_2079751
mouse anti-V5	Invitrogen	Cat# R960CUS; RRID: AB_2792973
rabbit anti-RFP	Rockland	Cat# 600-401-379; RRID: AB_2209751
Donkey anti-goat Cy5	Invitrogen	Cat# A-21447; RRID: AB_2535864
Donkey anti-rabbit Cy3	Jackson Immuno Research	Cat#711-165-152; RRID: AB_2307443
Donkey anti-chicken 488	Jackson Immuno Research	Cat#703-545-155; RRID: AB_2340375
Donkey anti-chicken Cy5	Jackson Immuno Research	Cat#703-605-155; RRID: AB_2340379
Donkey anti-goat 488	Invitrogen	Cat# A-11055; RRID: AB_2534102
Donkey anti-mouse 647	Invitrogen	Cat# A-31571; RRID: AB_162542
Donkey anti-mouse Cy3	Invitrogen	Cat# A-31570; RRID: AB_2536180
Donkey anti-mouse DyL405	Jackson Immuno Research	Cat# 715-475-150; RRID: AB_2340839
Virus Strains		
AAV-flex-SynMyc	Pivetta et al., 2014	N/A
AAV-flex-TdTomato	Capelli et al., 2017	N/A
AAV-flex-H2B-V5	Ruder et al., 2021	N/A
AAV-H2B-10xMyc	Ruder et al., 2021	N/A
AAV-H2B-V5	Ruder et al., 2021	N/A
AAV-Cre	This study	N/A
AAV-Cre-H2B-GFP	This study	N/A
AAV-Cre-H2B-V5	This study	N/A
AAV--hChR2(H134R)-EYFP	Addgene	Addgene no. 20298
AAV-fDIO-EYFP	Addgene	Addgene no. 55641
AAV(1)-hSyn-Cre	Addgene	Addgene no. 105553
AAV(1)-hSyn-Flpo	Addgene	Addgene no. 60663
Experimental Models: Organisms/Strains		
Mouse: C57BL/6	Charles River	Strain Code: 027
Mouselight database		
AA0180	Janelia Research Campus	https://doi.org/10.25378/janelia.5527441
AA0012	Janelia Research	https://doi.org/10.25378/janelia.55

	Campus	21618
AA0250	Janelia Research Campus	https://doi.org/10.25378/janelia.5527678
AA0788	Janelia Research Campus	https://doi.org/10.25378/janelia.7739369
AA0179	Janelia Research Campus	https://doi.org/10.25378/janelia.5527438
AA0576	Janelia Research Campus	https://doi.org/10.25378/janelia.7649849
AA0726	Janelia Research Campus	https://doi.org/10.25378/janelia.7707194
AA1543	Janelia Research Campus	N/A
AA0133	Janelia Research Campus	https://doi.org/10.25378/janelia.5527273
AA0134	Janelia Research Campus	https://doi.org/10.25378/janelia.5527276
AA0169	Janelia Research Campus	https://doi.org/10.25378/janelia.5527408
AA1043	Janelia Research Campus	https://doi.org/10.25378/janelia.7822304
AA0956	Janelia Research Campus	https://doi.org/10.25378/janelia.7804088
Software and Algorithms		
MATLAB (v2017b)	Mathworks	https://www.mathworks.com/RRID:SCR_001622
Python (v3.7)	Python	https://www.python.org/RRID:SCR_008394
CorelDraw (vX9)	Corel	https://www.coreldraw.com/RRID:SCR_014235
Imaris (v9.1.2)	Oxford Instruments Group	http://www.bitplane.com/imaris/ RRID:SCR_007370
Bonsai (v2.3)	NeuroGEARS Ltd.	https://bonsai-rx.org RRID:SCR_017218
Fiji	Fiji	http://fiji.sc RRID:SCR_002285
TrackMate (v6.0.3)	TrackMate	https://imagej.net/plugins/trackmate/
Kilosort v2	Cortex lab	https://github.com/MouseLand/Kilosort/releases/tag/v2.0
Kilosort v3	Cortex lab	https://github.com/MouseLand/Kilosort
Phy2	Cortex lab	https://github.com/cortex-lab/phy
DeepLabCut	Mathis Lab (Mathis et al., 2018)	http://www.mousemotorlab.org/deeplabcut
Other		
Muscimol	Tocris	Cat. No.0289

Beads, Fluoro-Max Dyed Blue Aqueous Fluorescent Particles	Thermo Scientific	Catalog number: B500
Fiber specs: (.39/200) – active length 0.5mm Implant length: 1.5mm	OptogeniX	https://www.optogenix.com/
ASSY-156-H5	Cambridge NeuroTech	https://www.cambridgeneurotech.com/
Neuropixels 1.0	IMEC	https://www.neuropixels.org/
RHD USB interface board	Intan Technologies	https://intantech.com/
NI PXIe-1071, 4-Slot 3U PXI Express Chassis	National instrument	https://www.ni.com/
NI PXIe-PCIe8381,x8 Gen2 MXI-Express for PXI Express Interface,3m	National instrument	https://www.ni.com/
PXIe-6341, X Series DAQ	National instrument	https://www.ni.com/
Neuropixels fixture	ATLAS Neuro	https://www.atlasneuro.com/
FV1000 confocal microscope	Olympus	http://www.olympusconfocal.com/products/fv1000/index.html
ZEISS Axio Imager 2	Zeiss	https://www.zeiss.com/microscopy/int/products/light-microscopes/axio-imager-2-for-biology.html
CSU-W1 Confocal Scanner Unit	Yokogawa	https://www.yokogawa.com/solutions/products-platforms/life-science/spinning-disk-confocal/csu-w1-confocal-scanner-unit/
Ace 2 Area Scan Cameras	Basler AG	a2A1920-160umBAS
Cobolt 06-MLD; 473nm; 100mW	HÜBNER Photonics	https://hubner-photonics.com/products/lasers/diode-lasers/06-01-series/
Model 1900 Stereotaxic Alignment System	Kopf	http://kopfinstruments.com/product/model-1900-stereotaxic-alignment-system/
Mouse schemes	Zenodo, scidraw.io	doi.org/10.5281/zenodo.3926569 doi.org/10.5281/zenodo.3925937 doi.org/10.5281/zenodo.3925901

3.5.2. Resource availability

Lead Contact

Further information or requests for reagents and resources should be addressed to the Lead Contact, Silvia Arber (silvia.arber@unibas.ch).

Materials Availability

All originally made constructs for AAV production described in this manuscript are available upon request by contacting the lead author.

Data and Code Availability

All custom-made scripts and codes for analysis are available upon request by contacting the lead author.

3.5.3. Animals

We used wild-type C57BL/6 mice from Charles River. For behavioral experiments, we used 2-4 month-old male mice, individually housed with horizontal running wheels. For anatomical experiments, both male and female mice of 2-4 months were used. Experimental mice originating from different litters were used in individual experiments. No criteria were applied to allocate mice to experimental groups. All procedures pertaining to housing, surgery, behavioral experiments and euthanasia were performed in compliance with the Swiss Veterinary Law guidelines.

3.5.4. Method details

3.5.4.1. Virus production, injections and implantations

The following, previously described adeno-associated viruses (AAV), all based on a backbone derived from Allen Brain (AAV-CAG-flex-tdTomato-WPRE-bGH): AAV-flex-SynMyc (referred to as AAV-flex-SynTag) (Takeoka et al., 2014), AAV-flex-tdTomato (referred to as AAV-flex-CytTag) (Capelli et al., 2017), AAV-H2B-10×Myc, AAV-H2B-V5 (referred to as AAV-nTag), AAV-flex-H2B-V5 (referred to as AAV-flex-nTag) (Ruder et al., 2021). Not previously reported viral constructs were designed in analogy to above constructs: AAV-Cre-H2B-V5, AAV-Cre-H2B-GFP (referred to as AAV-Cre-nTag). AAV-Ef1a-double floxed-hChR2(H134R)-EYFP (Addgene no. 20298) and AAV-Ef1a-fDIO-EYFP (Addgene no. 55641, referred to as AAV-frt-CytTag) were from Addgene. For unconditional expression of constructs using Cre-conditional AAVs, mice were co-injected with AAV-Cre. To infect neurons through local infection, a 2.9 serotype plasmid was used for production as in previous studies (Basaldella et al., 2015; Esposito et al., 2014; Ferreira-Pinto et al., 2021; Pivetta et al., 2014; Ruder et al., 2021). For retrograde targeting of neurons by means of axonal infection, a rAAV2-retro capsid plasmid (Tervo et al., 2016) was used for coating as described previously (Capelli et al., 2017; Ferreira-Pinto et al., 2021; Ruder et al., 2021). For transsynaptic targeting of postsynaptic recipient neurons from cortex, a 2.1 serotype (Zingg et al., 2017, 2020) was used to produce AAV(1)-hSyn-Cre (Addgene no. 105553) or AAV(1)-hSyn-Flpo (Addgene no. 60663). All AAVs used in this study were produced following standard protocols. Genomic titers for rAAV2-retro and AAV2.1 were between $1\text{-}5 \times 10^{13}$, and for AAV2.9 were between 1×10^{12} to 1×10^{13} .

For surgery, viruses were delivered to the target brain regions via stereotaxic injection with high precision stereotaxic instruments (Kopf Instruments, Model 1900)

under isoflurane anesthesia as previously described (Capelli et al., 2017; Esposito et al., 2014; Ferreira-Pinto et al., 2021; Ruder et al., 2021). Injections in the spinal cord were targeted to either the cervical segments C5-C8 or the lumbar segments L1-L3 (Takeoka et al., 2014), with an approximate injection volume of 300-500nl. The stereotaxic coordinates for brain injections are defined as antero-posterior (AP), medio-lateral (ML) and dorso-ventral (DV) (AP; ML; DV; in mm; approximate injection volumes: 50-100nl), taking lambda as a reference for the AP and ML axis for medulla injections, while bregma was used as a reference point for the AP and ML axis for cortex: latRM (-1.4; -1.55; -4.7); MAC (1.8; 1; 0.8); LAC (1.8; 2; 0.8); InsC (0; 3.9; 3).

Retrograde tracings to map the location of cortical neurons with defined outputs using rAAV2-retro-nTag or rAAV2-retro-Cre-nTag viruses were carried out by injections in the spinal cord or latRM. For systematically mapping the cortical output, we injected a mixture (2:2:1:1) of AAV-flex-SynMyc (to visualize synaptic output), AAV-flex- tdTomato (to show neuronal processes including axons), AAV-flex-H2B-V5 (to reveal the extent of the injection site), AAV-Cre (to allow the expression of conditional viruses), and waited at least four weeks for expression before perfusion. The injection sites were designed to cover the areas defined by retrograde mapping experiments and the coordinates of the injection sites were measured by post hoc assessment based on cortical spreading of the nuclear tag signal. For mapping the recipient neurons targeted by the cortex, AAV(1)-hSyn-Cre and AAV(1)-hSyn-Flpo were injected into two cortical regions (MAC/LAC or LAC/InsC), respectively. This was followed by an injection of a mixture (1:1) of AAV(9)-flex-tdTomato and AAV(9)-Efla-fDIO-EYFP into latRM. To specifically label the latRM projecting cortical neurons, rAAV2-retro-Cre-nTag virus was injected in latRM, applying an injection of a mixture (1:1) of AAV(9)-flex-tdTomato and AAV-flex-SynMyc in the cortex.

For cortex inactivation, craniotomies were drilled bilaterally in the skull to expose the application sites accessed with high precision stereotaxic instruments. The coordinates of the craniotomies are as follows (AP; ML; in mm): MAC (1.8; ± 1); LAC (1.8; ± 2). Kwik-Cast sealant (WPI) was applied to cover the exposed dura. Injections were performed as previously described (Cao et al., 2015; Otchy et al., 2015). Briefly, 100 nl of 25 mM solution (Tocris, Cat. No.0289) was bilaterally injected into one cortical site at a depth of 0.8mm from dura, together with beads (Thermo Scientific, Cat. No. B500) to verify precision of injection sites. For control, cortical sites were injected with PBS. 45 mins after injections, mice were tested for behavioral performance (see Behavior experiments).

For optogenetic cortex activation during electrophysiological recordings from mice in the latRM, we performed unilateral injection with AAV-flex-ChR2 and AAV-Cre into the cortex (coordinates of MAC and LAC same as above). One week thereafter, mice were trained in the pellet reaching task (see Behavior experiments) for one week.

3.5.4.2. Immunohistochemistry and microscopy

All mice in this study from anatomical and behavior experiments were euthanized, and brains and spinal cords were collected for histological processing, as previously described (Capelli et al., 2017). In brief, transcardial perfusion was performed under deep anesthesia with Ketamine-Xylazine. Animals were first perfused with cold phosphate buffer saline (PBS) and subsequent fixation using a 4% paraformaldehyde (PFA) solution (Sigma). Brains and spinal cords were dissected, post-fixed overnight in 4% PFA, and incubated in 30% sucrose (w/v) in PBS for at least two days before cryopreservation. Brains and spinal cords were sliced at 80 μ m thickness on a cryostat (coronally for brain tissue and transversely for spinal cord). We collected floating sections sequentially into individual wells and incubated them for

one-hour in blocking solution (1% BSA/0.2% TritonX100/PBS). Primary antibodies diluted in blocking solution were applied and incubated for 1-3 days at 4°C. Fluorophore-coupled secondary antibodies (Jackson or Invitrogen) were used for one-day incubations at 4°C, after extensive washing of tissue sections. After final washing, sections were mounted on glass slides in anti-bleach preservative medium in sequential order along the rostro- caudal axis. Primary antibodies used in this study were: chicken anti-GFP (Invitrogen), sheep anti GFP (Bio-Rad), chicken anti-Myc (Invitrogen), goat anti-ChAT (Millipore), mouse anti-V5 (Invitrogen) and rabbit anti-RFP (Rockland), rabbit anti-GFAP (Millipore). To acquire low-resolution overview images, we used an Axioscan light microscope (Zeiss, 5x objective) and for higher resolution imaging, we used a FV1000 confocal microscope (Olympus) or an Axio Imager M2 microscope (Zeiss) with a Yokogawa CSU W1 Dual camera T2 spinning disk confocal scanning unit.

3.5.4.3. Behavioral experiments

The pellet reaching and handling task was performed as previously described (Esposito et al., 2014; Ruder et al., 2021; Xu et al., 2009). Briefly, food-restricted mice were placed in a custom-made chamber containing a slit and trained to protrude the arm through the slit, reaching for a food reward. The body weight of mice was monitored to not drop below 85% of the original weight. Videos were recorded from below and side for pose estimation with Basler cameras (Ace 2 series). Mice were allowed to obtain food pellets with their tongue only on the first day, to accustom them to the goal of retrieving food. On following days, mice were motivated to use the forelimb for reaching trials, by placing the food pellets at a marked, consistent position outside the slit further away and not accessible to the tongue. For loss-of-function experiments, mice were trained for at least 7 days aiming for a success rate of > 30% and with a goal

of retrieving >15 pellets or 35 reaches. All mice (n=9) were included in analysis. Depending on whether mice were right- or left-handed, the pellet position was slightly moved to the side relative to the slit. For electrophysiological recording experiments, mice were all trained to use their left hand for 7 days and only successful first attempt forelimb reaches were selected for analysis (see Electrophysiological recording and analysis).

3.5.4.4. Anatomical reconstructions and analysis

Viral injections and tissue processing were performed as described above (see Virus production, injections and implantations). To map the neuronal distribution of cortical populations stratified by projections to latRM or spinal cord, 80µm thick coronal sections encompassing the full cortical area along its rostro-caudal axis were acquired using the Axioscan light microscope with a 5x objective. Every section along the rostro- caudal axis is used for analysis; the position where lateral ventricles begin to be separated was determined as bregma (Paxinos and Franklin, 2007). To assess projections of cortical neurons to the medulla, superior colliculus, striatum, subthalamic/para-subthalamic nucleus, substantia nigra, and the position of postsynaptic neurons in the medulla receiving cortical input through anterograde virus transfer, 80µm thick coronal sections were acquired with a 20x objective of a confocal microscope (FV 1000, Olympus) or an Axio Imager M2 microscope (Zeiss) with a Yokogawa CSU W1 Dual camera T2 spinning disk confocal scanning unit, tiling mosaics of multiple fields of view (z-step = 1.2µm for synapses; = 5µm for neurons). Three rostro-caudal levels were selected along the axis of the medulla for analysis (Paxinos and Franklin, 2007). The three chosen levels for analysis were as follows: rostral medulla at mid-7N level (Bregma -6mm) (Ruder et al., 2021); caudal medulla at the hypoglossal (12N) level (Bregma -7.32mm) (Esposito et al., 2014); intermediate

medulla midway between these rostral and caudal medulla levels (Bregma -6.64mm) (Capelli et al., 2017). Three rostro-caudal levels of striatum were selected based on striatal domain parcellations as previously reported (Hintiryan et al., 2016), i.e., Bregma +1.42mm, +0.14mm and -0.7mm. Two rostro-caudal levels of superior colliculus (Bregma -3.64mm and -4.04mm), three levels of subthalamic/para- subthalamic nucleus (Bregma -1.82mm, -2.06mm and -2.30mm), two levels of substantia nigra (Bregma -3.08mm and -3.64mm) were selected to cover the extent of the regions depicted in the atlas (Paxinos and Franklin, 2007). Stitching and maximum intensity projection images were generated using custom-made macros in Fiji. Automatic nuclei and synaptic spot detection was carried out in Imaris (v9.1.2. Oxford Instruments, Bitplane). Automatic spot detection was visually validated on every section for all experiments. Neurons were detected using TrackMate (Tinevez et al., 2017) assisted by manual curation. The coordinates of detected markers were subsequently transformed into the Allen Brain Atlas Common Coordinate Framework as previously described (Takato et al., 2021). Coordinates of Bregma in Allen CCF were set at AP, 5400; ML, 5700; DV 0 (Shamash et al., 2018; Takato et al., 2021) and were divided by 1000 so that the coordinates in Allen CCF were converted to coordinates in mm (Takato et al., 2021) to fit with a widely-used brain atlas with a numerical coordinate frame (Paxinos and Franklin, 2007).

Extracted coordinates were used to plot the distribution of labeled neurons using custom-built scripts in Python 3.7. 1D density plots were generated using 1D-kernel density estimate (1D-KDE) on antero-posterior, dorso-ventral or medio-lateral axis. The laterality index in Figure 3.3.5D were estimated by calculating the medio-lateral distribution of the synaptic puncta using bins of 30 μ m and obtaining a weighted mean of the centers of the bins, weighted with the proportion of synapses in that bin. 2D

density plots were generated using 2D-kernel density estimate (2D-KDE), plotting 5 or 7 density lines covering the space of 10-100% or 30-100% of highest density using Scipy, a Python library for scientific computing. To perform spatial correlation analysis, the density of synapses (binning into 100x100 pixels for each injection site) from one or multiple sections calculated using 2D-KDE was vectorized, and a correlogram was formed by calculating pairwise cosine similarity (scikit-learn library) between any two injection sites. Hierarchical clustering was performed using the clustering package in Scipy with the Ward variance minimization algorithm in the linkage function using the cosine distances calculated above. For the 3D density of postsynaptically labelled neurons shown in Video S3, the converted cell coordinates were plotted with a custom written code based on the Points function and the PointsDensity function, with a cutoff of 10%, in Brainrender (Claudi et al., 2021) and the color gradient and transparency of the color reflects the density of the distribution of the labelled neurons.

3.5.4.5. Mouselight database analysis

Mouselight is a database from the Janelia Research Campus in which single neurons are reconstructed and registered to the Allen Reference Atlas (Winnubst et al., 2019). To make use of this resources, we turned to Mouselight NeuronBrowser (<http://ml-neuronbrowser.janelia.org/>) and searched for neurons with the following criteria: soma in the cerebral cortex and axon in the medulla, which yielded a total of 39 neurons. We then looked for the number of axon terminals in the medulla following an established method (Morita et al., 2019). Those with more than 5 axon terminals in medulla were further analyzed, resulting in a total of 17 neurons. To map the position of the soma in the cortex, the coordinates of the soma of each neuron in Allen CCF were subtracted by the coordinates of Bregma in Allen CCF (AP, 5400; ML, 5700; DV 0) (Shamash et al., 2018) and were divided by 1000 so that the coordinates in Allen

CCF were converted to coordinates in mm (Takato et al., 2021) to fit with a widely-used brain atlas with a numerical coordinate frame (Paxinos and Franklin, 2007). For neurons whose soma locations are at the left hemisphere, the ML coordinates were mirrored. From the 17 chosen neurons, 13 resided in the anterior cortex (AP coordinates more than 1mm from bregma, Figure 3.3.2C), which were included for further analysis. Among these 13 neurons, 7 neurons resided in the MAC region (ML coordinates less than 1.5mm from midline, Figure 3.3.2D; AA0180, AA0012, AA0250, AA0788, AA0179, AA0576, AA0726) and 6 neurons resided in the LAC region (ML coordinates more than 1.5mm from midline, Figure 3.3.2D; AA1543, AA0133, AA0134, AA0169, AA1043, AA0956). We also obtained the converted coordinates of axon terminals contralateral to the soma from each of these neurons. We plotted the distribution of axon terminals from each neuron along the AP axis in the medulla with the 1D-kernel density estimation. 2D density plots of the distribution of the axon terminals were generated using a 2D-kernel density estimate plotting 5 density lines covering the space of 10- 100% of highest density equally using Scipy. Here, the mediolateral and dorsoventral coordinates of all the terminals was used throughout the anteroposterior extent of the medulla.

3.5.4.6. Behavioral analysis of forelimb movements

To assess the behavior of mice in food reaching and handling under control conditions (PBS) or upon selective cortical silencing, mice were subjected to a behavior session of the reaching and handling task lasting 10 minutes. Mice had previously been trained in the reaching and handling task until proficiency for 7 days (Esposito et al., 2014; Ruder et al., 2021).

For analysis of the behavioral effects upon silencing of cortical domains compared to control conditions, we used deep neural network based markerless pose

estimation using DeepLabCut (Mathis et al., 2018) coupled with high-speed videography of the bottom view of the mouse using Basler Ace2 cameras controlled using Bonsai (Lopes et al., 2015). We used a DeepLabCut model trained using 1100 frames of different videos of mice from the bottom view over behavioral experiments in the lab, with at least 15 frames of each video corresponding to all the different sessions of each mouse in the silencing experiment. The training frames were annotated with the following body parts: nose, head base, forepaws, wrists, body center, hindlimb balls, hindlimb heel, genitals and tail base.

All trials of reaching and handling were annotated manually from the behavioral videos. In case of MAC silencing, all mice ($n=9$) were unable to substantially extend their forelimbs. We therefore annotated attempts where they arrived at the slit and tried to move their forelimb towards the pellet with an apparent desire to reach the pellet. Upon LAC silencing, mice often resorted to eating of the food pellet without forelimb manipulation and these trials were annotated separately and quantified in Figure 3.3.9E. When mice did handle the food pellet with their forelimbs, they displayed a tendency to drop the pellet, and these trials were annotated and quantified separately in Figure 3.3.9E (right). During food handling, we also annotated the number of regrips in each handling bout quantified in Figure 3.3.9F. For the analysis with DLC, the reaching and handling trials were filtered such that trials in which the reaching forelimb paw was not tracked reliably with a confidence level (p) below 0.4 for over 5 frames overall in the trial were excluded and at least 10 trials of each were included for each session. For the others, in case of p falling below the threshold of 0.4, we linearly interpolated the trajectories. For handling, we also annotated the number of regrips during food manipulation.

For the analysis of reaching trajectories as shown in Figure 3.3.9D, we plotted the trajectories for an example mouse. The trajectory was smoothed with a Savitzky-Golay filter. To obtain the average trajectory, we normalized the time from the start of the reach to the time of maximal extension between 0 and 1 and discretized it into 10 equal bins. The individual trials shown for the example mice have all timepoints displayed, with each point representing 1 frame (10ms) apart and color-coded with the normalized time. Three of the mice (3/9) were right handed and their reaching trajectories were flipped to make their trajectories comparable to the left handed mice. The trajectory obtained from each mouse was averaged and is displayed in Figure 3.3.9D (lower right). The maximum extension shown in Figure 3.3.9C was the maximum extension of the limb relative to the slit in the entire session. The reaching velocity was calculated using the differential of the trajectory in the two planes and the magnitude of the velocity was median filtered and estimated as the speed of the forelimb in Figure 3.3.9C. For handling, we again smoothed the trajectories of both forelimb paws using a Savitzky-Golay filter. The trajectories were then rotated such that the axis along the tailbase and midpoint of the forelimb paws at the start of the handling bout was vertically aligned. To study primarily the movement of the distal limbs, the coordinates were shifted such that the midpoint between the limbs was always at the origin at all timepoints. In Figure 3.3.9G, the trajectories of 7 handling trials are displayed for each condition, colored by normalized time. We quantified the movement of the distal limbs as the standard deviation (s.d.) of the forelimb paws' coordinates obtained above averaged for the two paws over all trials, for each mouse across each experimental condition. To account for differences between mice, the s.d. of the forepaws during handling was calculated for each mouse across three conditions.

To normalize s.d. across mice, we divided each of the values by the maximum s.d. for each mouse. The average normalized s.d. are shown in Figure 3.3.9F.

3.5.4.7. Electrophysiological recordings and analysis

To perform *in vivo* extracellular electrophysiological recordings, single-shank chronic 64-channel silicon probes (Cambridge NeuroTech Inc., H5, 0.8mm recording length) or Neuropixels probes (imec, NP1.0) (Jun et al., 2017) were implanted into the latRM contralateral to the side of cortex with virus injection. The implantation was performed essentially as previously described (Ruder et al., 2021). Briefly, a tapered optic fiber (OptogeniX, lambda fiber with 0.5mm active length, 0.39 numerical aperture and 200 μ m diameter) was implanted on the cortex at the location of virus injection. Before probe implantation, Cambridge NeuroTech probes were mounted on a nanodrive (Cambridge NeuroTech Inc.), while Neuropixels probes were mounted on 3D printed fixtures (ATLAS Neuroengineering). The probe was then implanted in the latRM (AP and ML coordinates as for virus injections) at a dorso-ventral depth of around -4.9 mm using light curable cement (Relyx Unicem 2, 3M Inc.). To confirm correct probe placement and to locate recordings sites, a lesion near the tip of the Cambridge NeuroTech probe was produced before perfusion, or a thin layer of Dil (Invitrogen) was applied on Neuropixels probes before implantation (Figure 3.5.1B). We assessed recording sites after termination of experiments by using ChAT immunohistochemistry (see Immunohistochemistry and microscopy) to visualize brainstem motor nuclei (Figure 3.5.1B).

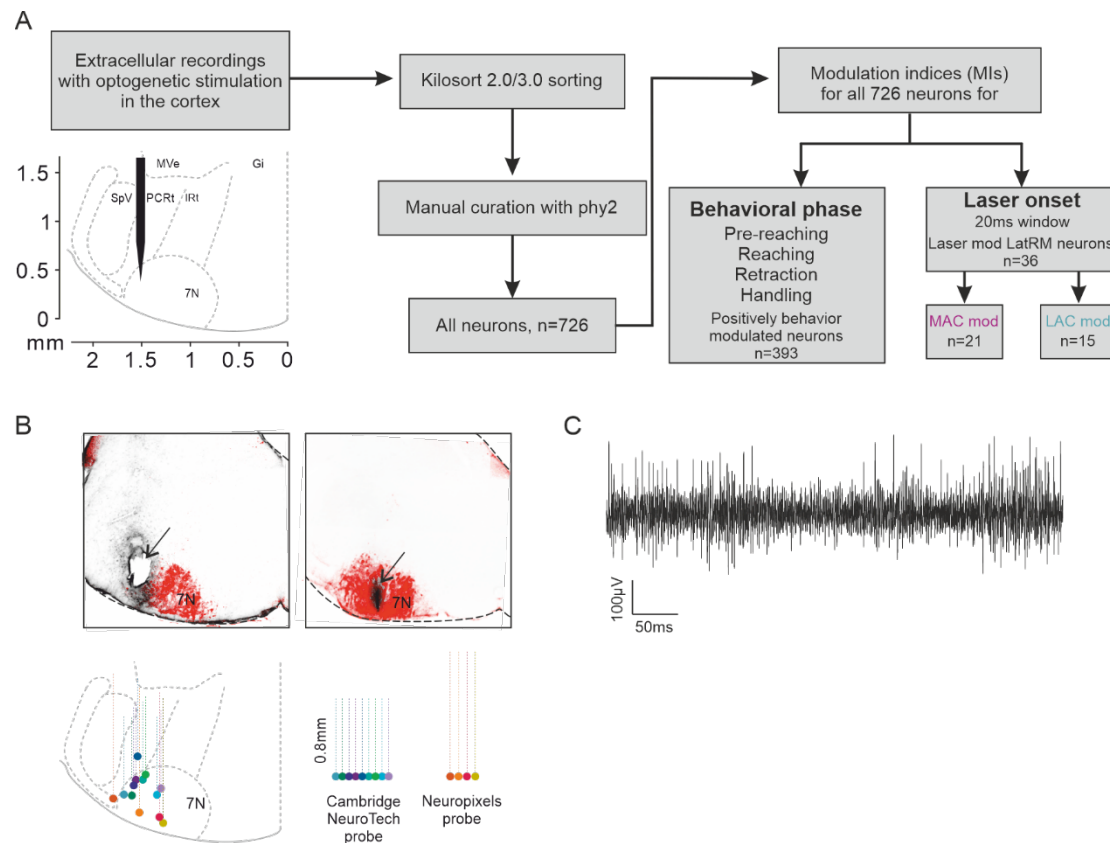


Figure 3.5.1 Analysis of electrophysiology data

(A) Scheme of the pipeline for extracellular electrophysiology recording and analysis.

(B) Upper panel: Representative latRM sections from mouse undergoing single-unit recordings with Cambridge NeuroTech probe (left) or Neuropixels probes (right). The end point of the silicon probe trajectory is either visualized through electrical lesion (left) performed at the end of all recording sessions or from Dil painted on probes before recording (right). Sections are counterstained for ChAT to visualize 7N neurons (red). Lower panel: Reconstruction of probe placements at the rostral medulla level. Dots denote the tips of the probe while the dashed lines show the estimated extension of the probes. Each color corresponds to one mouse analyzed for data shown in Figure 6.

(C) Example of a raw unsorted extracellular voltage trace.

Extracellular electrophysiological data with the Cambridge Neurotech probes was recorded using the Intan 64 channel headstage at an acquisition rate of 30kHz. The camera exposure pulses and laser pulses, from which the timestamps of the camera video frames and laser start were extracted, were obtained aligned to the electrophysiology signal recorded on the Intan RHD USB interface. The recordings were sorted using Kilosort2 (Pachirariu et al., 2016) to obtain isolated single units. The units were then curated using Phy2 (<https://github.com/cortex-lab/phy>) to obtain single

units which were used for subsequent analyses. To confirm correct probe placement and to locate recordings sites, a small current (3s at 200 mA) was delivered to produce a lesion near the tip of the Cambridge NeuroTech probe before withdrawing the probe using an electrical stimulator (WPI Inc., Stimulus isolator A360).

For Neuropixels 1.0 probes, we used the SpikeGLX system to record the electrophysiology signal in synchrony with the laser pulses and camera timestamps collected using the National Instruments PXIe-6341 multifunction IO module coupled with the BNC-2110 breakout box using the National Instruments PXIe/PCIe-8281 controller module. The data was processed using the ecephys spike sorting modules for SpikeGLX (https://github.com/jenniferColonell/ecephys_spike_sorting). Briefly, data collected from SpikeGLX was first processed with the CatGT module to apply demultiplexing corrections and for highpass filtering the data. Additionally, the edges of the synchronization pulses from the IMEC base station on which the Neuropixels data was recorded, the camera exposure pulses and laser pulses were extracted. Subsequently, using the Kilosort helper module, channels with firing rate below 0.05 Hz were excluded as noisy channels and the channel map for the spatial location of the remaining channels was constructed using the metadata from the recordings. We used Bank 0 on the Neuropixels 1.0 to record from the ventral most 384 channels on the probe. Subsequently, Kilosort3 was run on the data. Following the sorting, TPrime module helped synchronize all the datastreams precisely with the IMEC basestation recording used as the reference time stream using the synchronization pulse recorded on both the multifunctional IO device and the IMEC base station. To identify the units in the LatRM, we registered the probe tract identified using the DiI, which was used to mark the Neuropixels probes, to the Allen CCF (https://github.com/petersaj/AP_histology). Using the “ephys alignment tool” from the

International Brain Laboratory (<https://github.com/int-brain-lab/iblapps/wiki>), we aligned the electrophysiological features from the data with the anatomical landmarks to obtain the precise trajectory of the probe. Subsequently, the units on the channels in the LatRM were identified and used for further analysis. We then performed the manual curation of the output of Kilosort3 to obtain isolated single units.

We recorded a total of 726 single units across 13 mice. To determine latRM neurons that modulated their firing in response to different phases of the forelimb reaching and handling task, we calculated Modulation Indices (MIs) for the pre-reaching, reaching, retraction and handling phases. The firing rate was binned into bins of 5ms for subsequent analysis. Briefly, for these behaviors, we calculated the MIs for each trial of the behavior for each neuron as the average firing rate in the behavior window in that trial above the baseline. The distribution of MIs obtained was compared to the distribution of MIs obtained for the same neuron from 1000 random timepoints in a time window equal to the average length of the behavior phase in question using a Mann Whitney U-test. A neuron was classified as positively modulated to a behavioral phase if it had a p-value < 0.01 for this comparison and the average of the MI over all the trials of the behavior was greater than 3. It was classified as negatively modulated at a p-value < 0.01 and MI value < -3 . The validity of this approach can be seen on the heatmap showing the activity of all neurons identified as positively modulated to one of the behavioral phases (Figure 3.3.12). Using the same method, we defined neurons modulated to application of laser light to the cortex as those that significantly changed their firing rate (p-value < 0.001 and MI > 3) in the first 20ms following the onset of the laser that stimulated the cortical neurons. The time windows to calculate the baseline for each trial for each behavioral phase or laser stimulation are defined as following: -0.75s to -0.5s for pre-reach and reach (0s as reach onset); -1s to -0.75s for

retract (0s as retract onset); -1.25s to -1s for handle (0s as handle onset); -0.75s to -0.25s for laser (0s as laser onset). This pipeline is briefly summarized in Figure 3.5.1A. The overall baseline firing rate of each neuron displayed in the activity heatmaps was determined as the average firing rate over the recording session.

In the heatmaps used to display the average activity of the single neurons in Figure 3.3.11D, we first baseline subtracted the activity of the neuron and then normalized the baseline subtracted activity between 0 and 1. For the average activity of the population of neurons tagged from the MAC or the LAC aligned to reach or handle start, we first normalized the activity of all neurons and subtracted the baseline activity of each neuron estimated as the average activity in the time window of -4s to -3s from the onset of the behavior. The normalized average population activity is displayed in Figure 3.3.11D.

3.5.4.8. Statistical analysis

Significance levels indicated are as follows: $*p < 0.05$, $**p < 0.01$, $***p < 0.001$. All values reported in the text and figures represent mean \pm SEM. All statistical analyses were performed using Scipy, statsmodels, and Pingouin packages in Python 3.7. Shapiro-Wilk normality test was applied to check if the data set was normally distributed. Non-normally distributed data were subsequently compared with non-parametric tests. The following statistical tests were used to assess significance when indicated. To compare the number of synapses from different cortical sites in Fig. 2 and S2, we used one-way ANOVA followed by the Tukey HSD test. For rostral medulla levels, $F(4, 25) = 26.04$, $p < 0.001$, pairwise comparison as follows: MAC vs. LAC, $p = 0.2149$, MAC vs. CFA, $p < 0.001$; MAC vs. InsC, $p < 0.001$; MAC vs. Pos, $p < 0.001$; LAC vs. CFA, $p = 0.0349$; LAC vs. InsC, $p = 0.0376$; LAC vs. Pos, $p < 0.001$; CFA vs. InsC, $p = 0.9$; CFA vs. Pos, $p < 0.001$; InsC vs. Pos, $p = 0.0444$. For

intermediate medulla levels, $F(4, 25) = 11.33$, $p < 0.001$, pairwise comparison as follows: MAC vs. LAC, $p = 0.9$; MAC vs. CFA, $p = 0.018$; MAC vs. InsC, $p = 0.0244$; MAC vs. Pos, $p < 0.001$; LAC vs. CFA, $p = 0.0344$; LAC vs. InsC, $p = 0.042$; LAC vs. Pos, $p < 0.001$; CFA vs. InsC, $p = 0.9$; CFA vs. Pos, $p = 0.1054$; InsC vs. Pos, $p = 0.6736$. For caudal medulla levels, $F(4, 25) = 15.28$, $p < 0.001$, pairwise comparison as follows: MAC vs. LAC, $p = 0.2838$; MAC vs. CFA, $p < 0.001$; MAC vs. InsC, $p < 0.001$; MAC vs. Pos, $p < 0.001$; LAC vs. CFA, $p = 0.0424$; LAC vs. InsC, $p = 0.0198$; LAC vs. Pos, $p < 0.001$; CFA vs. InsC, $p = 0.7757$; CFA vs. Pos, $p = 0.1813$; InsC vs. Pos, $p = 0.9$. To compare the peak of synaptic distribution along the dorso-ventral axis in Fig. 3, we used two-way ANOVA followed by the Tukey HSD test. For D-V peak across medullary levels, $F(2, 60) = 1.359$, $p = 0.265$; For D-V peak across cortical regions, $F(3, 60) = 48.779$, $p < 0.001$, pairwise comparison as follows: MAC vs. LAC, $p < 0.001$; MAC vs. CFA, $p = 0.00896$; MAC vs. InsC, $p < 0.001$; LAC vs. CFA, $p < 0.001$; LAC vs. InsC, $p < 0.001$; CFA vs. InsC, $p < 0.001$. To compare the behavioral performance in Fig. 5, we used two-way ANOVA followed by the Tukey HSD test, except for the reach speed which was compared with the paired t-test. For the number of reaches per minute, $F(2, 16) = 13.116$, $p < 0.001$, pairwise comparison as follows: MAC vs. LAC, $p < 0.001$; MAC vs. Con, $p = 0.0025$; LAC vs. Con, $p = 0.2107$. For maximum extension, $F(2, 16) = 47.071$, $p < 0.001$, pairwise comparison as follows: MAC vs. LAC, $p < 0.001$; MAC vs. Con, $p < 0.001$; LAC vs. Con, $p = 0.026$. For reach speed, $p = 0.676$. For percentage of eating without forelimb, $F(2, 16) = 72.166$, $p < 0.001$, pairwise comparison as follows: MAC vs. LAC, $p < 0.001$; MAC vs. Con, $p = 0.3466$; LAC vs. Con, $p < 0.001$. For percentage of pellet drop during eating, $F(2, 14) = 40.311$, $p < 0.001$, pairwise comparison as follows: MAC vs. LAC, $p < 0.001$; MAC vs. Con, $p = 0.966$; LAC vs. Con, $p < 0.001$. For the number of regrips per second, $F(2,$

14) = 15.72, $p < 0.001$, pairwise comparison as follows: MAC vs. LAC, $p = 0.00898$; MAC vs. Con, $p = 0.7747$; LAC vs. Con, $p < 0.001$. For normalized SD of FLs during handling, $F(2, 14) = 8.93$, $p = 0.00316$, pairwise comparison as follows: MAC vs. LAC, $p = 0.0457$; MAC vs. Con, $p = 0.0841$; LAC vs. Con, $p < 0.001$. To compare the averaged firing rate between tagged neurons in Fig. 7, we used the Wilcoxon signed rank test. For firing rate aligned to reach onset, the task window is defined by -0.5 to 0.5s from reach onset, MAC vs. LAC, $p < 0.001$. For firing rate aligned to handle onset, the task window is defined by handle onset to 1s, MAC vs. LAC, $p < 0.001$.

Acknowledgements

We are grateful to M. Sigrist, M. Mielich, C. Nyerges, A. Schwarzmüller, A. Gerber, T. Brumm, S. Voggensperger for expert experimental help, to K. Bhandari and P. Caroni for help and advice with loss-of-function experiments, to P. Caroni, F. Donato, B. Roska and A. Falasconi for discussions and comments on the manuscript, and to all members of the Arber laboratory for feedback throughout the project. W.Y. and H.K. were supported by a Biozentrum PhD Fellowship, and all authors by an ERC Advanced Grant (No 692617), the Swiss National Science Foundation, the Kanton Basel-Stadt, the Novartis Research Foundation, and the Louis Jeantet Prize for Medicine.

Author Contributions

All authors were involved in the design of experiments and data analysis. W.Y. carried out most anatomy experiments, and these were analyzed jointly by W.Y. and H.K. Neuronal recording and silencing experiments were carried out and analyzed jointly by W.Y. and H.K. S.A. initiated the project and wrote the manuscript with contributions from W.Y. and H.K. All authors discussed the experiments and commented on the manuscript.

Declaration of interests

The authors declare no competing interests.

4. Conclusions and outlook

4.1. Hierarchical and interconnected motor pathways

Our results, together with other studies, demonstrate a wide broadcasting system for cortical control of movement while maintaining the specificity when contacting specific brain regions (Arber and Costa, 2018). Specialized neuronal networks for motor control are distributed across the brain and cortex has access to many of them. This feature likely suggests an important role of the cortex in the orchestration of neuronal activity in different brain regions to produce coherent motor outputs. Importantly, neuronal circuits in different cortical regions influence distinct subnetworks in connected structures, emphasizing the highly organized neuronal circuits for specialized functions.

Evolutionally, the cerebral cortex is a relatively new structure. Therefore, cortical neurons must build their functions based on existing foundations and by interacting with existing structures. The adoption of cortex might, in turn, lead to the attenuation or downgrading of some structures as their functions are being taken over. For example, in rodents, the red nucleus contains a big portion of magnocellular neurons which project to the spinal cord, while in primates, the magnocellular part of the red nucleus is small and the rubrospinal pathway becomes dispensable, which might be owing to the development of cortico-spinal projections (Basile et al., 2020). The placement of the cortex which is at the very exterior of the brain allows for easy expansion of cortical areas and volume (Figure 2.1.2A). The benefit of these enlarged areas is obvious for its expanded capacity to host more neurons and therefore possibly also more specialized functions (Berg et al., 2021). For example, in the visual cortex of cat and primate, neurons are organized into orientation columns (Hubel and Wiesel, 1962; Kaschube et al., 2010), but in rodent, neurons with different visual orientation

are intermingled likely due to limited cortical area which is correlated with reduced visual sensation (Kondo et al., 2016). The expansion of motor and premotor areas in primate is conceptually beneficial in generating complex movements as the cortical magnification allows for more detailed neuronal representation (Kaas, 2008). Therefore, more specialized cortical regions, with the collaboration of evolutionarily old subcortical structures, might help to realize more functions which would not be possible to achieve without cortical expansion (Figure 2.1.2A).

However, regional specificity cannot explain the diverse behaviors that animals can perform. For example, playing the piano needs not only a sequence of figure movements but also the force of each finger to apply on the keys, the temporal intervals of the notes and many more parameters. That is why it is important to increase the granularity to dissect neuronal circuits (Figure 2.3.1C). Some studies suggest that highly selective neurons encode different details. This hypothesis is supported by the place cells in hippocampus which only fire if the animal moves through a particular spatial location (Wilson and McNaughton, 1993; Ekstrom et al., 2003) as well as a more extreme example, the so-called “grandma cell” that fires in response to particular people (Young and Yamane, 1992; Quiroga et al., 2005). In motor cortex, it is also reported that stimulation of one single neuron is able to elicit movement (Brecht et al., 2004). However, neurons cannot be functional if not interconnected with other neurons and the specificity of neurons relies on broadly distributed neuronal networks. For example, the representation of spatial location in the place cells can be derived from the neuronal activity of grid cells in the medial entorhinal cortex (Moser et al., 2008). Following this line of arguments, it will be interesting to reveal how specialized subcircuits in the motor cortex emerged and control detailed movement-related parameters of movements (Figure 2.3.1C). The specialized subcircuits might be responsible for simple parameters

such as the direction of movement, velocity, acceleration, posture and joint torques, and the combination of subcircuits constructs the whole movement. In addition, those subcircuits might be reusable in other motor programs, expanding the capacity of cortical control of movement while avoiding the demands to overwhelmingly increase the number of neurons.

4.2. Closed-loop organization for motor control

In the most simplistic model, the brain is an input-output device which receives sensory input while executes motor output. However, this feedforward model can only be explanatory if the brain has all required motor programs imprinted, which is not the case for biological brain because motor functions are shaped based on postnatal experience and constant learning (Dominici et al., 2011; Makino et al., 2016). As an autonomous learning machine, the brain requires “closed-loop” feedback control so that it can learn to correct its errors, whereas open-loop systems cannot automatically correct errors from outcomes, and are not able to adapt to changes in the environment (Wiener, 1961). The closed-loop organization provides a mechanism for a system to be self-consistent, which has been suggested to sufficiently lead learning to be autonomous and adaptive (Ma et al., 2022). To allow such closed-loop feedback control, the brain needs not only to generate motor planning based on bottom-up sensory input from peripheral, but also to estimate and to predict the context changes during movement, as well as to compare the internal estimation and prediction with the consequences of the motor output using motor error signals (Figure 2.4.4A) (Wolpert and Ghahramani, 2000).

Interesting, as reviewed above, the cortex appears to be a hub involved in cortico-cortical, cortico-basal ganglia and cortico-thalamic circuits, all of which exhibit

the closed-loop organization, and other brain structures including cerebellum, superior colliculus, pontine nucleus, etc., also participate in those circuits, forming complex networks and providing ample possibilities to realized closed-loop feedback control. For example, one recent study reports that the cortex is necessary for corrective sub-movements to timely adjust the motor control of the tongue (Bollu et al., 2021), but the circuit mechanisms remain unknown. Our results reveal the topographical organization of the cortico-medullary projections and the cortico-medullary neurons send collaterals to other subcortical structures including striatum and superior colliculus, delivering copies of motor command to other motor structures. These collateral information streams transmitted to different domains might not only be used for different parameters of movement, but also contribute to the closed-loop feedback organization for precise control and motor learning, such as an update of the movement plan to other motor centers, a comparison with the information from the external circumstances through the sensory afferent pathway, and fine adjustments according to the outcomes with motor error signals. The cortical signal can also be a driver to initiate the operation of subcortical networks for automatic motor correction independently of cortex. Future work assigning specific functions to these circuits with the overarching goal to achieve a coherent model and to understand how they influence motor control will be particularly instructive.

4.3. Open questions and challenges

Neuroscience has made much progress in dissecting neuronal circuits at high granularity and assigning functions to different circuits. But it is a long-term challenge to align the carefully dissected circuits with well-defined functions. This requires tools to disentangle the spatially intermingled neurons and at the same time tracking their activity *in vivo* while the animal is performing behavioral tasks. For example,

tremendous efforts have been made to align the neuronal population in motor cortex on the basis of neuronal morphology, molecular, genetic and epigenetic traits, developmental programs as well as electrophysiological properties (BRAIN Initiative Cell Census Network (BICCN), 2021). However, it is still unknown how these neurons are assemble into circuits and their functions in motor control. To tackle those questions, state-of-the-art approaches to trace presynaptic and postsynaptic components of defined neuronal populations would be handy, which might require recently developed rabies virus whose expression can be stopped so as to avoid killing the infected neurons (Ciabatti et al., 2017), and yellow fever virus anterogradely monosynaptic tracing of downstream neurons (Li et al., 2021). Together with such viral tools, advanced recording techniques such as Neuropixels silicon probes for simultaneous recordings across a wide range of brain regions (Steinmetz et al., 2021), as well as miniature two photon microscopy to image the calcium activity of neurons and subcellular compartment like dendrite over a long period of time in free moving animals (Zong et al., 2022), will be particularly useful to uncover the organization and the functions of the neuronal circuits. In addition, more and more efficient tools to activate (Fenno et al., 2011; Chen et al., 2020) or silence (Wiegert et al., 2017; Mahn et al., 2018) specific neuronal populations and synapses provide the opportunity to build the causality between recording data of circuits and their functional contributions. All this progress will lead research in neuroscience to another level for understanding the nature of the nervous system.

5. Acknowledgments

First and foremost, I would like to thank my PhD supervisor, Professor Silvia Arber. During my whole PhD time, she shows enormous passion for science, excellent expertise and knowledge of the nervous system and great patient for educating students. All the training I received from her is extremely valuable for my further career. I am really appreciated to all her efforts for my education.

Moreover, I would like to thank my committee members, Prof. Botond Roska and Prof. Pico Caroni, for providing insightful suggestions throughout the years and being an inspiration to me in my scientific journey. I would also like to thank Prof. Carl Petersen for his time in reviewing my thesis. I am looking forward to the discussion with them on my defense.

A heartfelt thank you goes to all present and past members of the Arber lab. All of your kindness and warmth makes the lab as a big family. Ludwig Ruder guided me experiment and fitted me to the lab at the very beginning when I joined. Harsh Kanodia offered great help to push the project to finish; it would not have been successful without your help. Riccardo Schina supported me in difficult times and brought me joy of life both inside and outside the lab. A big thank you to Staci Thornton who has always been the best companion sharing this journey with me, and to Ana Rita Afonso, I shall never forget the stimulating scientific and philosophical discussions with you.

Most importantly, I would like to show my love to my parents. No matter I got little progress or a big failure, they are always supportive and caring. Without their love and encouragement, I will never be able to have the faith of finishing my study. 谢谢你们!

6. References

- Adams, J.H., Graham, D.I., and Jennett, B. (2000). The neuropathology of the vegetative state after an acute brain insult. *Brain* 123, 1327–1338. <https://doi.org/10.1093/brain/123.7.1327>.
- Alexander, G.E., DeLong, M.R., and Strick, P.L. (1986). Parallel Organization of Functionally Segregated Circuits Linking Basal Ganglia and Cortex. *Annu. Rev. Neurosci.* 9, 357–381. <https://doi.org/10.1146/annurev.ne.09.030186.002041>.
- Araneda, R., and Andrade, R. (1991). 5-Hydroxytryptamine₂ and 5-hydroxytryptamine_{1A} receptors mediate opposing responses on membrane excitability in rat association cortex. *Neuroscience* 40, 399–412. [https://doi.org/10.1016/0306-4522\(91\)90128-B](https://doi.org/10.1016/0306-4522(91)90128-B).
- Arber, S., and Costa, R.M. (2018). Connecting neuronal circuits for movement. *Science* 360, 1403–1404. <https://doi.org/10.1126/science.aat5994>.
- Arber, S., and Costa, R.M. (2022). Networking brainstem and basal ganglia circuits for movement. *Nat. Rev. Neurosci.* 1–19. <https://doi.org/10.1038/s41583-022-00581-w>.
- Ascoli, G.A., Alonso-Nanclares, L., Anderson, S.A., Barrionuevo, G., Benavides-Piccione, R., Burkhalter, A., Buzsáki, G., Cauli, B., DeFelipe, J., Fairén, A., et al. (2008). Petilla terminology: nomenclature of features of GABAergic interneurons of the cerebral cortex. *Nat. Rev. Neurosci.* 9, 557–568. <https://doi.org/10.1038/nrn2402>.
- Barbier, M., Chometton, S., Pautrat, A., Miguët-Alfonsi, C., Datiche, F., Gascuel, J., Fellmann, D., Peterschmitt, Y., Coizet, V., and Risold, P.-Y. (2020). A basal ganglia-like cortical–amygdalar–hypothalamic network mediates feeding behavior. *Proc. Natl. Acad. Sci.* 117, 15967–15976. <https://doi.org/10.1073/pnas.2004914117>.
- Barnes, T.D., Kubota, Y., Hu, D., Jin, D.Z., and Graybiel, A.M. (2005). Activity of striatal neurons reflects dynamic encoding and recoding of procedural memories. *Nature* 437, 1158–1161. <https://doi.org/10.1038/nature04053>.
- Basaldella, E., Takeoka, A., Sigrist, M., and Arber, S. (2015). Multisensory Signaling Shapes Vestibulo-Motor Circuit Specificity. *Cell* 163, 301–312. <https://doi.org/10.1016/j.cell.2015.09.023>.
- Basile, G.A., Quartu, M., Bertino, S., Serra, M.P., Boi, M., Bramanti, A., Anastasi, G.P., Milardi, D., and Cacciola, A. (2020). Red nucleus structure and function: from anatomy to clinical neurosciences. *Brain Struct. Funct.* <https://doi.org/10.1007/s00429-020-02171-x>.
- Berg, J., Sorensen, S.A., Ting, J.T., Miller, J.A., Chartrand, T., Buchin, A., Bakken, T.E., Budzillo, A., Dee, N., Ding, S.-L., et al. (2021). Human neocortical expansion involves glutamatergic neuron diversification. *Nature* 598, 151–158. <https://doi.org/10.1038/s41586-021-03813-8>.

Berridge, K.C. (1989). Progressive degradation of serial grooming chains by descending decerebration. *Behav. Brain Res.* 33, 241–253. [https://doi.org/10.1016/S0166-4328\(89\)80119-6](https://doi.org/10.1016/S0166-4328(89)80119-6).

Bobadilla, A.-C., Heinsbroek, J.A., Gipson, C.D., Griffin, W.C., Fowler, C.D., Kenny, P.J., and Kalivas, P.W. (2017). Chapter 4 - Corticostriatal plasticity, neuronal ensembles, and regulation of drug-seeking behavior. In *Progress in Brain Research*, T. Calvey, and W.M.U. Daniels, eds. (Elsevier), pp. 93–112.

Bollu, T., Ito, B.S., Whitehead, S.C., Kardon, B., Redd, J., Liu, M.H., and Goldberg, J.H. (2021). Cortex-dependent corrections as the tongue reaches for and misses targets. *Nature* 594, 82–87. <https://doi.org/10.1038/s41586-021-03561-9>.

Born, R.T., and Bradley, D.C. (2005). Structure and Function of Visual Area Mt. *Annu. Rev. Neurosci.* 28, 157–189. <https://doi.org/10.1146/annurev.neuro.26.041002.131052>.

Bortone, D.S., Olsen, S.R., and Scanziani, M. (2014). Translaminar Inhibitory Cells Recruited by Layer 6 Corticothalamic Neurons Suppress Visual Cortex. *Neuron* 82, 474–485. <https://doi.org/10.1016/j.neuron.2014.02.021>.

BRAIN Initiative Cell Census Network (BICCN) (2021). A multimodal cell census and atlas of the mammalian primary motor cortex. *Nature* 598, 86–102. <https://doi.org/10.1038/s41586-021-03950-0>.

Brecht, M., Schneider, M., Sakmann, B., and Margrie, T.W. (2004). Whisker movements evoked by stimulation of single pyramidal cells in rat motor cortex. *Nature* 427, 704–710. <https://doi.org/10.1038/nature02266>.

Brodmann, K. (1909). *Vergleichende Lokalisationslehre der Großhirnrinde : in ihren Prinzipien dargestellt auf Grund des Zellenbaues* / von K. Brodmann (Leipzig: Barth).

Brown, J.A. (2006). Recovery of motor function after stroke. In *Progress in Brain Research*, A.R. Möller, ed. (Elsevier), pp. 223–228.

Brown, S.P., and Hestrin, S. (2009). Intracortical circuits of pyramidal neurons reflect their long-range axonal targets. *Nature* 457, 1133–1136. <https://doi.org/10.1038/nature07658>.

Bruno, R.M., and Sakmann, B. (2006). Cortex Is Driven by Weak but Synchronously Active Thalamocortical Synapses. *Science* 312, 1622–1627. <https://doi.org/10.1126/science.1124593>.

Cajal, S.R. y (1899). *Comparative study of the sensory areas of the human cortex*.

Cao, V.Y., Ye, Y., Mastwal, S., Ren, M., Coon, M., Liu, Q., Costa, R.M., and Wang, K.H. (2015). Motor Learning Consolidates Arc-Expressing Neuronal Ensembles in Secondary Motor Cortex. *Neuron* 86, 1385–1392. <https://doi.org/10.1016/j.neuron.2015.05.022>.

Capelli, P., Pivetta, C., Soledad Esposito, M., and Arber, S. (2017). Locomotor speed control circuits in the caudal brainstem. *Nature* 551, 373–377. <https://doi.org/10.1038/nature24064>.

- Chen, J.L., Carta, S., Soldado-Magraner, J., Schneider, B.L., and Helmchen, F. (2013). Behaviour-dependent recruitment of long-range projection neurons in somatosensory cortex. *Nature* 499, 336–340. <https://doi.org/10.1038/nature12236>.
- Chen, R., Gore, F., Nguyen, Q.-A., Ramakrishnan, C., Patel, S., Kim, S.H., Raffiee, M., Kim, Y.S., Hsueh, B., Krook-Magnusson, E., et al. (2020). Deep brain optogenetics without intracranial surgery. *Nat. Biotechnol.* 1–4. <https://doi.org/10.1038/s41587-020-0679-9>.
- Ciabatti, E., González-Rueda, A., Mariotti, L., Morgese, F., and Tripodi, M. (2017). Life-Long Genetic and Functional Access to Neural Circuits Using Self-Inactivating Rabies Virus. *Cell* 170, 382–392.e14. <https://doi.org/10.1016/j.cell.2017.06.014>.
- Claudi, F., Tyson, A.L., Petrucco, L., Margrie, T.W., Portugues, R., and Branco, T. (2021). Visualizing anatomically registered data with brainrender. *ELife* 10, e65751. <https://doi.org/10.7554/eLife.65751>.
- Collins, D.P., and Anastasiades, P.G. (2019). Cellular Specificity of Cortico-Thalamic Loops for Motor Planning. *J. Neurosci.* 39, 2577–2580. <https://doi.org/10.1523/JNEUROSCI.2964-18.2019>.
- Conner, J.M., Bohannon, A., Igarashi, M., Taniguchi, J., Baltar, N., and Azim, E. (2021). Modulation of tactile feedback for the execution of dexterous movement. *Science* 374, 316–323. <https://doi.org/10.1126/science.abh1123>.
- Constantinople, C.M., and Bruno, R.M. (2013). Deep Cortical Layers Are Activated Directly by Thalamus. *Science* 340, 1591–1594. <https://doi.org/10.1126/science.1236425>.
- Costa, R.M., Cohen, D., and Nicolelis, M.A.L. (2004). Differential Corticostriatal Plasticity during Fast and Slow Motor Skill Learning in Mice. *Curr. Biol.* 14, 1124–1134. <https://doi.org/10.1016/j.cub.2004.06.053>.
- Cragg, S.J. (2006). Meaningful silences: how dopamine listens to the ACh pause. *Trends Neurosci.* 29, 125–131. <https://doi.org/10.1016/j.tins.2006.01.003>.
- Crandall, S.R., Cruikshank, S.J., and Connors, B.W. (2015). A Corticothalamic Switch: Controlling the Thalamus with Dynamic Synapses. *Neuron* 86, 768–782. <https://doi.org/10.1016/j.neuron.2015.03.040>.
- Cregg, J.M., Leiras, R., Montalant, A., Wanken, P., Wickersham, I.R., and Kiehn, O. (2020). Brainstem neurons that command mammalian locomotor asymmetries. *Nat. Neurosci.* 23, 730–740. <https://doi.org/10.1038/s41593-020-0633-7>.
- Crick, F., and Koch, C. (1998). Constraints on cortical and thalamic projections: the no-strong-loops hypothesis. *Nature* 391, 245–250. <https://doi.org/10.1038/34584>.
- Cui, G., Jun, S.B., Jin, X., Pham, M.D., Vogel, S.S., Lovinger, D.M., and Costa, R.M. (2013). Concurrent activation of striatal direct and indirect pathways during action initiation. *Nature* 494, 238–242. <https://doi.org/10.1038/nature11846>.

- Dembrow, N.C., Chitwood, R.A., and Johnston, D. (2010). Projection-Specific Neuromodulation of Medial Prefrontal Cortex Neurons. *J. Neurosci.* *30*, 16922–16937. <https://doi.org/10.1523/JNEUROSCI.3644-10.2010>.
- Dhawale, A.K., Wolff, S.B.E., Ko, R., and Ölveczky, B.P. (2021). The basal ganglia control the detailed kinematics of learned motor skills. *Nat. Neurosci.* *24*, 1256–1269. <https://doi.org/10.1038/s41593-021-00889-3>.
- Di Bella, D.J., Habibi, E., Stickels, R.R., Scalia, G., Brown, J., Yadollahpour, P., Yang, S.M., Abbate, C., Biancalani, T., Macosko, E.Z., et al. (2021). Molecular logic of cellular diversification in the mouse cerebral cortex. *Nature* *595*, 554–559. <https://doi.org/10.1038/s41586-021-03670-5>.
- Di Filippo, M., Picconi, B., Tantucci, M., Ghiglieri, V., Bagetta, V., Sgobio, C., Tozzi, A., Parnetti, L., and Calabresi, P. (2009). Short-term and long-term plasticity at corticostriatal synapses: Implications for learning and memory. *Behav. Brain Res.* *199*, 108–118. <https://doi.org/10.1016/j.bbr.2008.09.025>.
- Dittrich, L., Heiss, J., Warrier, D., Perez, X., Quik, M., and Kilduff, T. (2012). Cortical nNOS neurons co-express the NK1 receptor and are depolarized by Substance P in multiple mammalian species. *Front. Neural Circuits* *6*.
- Dominici, N., Ivanenko, Y.P., Cappellini, G., d’Avella, A., Mondì, V., Cicchese, M., Fabiano, A., Silei, T., Paolo, A.D., Giannini, C., et al. (2011). Locomotor Primitives in Newborn Babies and Their Development. *Science* *334*, 997–999. <https://doi.org/10.1126/science.1210617>.
- Douglas, R.J., Koch, C., Mahowald, M., Martin, K.A.C., and Suarez, H.H. (1995). Recurrent Excitation in Neocortical Circuits. *Science* *269*, 981–985. <https://doi.org/10.1126/science.7638624>.
- Economo, M.N., Viswanathan, S., Tasic, B., Bas, E., Winnubst, J., Menon, V., Graybiack, L.T., Nguyen, T.N., Smith, K.A., Yao, Z., et al. (2018). Distinct descending motor cortex pathways and their roles in movement. *Nature* *563*, 79. <https://doi.org/10.1038/s41586-018-0642-9>.
- Ekstrom, A.D., Kahana, M.J., Caplan, J.B., Fields, T.A., Isham, E.A., Newman, E.L., and Fried, I. (2003). Cellular networks underlying human spatial navigation. *Nature* *425*, 184–188. <https://doi.org/10.1038/nature01964>.
- English, D.F., Ibanez-Sandoval, O., Stark, E., Tecuapetla, F., Buzsaki, G., Deisseroth, K., Tepper, J.M., and Koos, T. (2012). GABAergic circuits mediate the reinforcement-related signals of striatal cholinergic interneurons. *Nat Neurosci* *15*, 123–130. <https://doi.org/10.1038/nn.2984>.
- Erzurumlu, R.S., and Gaspar, P. (2012). Development and critical period plasticity of the barrel cortex. *Eur. J. Neurosci.* *35*, 1540–1553. <https://doi.org/10.1111/j.1460-9568.2012.08075.x>.
- Esposito, M.S., Capelli, P., and Arber, S. (2014). Brainstem nucleus MdV mediates skilled forelimb motor tasks. *Nature* *508*, 351–356. <https://doi.org/10.1038/nature13023>.

- Fang, R., Xia, C., Close, J.L., Zhang, M., He, J., Huang, Z., Halpern, A.R., Long, B., Miller, J.A., Lein, E.S., et al. (2022). Conservation and divergence of cortical cell organization in human and mouse revealed by MERFISH. *Science* 377, 56–62. <https://doi.org/10.1126/science.abm1741>.
- Fenno, L., Yizhar, O., and Deisseroth, K. (2011). The Development and Application of Optogenetics. *Annu. Rev. Neurosci.* 34, 389–412. <https://doi.org/10.1146/annurev-neuro-061010-113817>.
- Ferezou, I., Haiss, F., Gentet, L.J., Aronoff, R., Weber, B., and Petersen, C.C.H. (2007). Spatiotemporal Dynamics of Cortical Sensorimotor Integration in Behaving Mice. *Neuron* 56, 907–923. <https://doi.org/10.1016/j.neuron.2007.10.007>.
- Ferreira-Pinto, M.J., Kanodia, H., Falasconi, A., Sigrist, M., Esposito, M.S., and Arber, S. (2021). Functional diversity for body actions in the mesencephalic locomotor region. *Cell* 184, 4564–4578.e18. <https://doi.org/10.1016/j.cell.2021.07.002>.
- Ferrier, D., and Burdon-Sanderson, J.S. (1875). Experiments on the brain of monkeys.—No. I. *Proc. R. Soc. Lond.* 23, 409–430. <https://doi.org/10.1098/rspl.1874.0058>.
- Fino, E., Glowinski, J., and Venance, L. (2005). Bidirectional Activity-Dependent Plasticity at Corticostriatal Synapses. *J. Neurosci.* 25, 11279–11287. <https://doi.org/10.1523/JNEUROSCI.4476-05.2005>.
- Fisher, S.D., Robertson, P.B., Black, M.J., Redgrave, P., Sagar, M.A., Abraham, W.C., and Reynolds, J.N.J. (2017). Reinforcement determines the timing dependence of corticostriatal synaptic plasticity in vivo. *Nat. Commun.* 8, 334. <https://doi.org/10.1038/s41467-017-00394-x>.
- Foster, N.N., Barry, J., Korobkova, L., Garcia, L., Gao, L., Becerra, M., Sherafat, Y., Peng, B., Li, X., Choi, J.-H., et al. (2021). The mouse cortico–basal ganglia–thalamic network. *Nature* 598, 188–194. <https://doi.org/10.1038/s41586-021-03993-3>.
- Friel, K.M., Barbay, S., Frost, S.B., Plautz, E.J., Stowe, A.M., Dancause, N., Zoubina, E.V., and Nudo, R.J. (2007). Effects of a Rostral Motor Cortex Lesion on Primary Motor Cortex Hand Representation Topography in Primates. *Neurorehabil. Neural Repair* 21, 51–61. <https://doi.org/10.1177/1545968306291851>.
- Fritsch, G., and Hitzig, E. (2009). Electric excitability of the cerebrum (Über die elektrische Erregbarkeit des Grosshirns). *Epilepsy Behav.* 15, 123–130. <https://doi.org/10.1016/j.yebeh.2009.03.001>.
- Galiñanes, G.L., Bonardi, C., and Huber, D. (2018). Directional Reaching for Water as a Cortex-Dependent Behavioral Framework for Mice. *Cell Rep.* 22, 2767–2783. <https://doi.org/10.1016/j.celrep.2018.02.042>.
- Gaspar, P., Bloch, B., and Le Moine, C. (1995). D1 and D2 Receptor Gene Expression in the Rat Frontal Cortex: Cellular Localization in Different Classes of Efferent Neurons. *Eur. J. Neurosci.* 7, 1050–1063. <https://doi.org/10.1111/j.1460-9568.1995.tb01092.x>.

- Gerfen, C.R., and Sawchenko, P.E. (1984). An anterograde neuroanatomical tracing method that shows the detailed morphology of neurons, their axons and terminals: Immunohistochemical localization of an axonally transported plant lectin, Phaseolus vulgaris leucoagglutinin (PHA-L). *Brain Res.* 290, 219–238. [https://doi.org/10.1016/0006-8993\(84\)90940-5](https://doi.org/10.1016/0006-8993(84)90940-5).
- Goulding, M. (2009). Circuits controlling vertebrate locomotion: moving in a new direction. *Nat. Rev. Neurosci.* 10, 507–518. <https://doi.org/10.1038/nrn2608>.
- Graziano, M.S.A., Taylor, C.S.R., and Moore, T. (2002). Complex Movements Evoked by Microstimulation of Precentral Cortex. *Neuron* 34, 841–851. [https://doi.org/10.1016/S0896-6273\(02\)00698-0](https://doi.org/10.1016/S0896-6273(02)00698-0).
- Gu, Z., Kalamboglas, J., Yoshioka, S., Han, W., Li, Z., Kawasaki, Y.I., Pochareddy, S., Li, Z., Liu, F., Xu, X., et al. (2017). Control of species-dependent cortico-motoneuronal connections underlying manual dexterity. *Science* 357, 400–404. <https://doi.org/10.1126/science.aan3721>.
- Guillery, R.W., and Sherman, S.M. (2002). Thalamic Relay Functions and Their Role in Corticocortical Communication: Generalizations from the Visual System. *Neuron* 33, 163–175. [https://doi.org/10.1016/S0896-6273\(01\)00582-7](https://doi.org/10.1016/S0896-6273(01)00582-7).
- Guo, J.-Z., Graves, A.R., Guo, W.W., Zheng, J., Lee, A., Rodríguez-González, J., Li, N., Macklin, J.J., Phillips, J.W., Mensh, B.D., et al. (2015). Cortex commands the performance of skilled movement. *ELife* 4, e10774. <https://doi.org/10.7554/eLife.10774>.
- Guo, K., Yamawaki, N., Svoboda, K., and Shepherd, G.M.G. (2018). Anterolateral Motor Cortex Connects with a Medial Subdivision of Ventromedial Thalamus through Cell Type-Specific Circuits, Forming an Excitatory Thalamo-Cortico-Thalamic Loop via Layer 1 Apical Tuft Dendrites of Layer 5B Pyramidal Tract Type Neurons. *J. Neurosci.* 38, 8787–8797. <https://doi.org/10.1523/JNEUROSCI.1333-18.2018>.
- Guo, Z.V., Inagaki, H.K., Daie, K., Druckmann, S., Gerfen, C.R., and Svoboda, K. (2017). Maintenance of persistent activity in a frontal thalamocortical loop. *Nature* 545, 181–186. <https://doi.org/10.1038/nature22324>.
- Han, Y., Kebschull, J.M., Campbell, R.A.A., Cowan, D., Imhof, F., Zador, A.M., and Mrsic-Flogel, T.D. (2018). The logic of single-cell projections from visual cortex. *Nature* 556, 51–56. <https://doi.org/10.1038/nature26159>.
- Harris, K.D., and Mrsic-Flogel, T.D. (2013). Cortical connectivity and sensory coding. *Nature* 503, 51–58. <https://doi.org/10.1038/nature12654>.
- Harris, J.A., Mihalas, S., Hirokawa, K.E., Whitesell, J.D., Choi, H., Bernard, A., Bohn, P., Caldejon, S., Casal, L., Cho, A., et al. (2019). Hierarchical organization of cortical and thalamic connectivity. *Nature* 575, 195–202. <https://doi.org/10.1038/s41586-019-1716-z>.
- Harrison, T.C., Ayling, O.G.S., and Murphy, T.H. (2012). Distinct Cortical Circuit Mechanisms for Complex Forelimb Movement and Motor Map Topography. *Neuron* 74, 397–409. <https://doi.org/10.1016/j.neuron.2012.02.028>.

- Hebb, D.O. (2002). *The organization of behavior: a neuropsychological theory* (Mahwah, N.J: L. Erlbaum Associates).
- Heekeren, H.R., Marrett, S., and Ungerleider, L.G. (2008). The neural systems that mediate human perceptual decision making. *Nat. Rev. Neurosci.* 9, 467–479. <https://doi.org/10.1038/nrn2374>.
- Heffner, R., and Masterton, B. (1975). Variation in Form of the Pyramidal Tract and Its Relationship to Digital Dexterity; pp. 161–174. *Brain. Behav. Evol.* 12, 161–174. <https://doi.org/10.1159/000124401>.
- Heindorf, M., Arber, S., and Keller, G.B. (2018). Mouse Motor Cortex Coordinates the Behavioral Response to Unpredicted Sensory Feedback. *Neuron* 99, 1040-1054.e5. <https://doi.org/10.1016/j.neuron.2018.07.046>.
- Hensch, T.K. (2005). Critical period plasticity in local cortical circuits. *Nat Rev Neurosci* 6, 877–888. <https://doi.org/10.1038/nrn1787>.
- Hikosaka, O., Takikawa, Y., and Kawagoe, R. (2000). Role of the Basal Ganglia in the Control of Purposive Saccadic Eye Movements. *Physiol. Rev.* 80, 953–978. <https://doi.org/10.1152/physrev.2000.80.3.953>.
- Hilscher, M.M., Leão, R.N., Edwards, S.J., Leão, K.E., and Kullander, K. (2017). ChRNA2-Martinotti Cells Synchronize Layer 5 Type A Pyramidal Cells via Rebound Excitation. *PLOS Biol.* 15, e2001392. <https://doi.org/10.1371/journal.pbio.2001392>.
- Hintiryan, H., Foster, N.N., Bowman, I., Bay, M., Song, M.Y., Gou, L., Yamashita, S., Bienkowski, M.S., Zingg, B., Zhu, M., et al. (2016). The mouse cortico-striatal projectome. *Nat. Neurosci.* 19, 1100–1114. <https://doi.org/10.1038/nn.4332>.
- Howe, M.W., and Dombeck, D.A. (2016). Rapid signalling in distinct dopaminergic axons during locomotion and reward. *Nature* 535, 505–510. <https://doi.org/10.1038/nature18942>.
- Hu, H., Gan, J., and Jonas, P. (2014). Fast-spiking, parvalbumin+ GABAergic interneurons: From cellular design to microcircuit function. *Science* 345, 1255263. <https://doi.org/10.1126/science.1255263>.
- Hubel, D.H., and Wiesel, T.N. (1962). Receptive fields, binocular interaction and functional architecture in the cat's visual cortex. *J. Physiol.* 160, 106–154. <https://doi.org/10.1113/jphysiol.1962.sp006837>.
- Huerta-Ocampo, I., Mena-Segovia, J., and Bolam, J.P. (2014). Convergence of cortical and thalamic input to direct and indirect pathway medium spiny neurons in the striatum. *Brain Struct. Funct.* 219, 1787–1800. <https://doi.org/10.1007/s00429-013-0601-z>.
- Hunnicutt, B.J., Long, B.R., Kusefoglu, D., Gertz, K.J., Zhong, H., and Mao, T. (2014). A comprehensive thalamocortical projection map at the mesoscopic level. *Nat. Neurosci.* 17, 1276–1285. <https://doi.org/10.1038/nn.3780>.

- Huo, Y., Chen, H., and Guo, Z.V. (2020). Mapping Functional Connectivity from the Dorsal Cortex to the Thalamus. *Neuron* 107, 1080-1094.e5. <https://doi.org/10.1016/j.neuron.2020.06.038>.
- Hwang, E.J., Dahlen, J.E., Hu, Y.Y., Aguilar, K., Yu, B., Mukundan, M., Mitani, A., and Komiyama, T. (2019). Disengagement of motor cortex from movement control during long-term learning. *Sci. Adv.* 5, eaay0001. <https://doi.org/10.1126/sciadv.aay0001>.
- Hyland, B.I., and Jordan, V.M.B. (1997). Muscle activity during forelimb reaching movements in rats. *Behav. Brain Res.* 85, 175–186. [https://doi.org/10.1016/S0166-4328\(97\)87582-1](https://doi.org/10.1016/S0166-4328(97)87582-1).
- Iacaruso, M.F., Gasler, I.T., and Hofer, S.B. (2017). Synaptic organization of visual space in primary visual cortex. *Nature* 547, 449–452. <https://doi.org/10.1038/nature23019>.
- Inagaki, H.K., Fontolan, L., Romani, S., and Svoboda, K. (2019). Discrete attractor dynamics underlies persistent activity in the frontal cortex. *Nature* 566, 212–217. <https://doi.org/10.1038/s41586-019-0919-7>.
- Inagaki, H.K., Chen, S., Ridder, M.C., Sah, P., Li, N., Yang, Z., Hasanbegovic, H., Gao, Z., Gerfen, C.R., and Svoboda, K. (2022). A midbrain-thalamus-cortex circuit reorganizes cortical dynamics to initiate movement. *Cell* <https://doi.org/10.1016/j.cell.2022.02.006>.
- Iwaniuk, A.N., and Whishaw, I.Q. (2000). On the origin of skilled forelimb movements. *Trends Neurosci.* 23, 372–376. [https://doi.org/10.1016/S0166-2236\(00\)01618-0](https://doi.org/10.1016/S0166-2236(00)01618-0).
- Jia, H., Rochefort, N.L., Chen, X., and Konnerth, A. (2010). Dendritic organization of sensory input to cortical neurons in vivo. *Nature* 464, 1307–1312. <https://doi.org/10.1038/nature08947>.
- Jiang, X., Shen, S., Cadwell, C.R., Berens, P., Sinz, F., Ecker, A.S., Patel, S., and Tolia, A.S. (2015). Principles of connectivity among morphologically defined cell types in adult neocortex. *Science* 350, aac9462. <https://doi.org/10.1126/science.aac9462>.
- Jones, T.A., and Adkins, D.L. (2015). Motor System Reorganization After Stroke: Stimulating and Training Toward Perfection. *Physiology* 30, 358–370. <https://doi.org/10.1152/physiol.00014.2015>.
- Ju, A., Fernandez-Arroyo, B., Wu, Y., Jacky, D., and Beyeler, A. (2020). Expression of serotonin 1A and 2A receptors in molecular- and projection-defined neurons of the mouse insular cortex. *Mol. Brain* 13, 99. <https://doi.org/10.1186/s13041-020-00605-5>.
- Jun, J.J., Steinmetz, N.A., Siegle, J.H., Denman, D.J., Bauza, M., Barbarits, B., Lee, A.K., Anastassiou, C.A., Andrei, A., Aydın, Ç., et al. (2017). Fully integrated silicon probes for high-density recording of neural activity. *Nature* 551, 232–236. <https://doi.org/10.1038/nature24636>.

- Kaas, J.H. (2008). The evolution of the complex sensory and motor systems of the human brain. *Brain Res. Bull.* 75, 384–390. <https://doi.org/10.1016/j.brainresbull.2007.10.009>.
- Kaas, J.H., and Hackett, T.A. (2000). Subdivisions of auditory cortex and processing streams in primates. *Proc. Natl. Acad. Sci.* 97, 11793–11799. <https://doi.org/10.1073/pnas.97.22.11793>.
- Kamiyama, T., Kameda, H., Murabe, N., Fukuda, S., Yoshioka, N., Mizukami, H., Ozawa, K., and Sakurai, M. (2015). Corticospinal Tract Development and Spinal Cord Innervation Differ between Cervical and Lumbar Targets. *J. Neurosci.* 35, 1181–1191. <https://doi.org/10.1523/JNEUROSCI.2842-13.2015>.
- Kaschube, M., Schnabel, M., Löwel, S., Coppola, D.M., White, L.E., and Wolf, F. (2010). Universality in the Evolution of Orientation Columns in the Visual Cortex. *Science* 330, 1113–1116. <https://doi.org/10.1126/science.1194869>.
- Kawaguchi, Y., and Kubota, Y. (1998). Neurochemical features and synaptic connections of large physiologically-identified GABAergic cells in the rat frontal cortex. *Neuroscience* 85, 677–701. [https://doi.org/10.1016/S0306-4522\(97\)00685-4](https://doi.org/10.1016/S0306-4522(97)00685-4).
- Kawai, R., Markman, T., Poddar, R., Ko, R., Fantana, A.L., Dhawale, A.K., Kampff, A.R., and Ölveczky, B.P. (2015). Motor Cortex Is Required for Learning but Not for Executing a Motor Skill. *Neuron* 86, 800–812. <https://doi.org/10.1016/j.neuron.2015.03.024>.
- Keller, G.B., and Mrsic-Flogel, T.D. (2018). Predictive Processing: A Canonical Cortical Computation. *Neuron* 100, 424–435. <https://doi.org/10.1016/j.neuron.2018.10.003>.
- Kepecs, A., and Fishell, G. (2014). Interneuron cell types are fit to function. *Nature* 505, 318–326. <https://doi.org/10.1038/nature12983>.
- Klaus, A., Martins, G.J., Paixao, V.B., Zhou, P., Paninski, L., and Costa, R.M. (2017). The Spatiotemporal Organization of the Striatum Encodes Action Space. *Neuron* 95, 1171–1180.e7. <https://doi.org/10.1016/j.neuron.2017.08.015>.
- Klaus, A., Alves da Silva, J., and Costa, R.M. (2019). What, If, and When to Move: Basal Ganglia Circuits and Self-Paced Action Initiation. *Annu. Rev. Neurosci.* 42, 459–483. <https://doi.org/10.1146/annurev-neuro-072116-031033>.
- Ko, H., Hofer, S.B., Pichler, B., Buchanan, K.A., Sjöström, P.J., and Mrsic-Flogel, T.D. (2011). Functional specificity of local synaptic connections in neocortical networks. *Nature* 473, 87–91. <https://doi.org/10.1038/nature09880>.
- Kohn, A., Jasper, A.I., Semedo, J.D., Gokcen, E., Machens, C.K., and Yu, B.M. (2020). Principles of Corticocortical Communication: Proposed Schemes and Design Considerations. *Trends Neurosci.* 43, 725–737. <https://doi.org/10.1016/j.tins.2020.07.001>.

- Kondo, S., Yoshida, T., and Ohki, K. (2016). Mixed functional microarchitectures for orientation selectivity in the mouse primary visual cortex. *Nat. Commun.* 7, 13210. <https://doi.org/10.1038/ncomms13210>.
- Koralek, A.C., Jin, X., Long Li, J.D., Costa, R.M., and Carmena, J.M. (2012). Corticostriatal plasticity is necessary for learning intentional neuroprosthetic skills. *Nature* 483, 331–335. <https://doi.org/10.1038/nature10845>.
- Kreitzer, A.C., and Malenka, R.C. (2008). Striatal Plasticity and Basal Ganglia Circuit Function. *Neuron* 60, 543–554. <https://doi.org/10.1016/j.neuron.2008.11.005>.
- Kuypers, H.G.J.M. (1982). A New Look at the Organization of the Motor System. In *Progress in Brain Research*, H.G.J.M. Kuypers, and G.F. Martin, eds. (Elsevier), pp. 381–403.
- Lam, Y.-W., and Sherman, S.M. (2015). Functional topographic organization of the motor reticulothalamic pathway. *J. Neurophysiol.* 113, 3090–3097. <https://doi.org/10.1152/jn.00847.2014>.
- Lanciego, J.L., and Wouterlood, F.G. (2020). Neuroanatomical tract-tracing techniques that did go viral. *Brain Struct. Funct.* 225, 1193–1224. <https://doi.org/10.1007/s00429-020-02041-6>.
- Lang, C.E., and Schieber, M.H. (2004). Reduced Muscle Selectivity During Individuated Finger Movements in Humans After Damage to the Motor Cortex or Corticospinal Tract. *J. Neurophysiol.* 91, 1722–1733. <https://doi.org/10.1152/jn.00805.2003>.
- Larkum, M.E., Zhu, J.J., and Sakmann, B. (1999). A new cellular mechanism for coupling inputs arriving at different cortical layers. *Nature* 398, 338–341. <https://doi.org/10.1038/18686>.
- Laureys, S., Faymonville, M., Luxen, A., Lamy, M., Franck, G., and Maquet, P. (2000). Restoration of thalamocortical connectivity after recovery from persistent vegetative state. *The Lancet* 355, 1790–1791. [https://doi.org/10.1016/S0140-6736\(00\)02271-6](https://doi.org/10.1016/S0140-6736(00)02271-6).
- Lee, J., Wang, W., and Sabatini, B.L. (2020). Anatomically segregated basal ganglia pathways allow parallel behavioral modulation. *Nat. Neurosci.* 23, 1388–1398. <https://doi.org/10.1038/s41593-020-00712-5>.
- Lee, S., Hjerling-Leffler, J., Zagha, E., Fishell, G., and Rudy, B. (2010). The Largest Group of Superficial Neocortical GABAergic Interneurons Expresses Ionotropic Serotonin Receptors. *J. Neurosci.* 30, 16796–16808. <https://doi.org/10.1523/JNEUROSCI.1869-10.2010>.
- Lemke, S.M., Ramanathan, D.S., Guo, L., Won, S.J., and Ganguly, K. (2019). Emergent modular neural control drives coordinated motor actions. *Nat. Neurosci.* 22, 1122–1131. <https://doi.org/10.1038/s41593-019-0407-2>.
- Lemon, R.N. (2008). Descending Pathways in Motor Control. *Annu. Rev. Neurosci.* 31, 195–218. <https://doi.org/10.1146/annurev.neuro.31.060407.125547>.

- Lemon, R.N., Landau, W., Tutssel, D., and Lawrence, D.G. (2012). Lawrence and Kuypers (1968a, b) revisited: copies of the original filmed material from their classic papers in *Brain*. *Brain* 135, 2290–2295. <https://doi.org/10.1093/brain/aws037>.
- Li, E., Guo, J., Oh, S.J., Luo, Y., Oliveros, H.C., Du, W., Arano, R., Kim, Y., Chen, Y.-T., Eitson, J., et al. (2021). Anterograde transneuronal tracing and genetic control with engineered yellow fever vaccine YFV-17D. *Nat. Methods* 18, 1542–1551. <https://doi.org/10.1038/s41592-021-01319-9>.
- Li, N., Chen, T.-W., Guo, Z.V., Gerfen, C.R., and Svoboda, K. (2015). A motor cortex circuit for motor planning and movement. *Nature* 519, 51–56. <https://doi.org/10.1038/nature14178>.
- Li, Y., Lu, H., Cheng, P., Ge, S., Xu, H., Shi, S.-H., and Dan, Y. (2012). Clonally related visual cortical neurons show similar stimulus feature selectivity. *Nature* <https://doi.org/10.1038/nature11110>.
- Li, Y., Lopez-Huerta, V.G., Adiconis, X., Levandowski, K., Choi, S., Simmons, S.K., Arias-Garcia, M.A., Guo, B., Yao, A.Y., Blosser, T.R., et al. (2020). Distinct subnetworks of the thalamic reticular nucleus. *Nature* 583, 819–824. <https://doi.org/10.1038/s41586-020-2504-5>.
- Lim, L., Mi, D., Llorca, A., and Marín, O. (2018). Development and Functional Diversification of Cortical Interneurons. *Neuron* 100, 294–313. <https://doi.org/10.1016/j.neuron.2018.10.009>.
- Liu, C., Cai, X., Ritzau-Jost, A., Kramer, P.F., Li, Y., Khaliq, Z.M., Hallermann, S., and Kaeser, P.S. (2022). An action potential initiation mechanism in distal axons for the control of dopamine release. *Science* 375, 1378–1385. <https://doi.org/10.1126/science.abn0532>.
- London, M., and Häusser, M. (2005). DENDRITIC COMPUTATION. *Annu. Rev. Neurosci.* 28, 503–532. <https://doi.org/10.1146/annurev.neuro.28.061604.135703>.
- Lopes, G., Bonacchi, N., Frazão, J., Neto, J.P., Atallah, B.V., Soares, S., Moreira, L., Matias, S., Itskov, P.M., Correia, P.A., et al. (2015). Bonsai: an event-based framework for processing and controlling data streams. *Front. Neuroinformatics* 9. .
- Luo, L. (2021). Architectures of neuronal circuits. *Science* 373, eabg7285. <https://doi.org/10.1126/science.abg7285>.
- Ma, Y., Tsao, D., and Shum, H.-Y. (2022). On the principles of Parsimony and Self-consistency for the emergence of intelligence. *Front. Inf. Technol. Electron. Eng.* <https://doi.org/10.1631/FITEE.2200297>.
- Mahn, M., Gibor, L., Patil, P., Cohen-Kashi Malina, K., Oring, S., Printz, Y., Levy, R., Lampl, I., and Yizhar, O. (2018). High-efficiency optogenetic silencing with soma-targeted anion-conducting channelrhodopsins. *Nat. Commun.* 9, 4125. <https://doi.org/10.1038/s41467-018-06511-8>.

- Makino, H., Hwang, E.J., Hedrick, N.G., and Komiyama, T. (2016). Circuit Mechanisms of Sensorimotor Learning. *Neuron* 92, 705–721. <https://doi.org/10.1016/j.neuron.2016.10.029>.
- Maltese, M., March, J.R., Bashaw, A.G., and Tritsch, N.X. (2021). Dopamine differentially modulates the size of projection neuron ensembles in the intact and dopamine-depleted striatum. *ELife* 10, e68041. <https://doi.org/10.7554/eLife.68041>.
- Mandelbaum, G., Taranda, J., Haynes, T.M., Hochbaum, D.R., Huang, K.W., Hyun, M., Umadevi Venkataraju, K., Straub, C., Wang, W., Robertson, K., et al. (2019). Distinct Cortical-Thalamic-Striatal Circuits through the Parafascicular Nucleus. *Neuron* 102, 636–652.e7. <https://doi.org/10.1016/j.neuron.2019.02.035>.
- Markov, N.T., Ercsey-Ravasz, M., Van Essen, D.C., Knoblauch, K., Toroczkai, Z., and Kennedy, H. (2013). Cortical High-Density Counterstream Architectures. *Science* 342, 1238406. <https://doi.org/10.1126/science.1238406>.
- Markram, H., Lübke, J., Frotscher, M., and Sakmann, B. (1997). Regulation of Synaptic Efficacy by Coincidence of Postsynaptic APs and EPSPs. *Science* 275, 213–215. <https://doi.org/10.1126/science.275.5297.213>.
- Markram, H., Gerstner, W., and Sjöström, P.J. (2011). A History of Spike-Timing-Dependent Plasticity. *Front. Synaptic Neurosci.* 3. <https://doi.org/10.3389/fnsyn.2011.00004>.
- Martinez-Conde, S., Macknik, S.L., and Hubel, D.H. (2004). The role of fixational eye movements in visual perception. *Nat. Rev. Neurosci.* 5, 229–240. <https://doi.org/10.1038/nrn1348>.
- Martinez-Garcia, R.I., Voelcker, B., Zaltsman, J.B., Patrick, S.L., Stevens, T.R., Connors, B.W., and Cruikshank, S.J. (2020). Two dynamically distinct circuits drive inhibition in the sensory thalamus. *Nature* 583, 813–818. <https://doi.org/10.1038/s41586-020-2512-5>.
- Mathis, A., Mamidanna, P., Cury, K.M., Abe, T., Murthy, V.N., Mathis, M.W., and Bethge, M. (2018). DeepLabCut: markerless pose estimation of user-defined body parts with deep learning. *Nat. Neurosci.* 21, 1281–1289. <https://doi.org/10.1038/s41593-018-0209-y>.
- Mathis, M.W., Mathis, A., and Uchida, N. (2017). Somatosensory Cortex Plays an Essential Role in Forelimb Motor Adaptation in Mice. *Neuron* 93, 1493–1503.e6. <https://doi.org/10.1016/j.neuron.2017.02.049>.
- Matsuda, W., Furuta, T., Nakamura, K.C., Hioki, H., Fujiyama, F., Arai, R., and Kaneko, T. (2009). Single Nigrostriatal Dopaminergic Neurons Form Widely Spread and Highly Dense Axonal Arborizations in the Neostriatum. *J. Neurosci.* 29, 444–453. <https://doi.org/10.1523/JNEUROSCI.4029-08.2009>.
- Matyas, F., Sreenivasan, V., Marbach, F., Wacongne, C., Barsy, B., Mateo, C., Aronoff, R., and Carl C. H. Petersen (2010). Motor Control by Sensory Cortex. *Science* 330, 1240–1243. <https://doi.org/10.1126/science.1195797>.

Maurice, N., Liberge, M., Jaouen, F., Ztaou, S., Hanini, M., Camon, J., Deisseroth, K., Amalric, M., Kerkerian-Le Goff, L., and Beurrier, C. (2015). Striatal Cholinergic Interneurons Control Motor Behavior and Basal Ganglia Function in Experimental Parkinsonism. *Cell Rep.* 13, 657–666. <https://doi.org/10.1016/j.celrep.2015.09.034>.

Mayrhofer, J.M., El-Boustani, S., Foustoukos, G., Auffret, M., Tamura, K., and Petersen, C.C.H. (2019). Distinct Contributions of Whisker Sensory Cortex and Tongue-Jaw Motor Cortex in a Goal-Directed Sensorimotor Transformation. *Neuron* 103, 1034–1043.e5. <https://doi.org/10.1016/j.neuron.2019.07.008>.

McElvain, L.E., Chen, Y., Moore, J.D., Brigidi, G.S., Bloodgood, B.L., Lim, B.K., Costa, R.M., and Kleinfeld, D. (2021). Specific populations of basal ganglia output neurons target distinct brain stem areas while collateralizing throughout the diencephalon. *Neuron* 109, 1721–1738.e4. <https://doi.org/10.1016/j.neuron.2021.03.017>.

Mercer Lindsay, N., Knutsen, P.M., Lozada, A.F., Gibbs, D., Karten, H.J., and Kleinfeld, D. (2019). Orofacial Movements Involve Parallel Corticobulbar Projections from Motor Cortex to Trigeminal Premotor Nuclei. *Neuron* 104, 765–780.e3. <https://doi.org/10.1016/j.neuron.2019.08.032>.

Miri, A., Warriner, C.L., Seely, J.S., Elsayed, G.F., Cunningham, J.P., Churchland, M.M., and Jessell, T.M. (2017). Behaviorally Selective Engagement of Short-Latency Effector Pathways by Motor Cortex. *Neuron* 95, 683–696.e11. <https://doi.org/10.1016/j.neuron.2017.06.042>.

Moore, J.D., Kleinfeld, D., and Wang, F. (2014). How the brainstem controls orofacial behaviors comprised of rhythmic actions. *Trends Neurosci.* 37, 370–380. <https://doi.org/10.1016/j.tins.2014.05.001>.

Morandell, K., and Huber, D. (2017). The role of forelimb motor cortex areas in goal directed action in mice. *Sci. Rep.* 7, 15759. <https://doi.org/10.1038/s41598-017-15835-2>.

Morecraft, R.J., Ge, J., Stilwell-Morecraft, K.S., McNeal, D.W., Pizzimenti, M.A., and Darling, W.G. (2013). Terminal distribution of the corticospinal projection from the hand/arm region of the primary motor cortex to the cervical enlargement in rhesus monkey. *J. Comp. Neurol.* 521, 4205–4235. <https://doi.org/10.1002/cne.23410>.

Morita, K., Im, S., and Kawaguchi, Y. (2019). Differential Striatal Axonal Arborizations of the Intratelencephalic and Pyramidal-Tract Neurons: Analysis of the Data in the MouseLight Database. *Front. Neural Circuits* 13, 71. <https://doi.org/10.3389/fncir.2019.00071>.

Moser, E.I., Kropff, E., and Moser, M.-B. (2008). Place Cells, Grid Cells, and the Brain's Spatial Representation System. *Annu. Rev. Neurosci.* 31, 69–89. <https://doi.org/10.1146/annurev.neuro.31.061307.090723>.

Muñoz-Castañeda, R., Zingg, B., Matho, K.S., Chen, X., Wang, Q., Foster, N.N., Li, A., Narasimhan, A., Hirokawa, K.E., Huo, B., et al. (2021). Cellular anatomy of the

mouse primary motor cortex. *Nature* 598, 159–166. <https://doi.org/10.1038/s41586-021-03970-w>.

Murata, Y., Higo, N., Oishi, T., Yamashita, A., Matsuda, K., Hayashi, M., and Yamane, S. (2008). Effects of Motor Training on the Recovery of Manual Dexterity After Primary Motor Cortex Lesion in Macaque Monkeys. *J. Neurophysiol.* 99, 773–786. <https://doi.org/10.1152/jn.01001.2007>.

Nakajima, K., Maier, M.A., Kirkwood, P.A., and Lemon, R.N. (2000). Striking Differences in Transmission of Corticospinal Excitation to Upper Limb Motoneurons in Two Primate Species. *J. Neurophysiol.* 84, 698–709. <https://doi.org/10.1152/jn.2000.84.2.698>.

Nambu, A. (2008). Seven problems on the basal ganglia. *Curr. Opin. Neurobiol.* 18, 595–604. <https://doi.org/10.1016/j.conb.2008.11.001>.

Nelson, A., Abdelmesih, B., and Costa, R.M. (2021). Corticospinal populations broadcast complex motor signals to coordinated spinal and striatal circuits. *Nat. Neurosci.* 24, 1721–1732. <https://doi.org/10.1038/s41593-021-00939-w>.

Niell, C.M., and Scanziani, M. (2021). How Cortical Circuits Implement Cortical Computations: Mouse Visual Cortex as a Model. *Annu. Rev. Neurosci.* <https://doi.org/10.1146/annurev-neuro-102320-085825>.

Oh, S.W., Harris, J.A., Ng, L., Winslow, B., Cain, N., Mihalas, S., Wang, Q., Lau, C., Kuan, L., Henry, A.M., et al. (2014). A mesoscale connectome of the mouse brain. *Nature* 508, 207–214. <https://doi.org/10.1038/nature13186>.

Okobi, D.E., Banerjee, A., Matheson, A.M.M., Phelps, S.M., and Long, M.A. (2019). Motor cortical control of vocal interaction in neotropical singing mice. *Science* 363, 983–988. <https://doi.org/10.1126/science.aau9480>.

Oláh, S., Komlósi, G., Szabadics, J., Varga, C., Tóth, É., Barzó, P., and Tamás, G. (2007). Output of neurogliaform cells to various neuron types in the human and rat cerebral cortex. *Front. Neural Circuits* 1. .

Olsen, S.R., Bortone, D.S., Adesnik, H., and Scanziani, M. (2012). Gain control by layer six in cortical circuits of vision. *Nature* 483, 47–52. <https://doi.org/10.1038/nature10835>.

Otchy, T.M., Wolff, S.B.E., Rhee, J.Y., Pehlevan, C., Kawai, R., Kempf, A., Gobes, S.M.H., and Ölveczky, B.P. (2015). Acute off-target effects of neural circuit manipulations. *Nature* 528, 358–363. <https://doi.org/10.1038/nature16442>.

Panigrahi, B., Martin, K.A., Li, Y., Graves, A.R., Vollmer, A., Olson, L., Mensh, B.D., Karpova, A.Y., and Dudman, J.T. (2015). Dopamine Is Required for the Neural Representation and Control of Movement Vigor. *Cell* 162, 1418–1430. <https://doi.org/10.1016/j.cell.2015.08.014>.

Park, J., Phillips, J.W., Guo, J.-Z., Martin, K.A., Hantman, A.W., and Dudman, J.T. (2022). Motor cortical output for skilled forelimb movement is selectively distributed

across projection neuron classes. *Sci. Adv.* 8, eabj5167. <https://doi.org/10.1126/sciadv.abj5167>.

Parker, J.G., Marshall, J.D., Ahanonu, B., Wu, Y.-W., Kim, T.H., Grewe, B.F., Zhang, Y., Li, J.Z., Ding, J.B., Ehlers, M.D., et al. (2018). Diametric neural ensemble dynamics in parkinsonian and dyskinetic states. *Nature* 557, 177–182. <https://doi.org/10.1038/s41586-018-0090-6>.

Paxinos, G., and Franklin, K.B.J. (2007). *The Mouse Brain in Stereotaxic Coordinates, Compact, Third Edition: The coronal plates and diagrams* (Academic Press).

Penfield, W., and Boldrey, E. (1937). SOMATIC MOTOR AND SENSORY REPRESENTATION IN THE CEREBRAL CORTEX OF MAN AS STUDIED BY ELECTRICAL STIMULATION. *Brain* 60, 389–443. <https://doi.org/10.1093/brain/60.4.389>.

Peters, A.J., Chen, S.X., and Komiyama, T. (2014). Emergence of reproducible spatiotemporal activity during motor learning. *Nature* 510, 263–267. <https://doi.org/10.1038/nature13235>.

Peters, A.J., Lee, J., Hedrick, N.G., O’Neil, K., and Komiyama, T. (2017). Reorganization of corticospinal output during motor learning. *Nat. Neurosci.* 20, 1133–1141. <https://doi.org/10.1038/nn.4596>.

Peters, A.J., Fabre, J.M.J., Steinmetz, N.A., Harris, K.D., and Carandini, M. (2021). Striatal activity topographically reflects cortical activity. *Nature* 591, 420–425. <https://doi.org/10.1038/s41586-020-03166-8>.

Petersen, C.C.H. (2019). Sensorimotor processing in the rodent barrel cortex. *Nat. Rev. Neurosci.* 20, 533–546. <https://doi.org/10.1038/s41583-019-0200-y>.

Pfeffer, C.K., Xue, M., He, M., Huang, Z.J., and Scanziani, M. (2013). Inhibition of inhibition in visual cortex: the logic of connections between molecularly distinct interneurons. *Nat. Neurosci.* 16, 1068–1076. <https://doi.org/10.1038/nn.3446>.

Pi, H.-J., Hangya, B., Kvitsiani, D., Sanders, J.I., Huang, Z.J., and Kepecs, A. (2013). Cortical interneurons that specialize in disinhibitory control. *Nature* 503, 521–524. <https://doi.org/10.1038/nature12676>.

Pinto, L., Rajan, K., DePasquale, B., Thiberge, S.Y., Tank, D.W., and Brody, C.D. (2019). Task-Dependent Changes in the Large-Scale Dynamics and Necessity of Cortical Regions. *Neuron* 104, 810–824.e9. <https://doi.org/10.1016/j.neuron.2019.08.025>.

Pivetta, C., Esposito, M.S., Sigrist, M., and Arber, S. (2014). Motor-Circuit Communication Matrix from Spinal Cord to Brainstem Neurons Revealed by Developmental Origin. *Cell* 156, 537–548. <https://doi.org/10.1016/j.cell.2013.12.014>.

Poewe, W., Seppi, K., Tanner, C.M., Halliday, G.M., Brundin, P., Volkmann, J., Schrag, A.-E., and Lang, A.E. (2017). Parkinson disease. *Nat. Rev. Dis. Primer* 3, 1–21. <https://doi.org/10.1038/nrdp.2017.13>.

- Poorthuis, R.B., Bloem, B., Schak, B., Wester, J., de Kock, C.P.J., and Mansvelder, H.D. (2013). Layer-Specific Modulation of the Prefrontal Cortex by Nicotinic Acetylcholine Receptors. *Cereb. Cortex* 23, 148–161. <https://doi.org/10.1093/cercor/bhr390>.
- Quiroga, R.Q., Reddy, L., Kreiman, G., Koch, C., and Fried, I. (2005). Invariant visual representation by single neurons in the human brain. *Nature* 435, 1102–1107. <https://doi.org/10.1038/nature03687>.
- Rakic, P. (2009). Evolution of the neocortex: a perspective from developmental biology. *Nat Rev Neurosci* 10, 724–735. <https://doi.org/10.1038/nrn2719>.
- Rathelot, J.-A., and Strick, P.L. (2006). Muscle representation in the macaque motor cortex: An anatomical perspective. *Proc. Natl. Acad. Sci.* 103, 8257–8262. <https://doi.org/10.1073/pnas.0602933103>.
- Rathelot, J.-A., and Strick, P.L. (2009). Subdivisions of primary motor cortex based on cortico-motoneuronal cells. *Proc. Natl. Acad. Sci.* 106, 918–923. <https://doi.org/10.1073/pnas.0808362106>.
- Reynolds, J.N.J., and Wickens, J.R. (2002). Dopamine-dependent plasticity of corticostriatal synapses. *Neural Netw.* 15, 507–521. [https://doi.org/10.1016/S0893-6080\(02\)00045-X](https://doi.org/10.1016/S0893-6080(02)00045-X).
- Rockland, K.S., and Pandya, D.N. (1979). Laminar origins and terminations of cortical connections of the occipital lobe in the rhesus monkey. *Brain Res.* 179, 3–20. [https://doi.org/10.1016/0006-8993\(79\)90485-2](https://doi.org/10.1016/0006-8993(79)90485-2).
- Roy, D.S., Zhang, Y., Halassa, M.M., and Feng, G. (2022). Thalamic subnetworks as units of function. *Nat. Neurosci.* 1–14. <https://doi.org/10.1038/s41593-021-00996-1>.
- Ruder, L., and Arber, S. (2019). Brainstem Circuits Controlling Action Diversification. *Annu. Rev. Neurosci.* 42, 485–504. <https://doi.org/10.1146/annurev-neuro-070918-050201>.
- Ruder, L., Schina, R., Kanodia, H., Valencia-Garcia, S., Pivetta, C., and Arber, S. (2021). A functional map for diverse forelimb actions within brainstem circuitry. *Nature* 590, 445–450. <https://doi.org/10.1038/s41586-020-03080-z>.
- Sahni, V., Shnider, S.J., Jabaudon, D., Song, J.H.T., Itoh, Y., Greig, L.C., and Macklis, J.D. (2021a). Corticospinal neuron subpopulation-specific developmental genes prospectively indicate mature segmentally specific axon projection targeting. *Cell Rep.* 37, 109843. <https://doi.org/10.1016/j.celrep.2021.109843>.
- Sahni, V., Itoh, Y., Shnider, S.J., and Macklis, J.D. (2021b). Crim1 and Kelch-like 14 exert complementary dual-directional developmental control over segmentally specific corticospinal axon projection targeting. *Cell Rep.* 37, 109842. <https://doi.org/10.1016/j.celrep.2021.109842>.
- Sanes, J.N., and Donoghue, J.P. (2000). Plasticity and Primary Motor Cortex. *Annu. Rev. Neurosci.* 23, 393–415. <https://doi.org/10.1146/annurev.neuro.23.1.393>.

- Sauerbrei, B.A., Guo, J.-Z., Cohen, J.D., Mischiati, M., Guo, W., Kabra, M., Verma, N., Mensh, B., Branson, K., and Hantman, A.W. (2020). Cortical pattern generation during dexterous movement is input-driven. *Nature* 577, 386–391. <https://doi.org/10.1038/s41586-019-1869-9>.
- Schneider, D.M., Nelson, A., and Mooney, R. (2014). A synaptic and circuit basis for corollary discharge in the auditory cortex. *Nature* 513, 189–194. <https://doi.org/10.1038/nature13724>.
- Seong, H.J., and Carter, A.G. (2012). D1 Receptor Modulation of Action Potential Firing in a Subpopulation of Layer 5 Pyramidal Neurons in the Prefrontal Cortex. *J. Neurosci.* 32, 10516–10521. <https://doi.org/10.1523/JNEUROSCI.1367-12.2012>.
- Seymour, B., Singer, T., and Dolan, R. (2007). The neurobiology of punishment. *Nat. Rev. Neurosci.* 8, 300–311. <https://doi.org/10.1038/nrn2119>.
- Shamash, P., Carandini, M., Harris, K., and Steinmetz, N. (2018). A tool for analyzing electrode tracks from slice histology. <https://doi.org/10.1101/447995>.
- Shen, W., Flajolet, M., Greengard, P., and Surmeier, D.J. (2008). Dichotomous Dopaminergic Control of Striatal Synaptic Plasticity. *Science* 321, 848–851. <https://doi.org/10.1126/science.1160575>.
- Shepherd, G.M.G. (2013). Corticostriatal connectivity and its role in disease. *Nat. Rev. Neurosci.* 14, 278–291. <https://doi.org/10.1038/nrn3469>.
- Sherman, S.M., and Guillery, R.W. (2005). *Exploring the Thalamus and Its Role in Cortical Function* (Cambridge, MA, USA: MIT Press).
- Silberberg, G., and Markram, H. (2007). Disynaptic Inhibition between Neocortical Pyramidal Cells Mediated by Martinotti Cells. *Neuron* 53, 735–746. <https://doi.org/10.1016/j.neuron.2007.02.012>.
- Silva, J.A. da, Tecuapetla, F., Paixão, V., and Costa, R.M. (2018). Dopamine neuron activity before action initiation gates and invigorates future movements. *Nature* <https://doi.org/10.1038/nature25457>.
- Sippy, T., Lapray, D., Crochet, S., and Petersen, C.C.H. (2015). Cell-Type-Specific Sensorimotor Processing in Striatal Projection Neurons during Goal-Directed Behavior. *Neuron* 88, 298–305. <https://doi.org/10.1016/j.neuron.2015.08.039>.
- Smith, J.C., Abdala, A.P.L., Borgmann, A., Rybak, I.A., and Paton, J.F.R. (2013). Brainstem respiratory networks: building blocks and microcircuits. *Trends Neurosci.* 36, 152–162. <https://doi.org/10.1016/j.tins.2012.11.004>.
- Sobinov, A.R., and Bensmaia, S.J. (2021). The neural mechanisms of manual dexterity. *Nat. Rev. Neurosci.* 1–17. <https://doi.org/10.1038/s41583-021-00528-7>.
- Sotelo, C. (2003). Viewing the brain through the master hand of Ramon y Cajal. *Nat. Rev. Neurosci.* 4, 71–77. <https://doi.org/10.1038/nrn1010>.

Sousa, A.M.M., Meyer, K.A., Santpere, G., Gulden, F.O., and Sestan, N. (2017). Evolution of the Human Nervous System Function, Structure, and Development. *Cell* 170, 226–247. <https://doi.org/10.1016/j.cell.2017.06.036>.

Sreenivasan, V., Karmakar, K., Rijli, F.M., and Carl C. H. Petersen (2015). Parallel pathways from motor and somatosensory cortex for controlling whisker movements in mice. *Eur. J. Neurosci.* 41, 354–367. <https://doi.org/10.1111/ejn.12800>.

Steinmetz, N.A., Zatka-Haas, P., Carandini, M., and Harris, K.D. (2019). Distributed coding of choice, action and engagement across the mouse brain. *Nature* 1–8. <https://doi.org/10.1038/s41586-019-1787-x>.

Steinmetz, N.A., Aydin, C., Lebedeva, A., Okun, M., Pachitariu, M., Bauza, M., Beau, M., Bhagat, J., Böhm, C., Broux, M., et al. (2021). Neuropixels 2.0: A miniaturized high-density probe for stable, long-term brain recordings. *Science* 372, eabf4588. <https://doi.org/10.1126/science.abf4588>.

Takata, N. (2020). Thalamic reticular nucleus in the thalamocortical loop. *Neurosci. Res.* 156, 32–40. <https://doi.org/10.1016/j.neures.2019.12.004>.

Takato, J., Park, J.H., Lu, J., Li, S., Thompson, P., Han, B.-X., Zhao, S., Kleinfeld, D., Friedman, B., and Wang, F. (2021). Constructing an adult orofacial premotor atlas in Allen mouse CCF. *ELife* 10, e67291. <https://doi.org/10.7554/eLife.67291>.

Takeoka, A., Vollenweider, I., Courtine, G., and Arber, S. (2014). Muscle Spindle Feedback Directs Locomotor Recovery and Circuit Reorganization after Spinal Cord Injury. *Cell* 159, 1626–1639. <https://doi.org/10.1016/j.cell.2014.11.019>.

Taniguchi, H., Lu, J., and Z. Josh Huang (2013). The Spatial and Temporal Origin of Chandelier Cells in Mouse Neocortex. *Science* 339, 70–74. <https://doi.org/10.1126/science.1227622>.

Tasic, B., Yao, Z., Graybiel, L.T., Smith, K.A., Nguyen, T.N., Bertagnolli, D., Goldy, J., Garren, E., Economou, M.N., Viswanathan, S., et al. (2018). Shared and distinct transcriptomic cell types across neocortical areas. *Nature* 563, 72. <https://doi.org/10.1038/s41586-018-0654-5>.

Tecuapetla, F., Jin, X., Lima, S.Q., and Costa, R.M. (2016). Complementary Contributions of Striatal Projection Pathways to Action Initiation and Execution. *Cell* 166, 703–715. <https://doi.org/10.1016/j.cell.2016.06.032>.

Tennant, K.A., Adkins, D.L., Donlan, N.A., Asay, A.L., Thomas, N., Kleim, J.A., and Jones, T.A. (2011). The Organization of the Forelimb Representation of the C57BL/6 Mouse Motor Cortex as Defined by Intracortical Microstimulation and Cytoarchitecture. *Cereb. Cortex* 21, 865–876. <https://doi.org/10.1093/cercor/bhq159>.

Tervo, D.G.R., Hwang, B.-Y., Viswanathan, S., Gaj, T., Lavzin, M., Ritola, K.D., Lindo, S., Michael, S., Kuleshova, E., Ojala, D., et al. (2016). A Designer AAV Variant Permits Efficient Retrograde Access to Projection Neurons. *Neuron* 92, 372–382. <https://doi.org/10.1016/j.neuron.2016.09.021>.

Thomson, A. (2010). Neocortical layer 6, a review. *Front. Neuroanat.* 4. .

- Tinevez, J.-Y., Perry, N., Schindelin, J., Hoopes, G.M., Reynolds, G.D., Laplantine, E., Bednarek, S.Y., Shorte, S.L., and Eliceiri, K.W. (2017). TrackMate: An open and extensible platform for single-particle tracking. *Methods* 115, 80–90. <https://doi.org/10.1016/j.ymeth.2016.09.016>.
- Ueno, M., Nakamura, Y., Li, J., Gu, Z., Niehaus, J., Maezawa, M., Crone, S.A., Goulding, M., Bacceti, M.L., and Yoshida, Y. (2018). Corticospinal Circuits from the Sensory and Motor Cortices Differentially Regulate Skilled Movements through Distinct Spinal Interneurons. *Cell Rep.* 23, 1286-1300.e7. <https://doi.org/10.1016/j.celrep.2018.03.137>.
- Usseglio, G., Gatier, E., Heuzé, A., Hérent, C., and Bouvier, J. (2020). Control of Orienting Movements and Locomotion by Projection-Defined Subsets of Brainstem V2a Neurons. *Curr. Biol.* 30, 4665-4681.e6. <https://doi.org/10.1016/j.cub.2020.09.014>.
- Wang, H.-P., Spencer, D., Fellous, J.-M., and Sejnowski, T.J. (2010). Synchrony of Thalamocortical Inputs Maximizes Cortical Reliability. *Science* 328, 106–109. <https://doi.org/10.1126/science.1183108>.
- Wang, M., Ramos, B.P., Paspalas, C.D., Shu, Y., Simen, A., Duque, A., Vijayraghavan, S., Brennan, A., Dudley, A., Nou, E., et al. (2007). α 2A-Adrenoceptors Strengthen Working Memory Networks by Inhibiting cAMP-HCN Channel Signaling in Prefrontal Cortex. *Cell* 129, 397–410. <https://doi.org/10.1016/j.cell.2007.03.015>.
- Wang, X., Liu, Y., Li, X., Zhang, Z., Yang, H., Zhang, Y., Williams, P.R., Alwahab, N.S.A., Kapur, K., Yu, B., et al. (2017). Deconstruction of Corticospinal Circuits for Goal-Directed Motor Skills. *Cell* 171, 440-455.e14. <https://doi.org/10.1016/j.cell.2017.08.014>.
- Wang, Y., Yin, X., Zhang, Z., Li, J., Zhao, W., and Guo, Z.V. (2021). A cortico-basal ganglia-thalamo-cortical channel underlying short-term memory. *Neuron* 109, 3486-3499.e7. <https://doi.org/10.1016/j.neuron.2021.08.002>.
- Watson, G.D.R., Hughes, R.N., Petter, E.A., Fallon, I.P., Kim, N., Severino, F.P.U., and Yin, H.H. (2021). Thalamic projections to the subthalamic nucleus contribute to movement initiation and rescue of parkinsonian symptoms. *Sci. Adv.* 7, eabe9192. <https://doi.org/10.1126/sciadv.abe9192>.
- Wiegert, J.S., Mahn, M., Prigge, M., Printz, Y., and Yizhar, O. (2017). Silencing Neurons: Tools, Applications, and Experimental Constraints. *Neuron* 95, 504–529. <https://doi.org/10.1016/j.neuron.2017.06.050>.
- Wiener, N. (1961). *Cybernetics or control and communication in the animal and the machine* (Cambridge, Mass: MIT Press).
- Williams, R.W., and Herrup, K. (1988). The Control of Neuron Number. *Annu. Rev. Neurosci.* 11, 423–453. <https://doi.org/10.1146/annurev.ne.11.030188.002231>.
- Williams, S.R., and Stuart, G.J. (2002). Dependence of EPSP Efficacy on Synapse Location in Neocortical Pyramidal Neurons. *Science* 295, 1907–1910. <https://doi.org/10.1126/science.1067903>.

- Wilson, M.A., and McNaughton, B.L. (1993). Dynamics of the Hippocampal Ensemble Code for Space. *Science* 261, 1055–1058. <https://doi.org/10.1126/science.8351520>.
- Winnubst, J., Bas, E., Ferreira, T.A., Wu, Z., Economo, M.N., Edson, P., Arthur, B.J., Bruns, C., Rokicki, K., Schauder, D., et al. (2019). Reconstruction of 1,000 Projection Neurons Reveals New Cell Types and Organization of Long-Range Connectivity in the Mouse Brain. *Cell* 179, 268–281.e13. <https://doi.org/10.1016/j.cell.2019.07.042>.
- Wolpert, D.M., and Ghahramani, Z. (2000). Computational principles of movement neuroscience. *Nat. Neurosci.* 3, 1212–1217. <https://doi.org/10.1038/81497>.
- Xiong, Q., Znamenskiy, P., and Zador, A.M. (2015). Selective corticostriatal plasticity during acquisition of an auditory discrimination task. *Nature* 521, 348–351. <https://doi.org/10.1038/nature14225>.
- Xu, H., Jeong, H.-Y., Tremblay, R., and Rudy, B. (2013). Neocortical Somatostatin-Expressing GABAergic Interneurons Disinhibit the Thalamorecipient Layer 4. *Neuron* 77, 155–167. <https://doi.org/10.1016/j.neuron.2012.11.004>.
- Xu, N., Harnett, M.T., Williams, S.R., Huber, D., O'Connor, D.H., Svoboda, K., and Magee, J.C. (2012). Nonlinear dendritic integration of sensory and motor input during an active sensing task. *Nature* 492, 247–251. <https://doi.org/10.1038/nature11601>.
- Xu, T., Yu, X., Perlik, A.J., Tobin, W.F., Zweig, J.A., Tennant, K., Jones, T., and Zuo, Y. (2009). Rapid formation and selective stabilization of synapses for enduring motor memories. *Nature* 462, 915–919. <https://doi.org/10.1038/nature08389>.
- Yakovenko, S., Krouchev, N., and Drew, T. (2011). Sequential Activation of Motor Cortical Neurons Contributes to Intralimb Coordination During Reaching in the Cat by Modulating Muscle Synergies. *J. Neurophysiol.* 105, 388–409. <https://doi.org/10.1152/jn.00469.2010>.
- Yamashita, T., Pala, A., Pedrido, L., Kremer, Y., Welker, E., and Petersen, C.C.H. (2013). Membrane Potential Dynamics of Neocortical Projection Neurons Driving Target-Specific Signals. *Neuron* 80, 1477–1490. <https://doi.org/10.1016/j.neuron.2013.10.059>.
- Yamawaki, N., Borges, K., Suter, B.A., Harris, K.D., and Shepherd, G.M.G. (2014). A genuine layer 4 in motor cortex with prototypical synaptic circuit connectivity. *ELife* 3, e05422. <https://doi.org/10.7554/eLife.05422>.
- Yin, H.H., and Knowlton, B.J. (2006). The role of the basal ganglia in habit formation. *Nat. Rev. Neurosci.* 7, 464–476. <https://doi.org/10.1038/nrn1919>.
- Yin, H.H., Mulcare, S.P., Hilário, M.R.F., Clouse, E., Holloway, T., Davis, M.I., Hansson, A.C., Lovinger, D.M., and Costa, R.M. (2009). Dynamic reorganization of striatal circuits during the acquisition and consolidation of a skill. *Nat. Neurosci.* 12, 333–341. <https://doi.org/10.1038/nn.2261>.
- Young, M.P., and Yamane, S. (1992). Sparse population coding of faces in the inferior temporal cortex. *Science* 256, 1327–1331. <https://doi.org/10.1126/science.1598577>.

- Yu, Y.-C., Bultje, R.S., Wang, X., and Shi, S.-H. (2009). Specific synapses develop preferentially among sister excitatory neurons in the neocortex. *Nature* 458, 501–504. <https://doi.org/10.1038/nature07722>.
- Yu, Y.-C., He, S., Chen, S., Fu, Y., Brown, K.N., Yao, X.-H., Ma, J., Gao, K.P., Sosinsky, G.E., Huang, K., et al. (2012). Preferential electrical coupling regulates neocortical lineage-dependent microcircuit assembly. *Nature* 486, 113–117. <https://doi.org/10.1038/nature10958>.
- Zaaimi, B., Edgley, S.A., Soteropoulos, D.S., and Baker, S.N. (2012). Changes in descending motor pathway connectivity after corticospinal tract lesion in macaque monkey. *Brain* 135, 2277–2289. <https://doi.org/10.1093/brain/aws115>.
- Zhang, Y., Roy, D.S., Zhu, Y., Chen, Y., Aida, T., Hou, Y., Shen, C., Lea, N.E., Schroeder, M.E., Skaggs, K.M., et al. (2022). Targeting thalamic circuits rescues motor and mood deficits in PD mice. *Nature* 1–9. <https://doi.org/10.1038/s41586-022-04806-x>.
- Zingg, B., Hintiryan, H., Gou, L., Song, M.Y., Bay, M., Bienkowski, M.S., Foster, N.N., Yamashita, S., Bowman, I., Toga, A.W., et al. (2014). Neural Networks of the Mouse Neocortex. *Cell* 156, 1096–1111. <https://doi.org/10.1016/j.cell.2014.02.023>.
- Zingg, B., Chou, X., Zhang, Z., Mesik, L., Liang, F., Tao, H.W., and Zhang, L.I. (2017). AAV-Mediated Anterograde Transsynaptic Tagging: Mapping Corticocollicular Input-Defined Neural Pathways for Defense Behaviors. *Neuron* 93, 33–47. <https://doi.org/10.1016/j.neuron.2016.11.045>.
- Zingg, B., Peng, B., Huang, J., Tao, H.W., and Zhang, L.I. (2020). Synaptic Specificity and Application of Anterograde Transsynaptic AAV for Probing Neural Circuitry. *J. Neurosci.* 40, 3250–3267. <https://doi.org/10.1523/JNEUROSCI.2158-19.2020>.
- Znamenskiy, P., and Zador, A.M. (2013). Corticostriatal neurons in auditory cortex drive decisions during auditory discrimination. *Nature* 497, 482–485. <https://doi.org/10.1038/nature12077>.
- Zong, W., Obenhaus, H.A., Skytøen, E.R., Eneqvist, H., de Jong, N.L., Vale, R., Jorge, M.R., Moser, M.-B., and Moser, E.I. (2022). Large-scale two-photon calcium imaging in freely moving mice. *Cell* 185, 1240–1256.e30. <https://doi.org/10.1016/j.cell.2022.02.017>.

7. Curriculum Vitae

Wuzhou Yang

Date of Birth: Jan. 9th, 1991 Nationality: Chinese

Address: Tangentenweg 34, 4058, Basel

E-Mail: wuzhou.yang@unibas.ch, yang.wuzh@gmail.com

Education

- Sep. 2007 to Jul. 2012 Bachelor of Medicine, Fudan University
 - Sep. 2012 to Jul. 2015 MSc in Neurobiology, Fudan University
 - Jan. 2016 to Mar. 2017 Student assistant, EPFL
 - Apr. 2017 to 2022 PhD in Neurobiology (expected), University of Basel
-

Research and Working Experiences

- Apr. 2017 to 2022 FMI & Biozentrum, University of Basel
Interaction between motor cortex and brainstem
Advisor: Professor Silvia Arber
 - Jan. 2016 to Mar. 2017 Brain Mind Institute, EPFL
Extracellular Calcium Impact on Synaptic Dynamics and Network Activity
Advisor: Professor Henry Markram
 - Sep. 2012 to Jul. 2015 Institute of Brain Science, Fudan University
Fear Erasure Facilitated by Immature Inhibitory Neuron Transplantation
Advisor: Professor Yong-Chun Yu
 - Sep. 2010 to Feb. 2011 Jinshan Hospital, Fudan University
Clinical Internship
-

Publications

- **Yang, W.**, Kanodia, H., Arber, S. (2022). Fine-grained structural and functional map for forelimb movement phases between cortex and medulla. Submitted to Cell, accepted.
- **Yang, W.-Z.***, Liu, T.-T.*, Cao, J.-W., Chen, X.-F., Liu, X., Wang, M., Su, X., Zhang, S.-Q., Qiu, B.-L., Hu, W.-X., et al. (2016). Fear Erasure Facilitated by Immature Inhibitory Neuron Transplantation. *Neuron* 92, 1352–1367. DOI: 10.1016/j.neuron.2016.11.018 *co-first author
- Cheng, L., Hu, W., Qiu, B., Zhao, J., Yu, Y., Guan, W., Wang, M., **Yang, W.**, and Pei, G. (2014). Generation of neural progenitor cells by chemical cocktails and hypoxia. *Cell Res* 24, 665–679. DOI: 10.1038/cr.2014.32